CHEMICAL SOLUTION DEPOSITION AND CHARACTERIZATION OF $Bi_4Ti_3O_{12}$ AND $BiFe_{1-x}Co_xO_3$ THIN FILMS

NGUYEN TRUONG THO

SEPTEMBER 2010

CHEMICAL SOLUTION DEPOSITION AND CHARACTERIZATION OF $Bi_4Ti_3O_{12}$ AND $BiFe_{1-x}Co_xO_3$ THIN FILMS

A dissertation submitted to
THE GRADUATE SCHOOL OF ENGINEERING SCIENCE
OSAKA UNIVERSITY

In partial fulfillment of the requirements for the degree of
DOCTOR OF PHYLOSOPHY IN ENGINEERING

BY

NGUYEN TRUONG THO

SEPTEMBER 2010

Abstract

Ferroelectric materials exhibit a number of desirable properties, such as switchable polarization, high piezoelectric responses and high dielectric constants. For this reason they are widely used in devices, for example memory elements, ultrasonic generators, capacitors, gas igniters in thin film and so on. There are two trends of ferroelectric random access memory (FeRAM), namely suppression of processing temperature in preparation of thin films and the improvement of insulation and ferroelectric property.

Among several candidates of these materials, $Bi_3Ti_4O_{12}$ (BIT) is attracting significant attention. Similar to $SrBi_2Ta_2O_9$ (SBT), BIT has a layered perovskite structure consisting of triple TiO_6 octahedral in perovskite-like layers separated by Bi_2O_3 layers. BIT has large remanent polarization, a small coercive field and high Curie temperature. Furthermore, BIT thin films are known to be crystallized at lower temperature compared with that of SBT. As a result, the ferroelectric thin film can be deposited on a large-scale integration (LSI) structure in a final process without mutual diffusion and any damage to either the Al wire or low-k layer. Meanwhile, hydrothermal synthesis is known as a method to decrease preparation temperature of ferroelectric thin films because of increasing pressure of the autoclave containing samples.

In this thesis, BIT thin films were prepared by low temperature hydrothermal synthesis. First, BIT or TiO_2 sol solutions were spin-coated on a $Pt/Ti/SiO_2/Si$ substrate at 500 rpm for 5 sec and 3000 rpm for 30 sec, and the coated sol film was transformed into a gel film by annealing in air at 350 °C for 20 min. Second, the gel film was immersed in KOH solution within an autoclave and transformed into a BIT hydrothermal synthesis. However, the obtained BIT gel films are amorphous and thus are not attached strongly to the substrate. Meanwhile, the crystallization of BIT thin films, synthesized by hydrothermal method, was able to be achieved on a TiO_2 layer. Hence, good crystallization of BIT thin films was realized by a hydrothermal treatment at 510 – 520 °C for 4 hours in a mixture solution of $Bi(OH)_3$ 0.2 M, TiO_2

0.1 M and KOH 0.012 M. The BIT thin film was observed to be ferroelectric and the polarization difference at zero-electric field was 1.16 $\mu C/cm^2$, although it was leaky.

As a giant ferroelectric polarization material, $BiFeO_3$ (BFO) was expected to exhibit a better ferroelectric property as a form of thin films synthesized by a hydrothermal method. The result indicated that quite good crystallization of BFO powder was successfully obtained by preparing at 200 °C for 12 h in solution of $Bi(NO_3)_3.5H_2O$ 0.1 M, $Fe(NO_3)_3.9H_2O$ 0.1 M with KOH 1 M. Meanwhile, BFO thin films prepared by hydrothermal synthesis on $Pt/Ti/SiO_2/Si$ substrates need to be deposited on a BFO nucleation with good crystallization. Therefore, the preparation of the BFO layer was carried out by a chemical solution depositon (CSD) method using rapid thermal annealing (RTA) at 430 °C in nitrogen. However, BFO thin films, synthesized by hysdrothermal method at high KOH concentration of 5 M and with a long processing time, just exhibit quite good crystallization in comparison with that of the previous BFO. High KOH concentration and a long processing time damage the substrate and strong enhance of a leakage current, so ferroelectricity of these films has not been found out yet.

From above results and discussion, $Bi_{1.1}Fe_{1-x}Co_xO_3$ (BFCO) with $x = 0 \sim 0.3$ thin films have been prepared by CSD method using RTA at high temperatures of 450 ~ 560 °C in nitrogen and oxygen. These films show good ferroelectric properties. By using iterative RTA for 8 times in nitrogen, Annealing at 520 °C enhaced the crystallization of BFO rhombohedral, the application of tolerant electric field up to 2 MV/cm without dielectric breakdown, and improve a piezoelectric property. On the other hand, $Bi_{1.1}Fe_{0.8}Co_{0.2}O_3$ thin films annealed at 520 °C in oxygen by iterative RTA for 8 times suppress a leakage current density so that *P-E* hysteresis loops at RT show very good saturation.

Acknowledgements

This dissertation represents the research work and result that I have studied almost time in the past Okuyama laboratory and the last period in the present Shiraishi laboratory. I would like to express my sincere gratitude to all people who helped and encouraged me during this doctor course.

Firstly, I own a great deal of gratitude to my supervisor, Prof. Masanori Okuyama, for giving me the opportunity to work in Osaka University. I also praise to his great guidance, advices, encouragement, financial support during all my study in doctor course. Once again, I would like to express my sincere gratitude to him. I am very grateful to my advisor and mentor, Ass Prof. T. Kanashima, for his detailed and constructive comments and important support throughout my research, especially for helping with the suggestion when I am facing problems with my study. This thesis would not have been completed without his continuous direction and support. I would like to express a special acknowledgement to my present supervisor, Prof. M. Shiraishi for his support and encouragement and comfort during the last period of my doctor course. I give special thanks to Prof. Le Van Hong for his comment, encouragement and support my schedule of doctor course. I would like to thank my vice-adviser Prof. H. Okamoto and Prof. M. Tonouchi for their valuable and effective advices and suggestions for preparing this thesis.

This is a chance for me to praise to Dr. Masayuki Sohgawa in Osaka University, Prof. Minoru Noda and Ass Prof. Kaoru Yamashita in Kyoto Institute of Technology, Dr. Le Van Hai in National Institute of Advanced Industrial Science and Technology (AIST), Dr. Dan Ricinschi in Tokyo Institute of Technology, Dr. Seiji Nakashima in Hyogo University for valuable suggestion, supportive wisdom and helping me in measurement. I also would like to express my sincere acknowledgment to Mr. C. Sada of Osaka University for his helps in experiment equipments. I thank Mr. Yoshitaka Nakamura of Kyoto University and Mr. Akihiro Inoue of Kyocera Corporation who helped me to get familiar with life in Japan and started work in laboratory. I thank also Dr. H. Morioka and Dr. Saito of Bruker AXS for measurement of reciprocal space mapping and my colleges, Mr. F. Gotoda and Mr. J. M. Park for their help of

M-H hysteresis measurement. I want to officially acknowledge my present and past lab members for valuable group interactions, friendship and support.

I am very grateful to Ms. Emiko Tasaka and Ms. Kanako Sawamoto and other member of the International Student Office for their help consideration and support. My special thanks go to my Japanese teacher, Ms. Aki Usunami for her kindness. My life at Japan would be much harder without their help.

I would like to thank my friends, Nguyen Thi Le Huyen, Nguyen Hoang Long, Duong Thi Hanh, Le Quoc Tuan, Nguyen Hoang Nam, Bui Huong, Tran Phuong Dung, Pham Tan Thi and many others for their help and friendship.

I give special thanks to Prof. Tadashi Itoh, Prof. Nguyen Xuan Phuc, and Prof. Nguyen Quang Liem for support my schedule of doctor course. My appreciation goes to the Vietnamese Government through the 322 Project and Japan Student Services Organization (JASSO) for grant of the scholarship during my study.

Finally, I would like to express my everlasting honor and gratitude my parent for their moral support, even they do not really understand what I am doing for my research, and financial support for my life and studies so far. It has been of immense encouragement for my life in past and future.

Osaka, August 2010
Nguyen Truong Tho

Contents

List of Figures

CHAPTER 1

Introduction

The prominent properties of ferroelectric materials such as polarization hysteresis, large dielectric constant, and remarkable piezoelectric, pyroelectric and electro-optical effects can be applied in electronic devices. Especially in the form of thin films, ferroelectrics show excellent features for electronic devices such as nonvolatile memories, capacitors, sensors, and actuators. Among these, non-volatile memories utilizing ferroelectric thin films have attracted special attention recently because of their low power dissipation and fast switching. I have prepared ferroelectric $Bi_4Ti_3O_{12}$ and $BiFeO_3$ thin films for electronic devices and characterized those properties.

1.1 BACKGROUND

Recently, ferroelectric materials have received much attention because of not only fundamental scientific interest but also their potential of technological applications utilizing their unique properties like large dielectric constant, piezoelectric, pyroelectric and electro-optic properties. One of the most important applications of ferroelectric thin films is ferroelectric random access memory (FeRAM). In fact, there are semiconductor memories like dynamic random access memory (DRAM) and static random access memory (SRAM) dominating the market. However, the disadvantage of these memories is their volatility i.e., the loss of stored data upon power off or failure. A universal memory has to show that it is non-volatile, non-destructive read and write, bit erasable, electrical re-programmable, low power consumption, durable, dense and low cost. FeRAM is a non-volatile memory using a ferroelectric thin film capacitor for storing data and satisfies the above requirements as the universal memory.

One of the most important components in FeRAM is the ferroelectric layer playing a role as a capacitor, which polarization can be reversed by the application of external electric field. Hence, FeRAM make use of this phenomena to store data i.e., the upward and downward polarizations in the ferroelectric capacitor are referred to "0" and "1" state or vice versa, as shown in Fig.1.1. The amount of remanent polarization is important for FeRAM because

memory cell size becomes very small in the highly integrated memory and total reversal charge is proportional to capacitor area. Many ferroelectric oxide materials having perovskite crystalline structure are frequently used for the capacitor. Typical ferroelectric materials are $BaTiO_3$, $PbTiO_3$ and $Pb(Zr,Ti)O_3$ (PZT). The Pb-based ferroelectrics show fantastic properties such as polarization reversal, piezoelectric and pyroelectric responses. Especially, PZT shows good ferroelectric property, but the inherent toxicity of lead is of great concern and its use in electronic devices will be regulated near future. Therefore, lead-free ferroelectric materials have been expected to be well available for various devices in recent years. Bismuth-layer-structured-ferroelectric (BLSF) materials such as $SrBi_2Ta_9O_3$ (SBT) and $Bi_4Ti_3O_{12}$ (BIT) are lead free and have considerably good ferroelectric property.

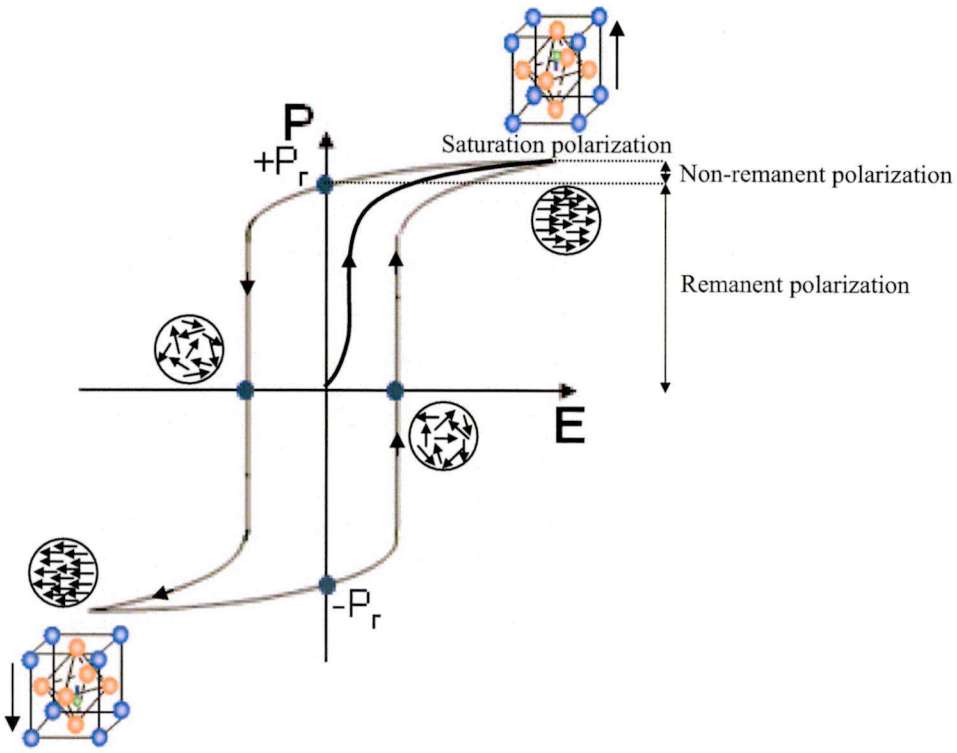

Figure 1.1 Polarization-electric-field hysteresis loop for ideal ferroelectrics.

Table 1.1 shows ferroelectric properties of typical ferroelectric thin films.

Table 1.1: Summary of typical properties in typical ferroelectric materials

Materials	T_C(K)	Experimental Polarization	Crystalline temperature (in CSD)	Preferences
$BaTiO_3$	~ 400K	~ 70 μC/cm^2	~ 1373K	[1-3]
$PbTiO_3$	~ 760K	~ 97 μC/cm^2	~ 923K	[4, 5]
$Pb(Zr,Ti)O_3$	~ 673K	~ 90 μC/cm^2	~ 973K	[6, 7]
$SrBi_2Ta_9O_3$ (SBT)	~ 573K	~ 10 μC/cm^2	~ 1023K	[8-11]
$Bi_4Ti_3O_{12}$ (BIT)	~ 950K	~ 50 μC/cm^2	~ 923K	[12]
$BiFeO_3$ (BFO)	~ 1123K	~ 90 μC/cm^2	~ 823 K	[13-15]

So far, PZT and SBT could have been applied as ferroelectric capacitors in FeRAM because they have enough remanent polarization, low coercive fields, promising fatigue, retention and aging characteristics which are necessary conditions for preparation of the ferroelectric capacitor in FeRAM [16, 17]. Although the SBT thin film has excellent fatigue-free properties [17], SBT has a higher crystallization temperature compared to PZT and the remanent polarization is small for the highly integrated memory [18]. On the other hand, BIT and BFO thin films show larger polarization and lower crystallization temperature compared to SBT thin films prepared by CSD. Thus, BFO and BIT are expected for lead-free ferroelectrics having excellent ferroelectric properties and low processing temperature, and have been studied in this thesis.

1.2 PROPERTIES OF $Bi_4Ti_3O_{12}$ AND $BiFeO_3$

1.2.1 Properties of $Bi_4Ti_3O_{12}$

$Bi_4Ti_3O_{12}$ (BIT) has been considered to be one of the promising candidates for suppression of processing temperature and enhancement of ferroelectric properties because of its low crystalline temperature and large polarization as mentioned above. Similar to SBT,

BIT has triple pseudo-perovskite layers sandwiched by bismuth oxide layers whose lattice constants are $a = 0.5448$, $b = 0.5410$, and $c = 3.284$ nm, as shown in Fig.1.2.

Synthesized BIT thin films show coercive fields (E_c) of 3.5 kV/cm and 50 kV/cm, and remanent polarization (P_r) values of 4 μC/cm^2 and 50 μC/cm^2, in the *c*-axis and *a*-*b* plane directions, respectively [19]. The low-coercive field and adequate remanent polarization along the *c*-axis makes BIT an attractive gate dielectric in a ferroelectric field effect transistor. However, the preparation methods have not recovered the high processing temperature yet. From this consideration, the CSD using hydrothermal treatment is considered to be suitable for the fabrication of ferroelectric BIT-based thin films [18], because the high pressure in the hydrothermal autoclave can suppress strongly processing temperature.

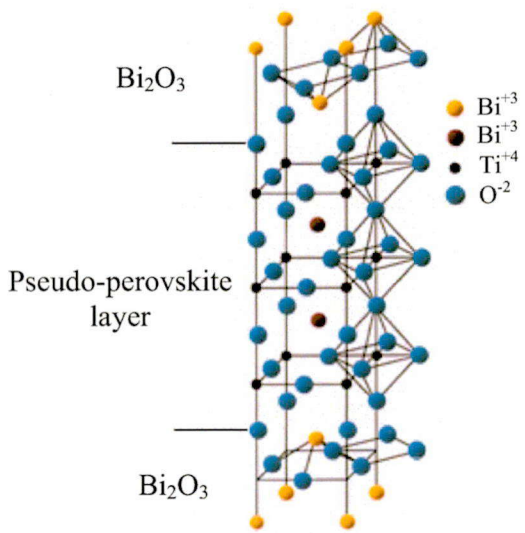

Figure 1.2 Crystal structure of $Bi_4Ti_3O_{12}$.

1.2.2 Properties of $BiFeO_3$

$BiFeO_3$ (BFO) is a promising candidate for high-density ferroelectric random-access memory (FeRAM) because of its large polarization value and low crystallization temperature [13-15]. The lattice structure of a $BiFeO_3$ single crystal is a rhombohedrally distorted perovskite, which belongs to the space group *R3c* (or *R3m*) with unit cell parameters a = 3.96 Å and $\alpha = 89.5^\circ$ (or a = 5.57 Å and $\alpha = 59.4^\circ$). Figure 1.3 shows the crystal structure of BFO with *R3c*. BFO belongs to the multiferroic family because it exhibits ferroelectric and

antiferromagnetic properties simultaneously [20]. It has ferroelectric properties with a high Curie temperature (T_C) of approximately 850 °C and antiferromagnetic behavior with a Neel temperature (T_N) of approximately 370 °C. The high Curie temperature makes it a suitable candidate for use as a ferroelectric at room temperature.

One of the major problems of BFO thin films is their low electrical resistivity, which affects the measurement of ferroelectric property at room temperature (RT). The relatively high conductivity of BFO thin film is known to be attributed to the morphology of the thin films, the valence fluctuations of Fe ions (Fe^{3+} to Fe^{2+}) and creation of oxygen vacancies for charge compensation [21, 22]. In order to overcome this problem, many kinds of doped BFO thin films have been prepared by several preparation methods. Thus, from this consideration, BIT and BFO thin films have been prepared and characterized in this thesis.

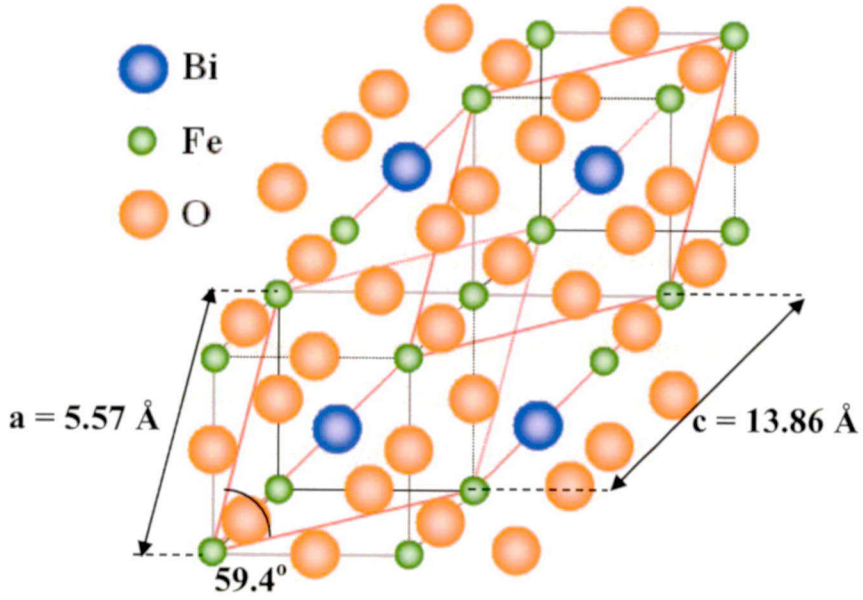

Figure 1.3 Crystal structure of $BiFeO_3$ with *R3c* space group.

1.3 PREPARATION METHODS OF FERROELECTRIC THIN FILMS

There are many deposition methods for ferroelectric thin films such as sputter deposition, metal organic chemical vapor deposition (MOCVD), pulsed laser deposition (PLD) and chemical solution deposition (CSD). These depositions can be divided mainly to two techniques, physical deposition and chemical deposition techniques.

1.3.1 Physical Deposition Technique

This technique uses ion impact or thermodynamic mean to produce vapor of source material for a thin film of solid. Then, physical deposition systems require a low-pressure vapor environment to function properly and most of the physical deposition methods can be classified as "physical vapor deposition" (PVD).

PVD covers a broad class of vacuum coating processes in which material is physically removed from a source by evaporation or sputtering. The vapor and particles are transported through a vacuum or low-pressure space and condensed as a film on the surfaces of appropriately placed substrates. Chemical compounds are deposited by either using a similar source material, and/or by introducing a reactive gas (nitrogen, oxygen, or simple hydrocarbons) containing the desired reactants, which react with vapor species in the space and condensed species on the substrate.

The material to be deposited is placed at high temperature and/or energetic particles impinge so that various particles of material such as atoms, ions and molecules tend to escape its surface. Therefore, volatile elements are deliberately added to a stoichiometric target. Here are typical examples of physical deposition including:

- **Electron beam evaporator** fires a high-energy beam from an electron gun to boil a small spot of material; since the heating is not uniform, lower vapor pressure materials can be evaporated easily and composition of the film might be changed from the target.

- **Sputtering** uses a plasma (usually a noble gas, such as argon) to knock target material at a time. The target can be kept at a relatively low temperature, since the process is not simple evaporation, making this one of the most flexible deposition techniques. It is especially useful for compounds or mixtures, where different components tend to evaporate at different rates. The sputtered ions can fly from the target in straight lines and impact energetically on the substrates or vacuum chamber causing re-sputtering which is re-emission of the deposited material during the deposition process by ion or atom bombardment. The sputtering gas is often an inert gas such as argon, but reactive gases can be also used to sputter compounds. This technique is a fast technique and also provides a good thickness control.

- **Pulsed laser deposition** uses laser for vaporization and is called also laser ablation. Pulses of focused laser light vaporize the surface of the target material and convert it to plasma including energetic elements, electrons and ions; this plasma emits light and reaches the substrate. Energetic particles promote chemical reaction on the substrate and the substrate temperature is lowered as compared with the other PVD methods.

1.3.2 Chemical Deposition Technique

Here a fluid precursor produces a chemical reaction at a solid surface, making a solid layer. Since the fluid surrounds the solid object, deposition happens on every surface, with little regard to direction; thin films obtained by chemical deposition techniques tend to be conformal.

Chemical deposition is further categorized by the phase of the precursor:

- **Chemical vapor deposition** (CVD) generally uses a gas-phase precursor, often metalorganic, halide or hydride compounds of the elements to be deposited. In the case of metal organic vapor deposition (**MOCVD**), an organometallic gas is used and various ferroelectric films have been prepared. This is often used at low pressures of precursor gas.
- **Chemical solution deposition** (CSD) uses liquid precursor, usually organometallic solution dissolved in organic solvent. This is a relatively inexpensive and simple thin film process that tends to produce stoichiometrically accurate crystalline-phases. The fabrication of thin films by this approach involves three basic steps: (i) Synthesis of the precursor solution; (ii) Deposition by spin-coating or dip-coating, where drying processes usually begin depending on the solvent; (iii) The as-deposited thin film is then heated to cause densification and crystallization [18].

  For most solution deposition approaches, the first three steps are similar despite differences in the characteristics of the precursor solution, and for electronic devices, spin-coating has been used almost exclusively. The solution route used will also determine the extent of intermixing of the metal species, formation of a network and formation of individual inorganic phases, the carbon content of the films after pyrolysis of organic species, the weight loss associated with oxide formation and the densification and crystallization behavior of the film follow.

Some of PVD and CVD deposition methods are generally high cost and limited in mass-production. Moreover, the deposition temperatures of these methods are typically above 400 °C. On the other hand, on annealing for 30 min at 450 °C aluminum migrates into the Si_3N_4 film [23]. When the stacked-type capacitor is formed, it is thought that processing temperature is required to be as low as possible (lower than 400 °C). Therefore, decrease of annealing temperature by selecting material and preparation method of ferroelectric thin films is one of crucial conditions.

- **Hydrothermal Synthesis**

Hydrothermal synthesis is known as a preparation method which can suppress crystallization temperature of material under a high pressure in the autoclave filled with high alkali ambient [24-26]. The synthesis is a technique of crystallization of the film at high-pressure in aqueous solutions, and can be carried out under mild conditions (T<350 °C, P<100 MPa). Hydrothermal synthesis is a process that utilizes single or heterogeneous phase reactions in aqueous media at elevated temperature (T>25 °C) and pressure (P>100 KPa) to crystallize ceramic materials directly from solution [27].

Low deposition temperature is sincerely expected for deposition of the stacked-type capacitor of FeRAMs because the high process temperature damages Al wires and device components fabricated before. Thus, hydrothermal preparation of BIT thin films at low temperature is the object of the study in this thesis.

1.3.3 Thermal Annealing

Thermal annealing is important process to promote chemical reaction of precursors such as metalorganic sources and metal oxides, crystallization of non-reacted species and amorphous materials and oxidization of oxygen-deficient materials. The annealing is used in many preparation processes of thin films and can be carried out by using some instruments. The typical ones are furnace annealing, laser annealing and rapid thermal annealing which are explained as follows,

- **Furnace annealing** is heat treatment in furnace for comparatively long time. This is used conveniently and frequently in CSD, but in some cases, high temperature for

long time tends to degrade the substrate including electronic circuit on silicon, and resolves the film itself by evaporation of volatile elements.

- **Laser annealing** is carried out by heating of the films induced by strong pulse of laser emission and so is very quick method. Chemical reaction is promoted for very short time at very high temperature and so the crystalline property of the irradiated film might not be sufficient. Moreover, irradiated area is limited by small area around the focused point and uniform annealing is very difficult even if the laser beam is scanned on the film.
- **Rapid thermal annealing** is carried out for comparatively short time mainly by the lamp irradiation or in a furnace. Generally process temperature is a little higher than that of the furnace annealing, process time is acceptable for chemical reaction and the film can be annealed uniformly. Recent results confirm the benefit of using high heating rates [28], and also suggest that increasing the ramp rate is useful to reduce the amount of profile broadening caused by enhanced diffusion. Conventional rapid thermal annealing (RTA) is used for one time after several processes of spin-coating and baking [29]. By repeating the RTA coating-by-coating, strains and damage inside thin films could be suppressed and better films can be obtained at low temperatures in comparison with one-time annealing. Iterative RTA was thus carried out to prepare ferroelectric thin films in this thesis.

1.4 PURPOSE OF THIS THESIS

As mentioned in the previous sections, various points are discussed for ferroelectric thin films. One of the most important applications of ferroelectric thin films is as the capacitor in FeRAM. Therefore, the suppression of the processing temperature is very important to avoid thermal damage to devices prepared before to suppress a leakage current and to improve ferroelectric property such as large remanent polarization and small coercive field.

BIT and BFO thin films are lead-free material and safe for human being. Moreover, they have large remanent polarization and very effective for future FeRAM application. On the other hand, hydrothermal synthesis is useful to prepare ferroelectric thin film as they can be grown around 200 °C due to high pressure in the autoclave [30-33].

Therefore, in my thesis work, BIT and BFO thin films have been prepared to realize their excellent ferroelectric properties. So, firstly, BIT thin films have been prepared by hydrothermal method and their structural and electronic properties have been characterized (chapter 2). Moreover, hydrothermal synthesis of BFO has been tried and the crystalline powder are obtained (chapter 3).

Secondly, BFO has a giant polarization, but leakage current is not so small. To utilize BFO thin films for FeRAM, leakage current must be suppressed. The origin of leakage current in BFO thin films is considered to be the thermal damage inside the thin films and the creation of oxygen vacancies during the preparation. In order to improve the damage inside the thin films, iterative RTA preparation was carried out in CSD preparation of BFO thin films. Especially, iterative RTA is useful to suppress strains and damages inside thin films induced at high temperature during annealing.

Here, oxygen vacancies are known to be created in BFO thin films [21, 22]. Thus the substitution of little amount of iron ions to other ions may suppress leakage current. On the other hand, $BiCoO_3$ is a perovskite material having tetragonal anisotropy (c/a = 1.267) [34]. It is expected that $BiFe_{1-x}Co_xO_3$ thin films could enhance ferroelectric and insulation properties. In order to improve the iterative RTA, both nitrogen and oxygen ambient is tried to be used to suppress oxygen vacancies in this thesis.

Co-substituted BFO ($Bi_{1.1}Fe_{1-x}Co_xO_3$; BFCO) has been characterized to improve the insulation. Thin films have been prepared by chemical solution deposition (CSD) method using iterative rapid thermal annealing (RTA) in nitrogen (chapter 4) and in oxygen (chapter 5).

Finally, I summarized this thesis in chapter 6.

The outline of this thesis is illustrated in Fig. 1.4.

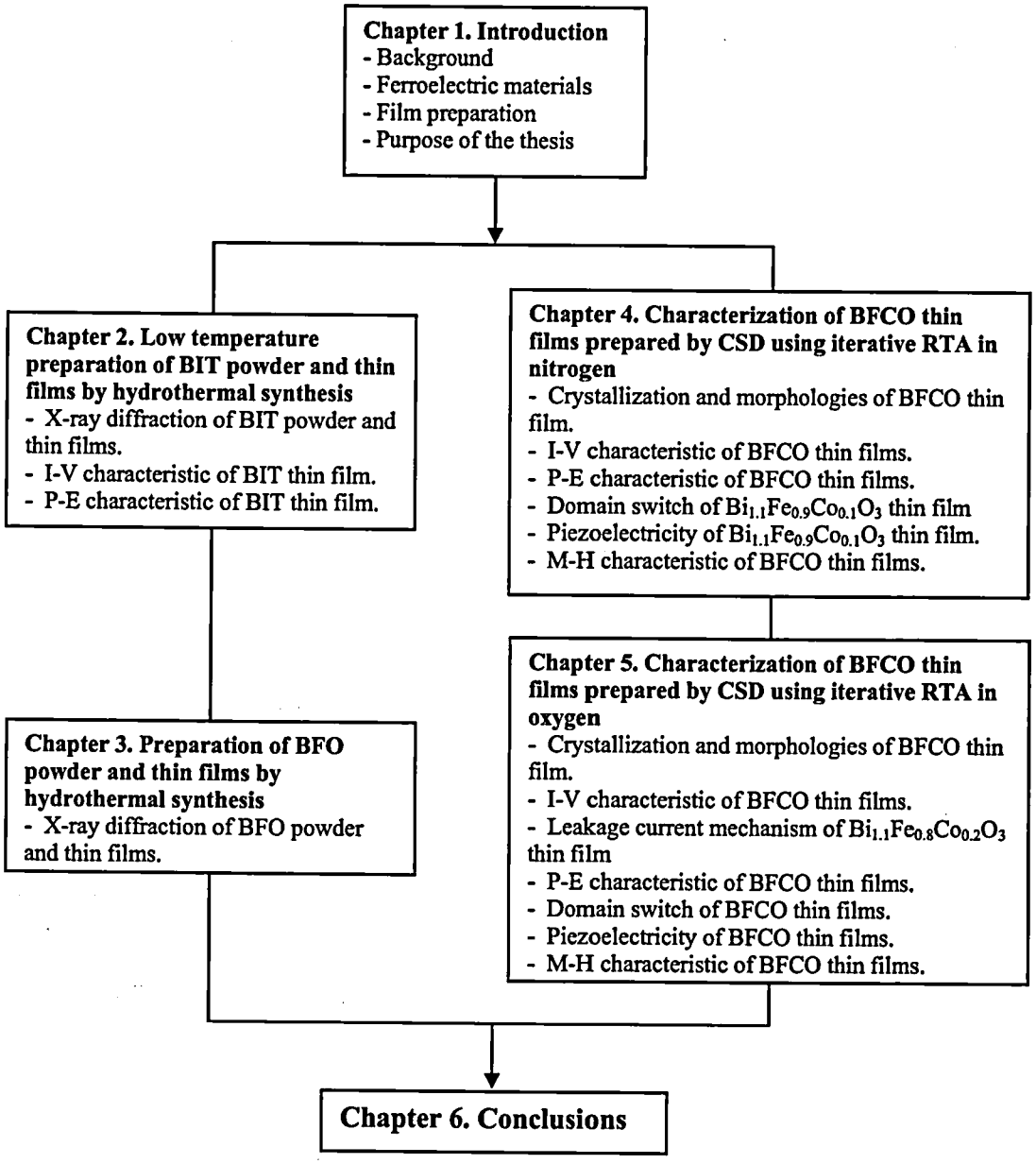

Figure 1.4 Outline of this thesis.

REFERENCES

[1] K. Sakayori, Y. Matsui, H. Abe, E. Nakamura, M. Kenmoku, T. Hara, D. Ishikawa, A. Kokubu, K. Hirota, and T. Ikeda: Jpn. J. Appl. Phys. **34** (1995) 5443.

[2] K. J. Choi, M. Biegalski, Y. L. Li, A. Sharan, J. Chubert, R. Uecker, P. Reiche, Y. B. Chen, X. Q. Pan, V. Gopalan, L. Q. Chen, D. G. Schlom, and C. B. Eom: Science **306** (2004) 1005.

[3] I. Maclaren and C. B. Ponton: J. Eur. Ceram. Soc. **20** (2000) 1267.

[4] T. Morita and Y. Cho: Appl. Phys. Lett. **83** (2003) 2408.

[5] M. C. Hsu., Y. M. Sun, I. C. Leu, and M. H. Hon: Appl. Surf. Scien. **253** (2007) 7639.

[6] S. Yokohama, Y. Honda, H. Morioka, T. Oikawa, H. Funakubo, T. Iijima, H. Matsuda, and K. Saito: Appl. Phys. Lett. **83** (2003) 2408.

[7] J. Liu, S. Zhang, C. Yang, and J. Zhou: J. Crystal. Growth. **264** (2004) 302.

[8] K. Y. Yun, D. Ricinschi, T. Kanashima, M. Noda and M. Okuyama: Jpn. J. Appl. Phys. **43** (2004) L647.

[9] Y. Shimakawa, Y. Kubo, Y. Nakagawa, T. Kamiyama, H. Asano, and F. Izumi: Appl. Phys. Lett. **74** (1999) 1904.

[10] Y. Ito, M. Ushikubo, S. Yokoyama, H. Matsunaga, T. Atsuki, T. Yonezawa, and K. Ogi: Jpn. J. Appl. Phys. **35** (1996) 4925.

[11] R. Dat, J. K. Lee, O.Auciello, and A. I. Kingo: Appl. Phys. Lett. **68** (1995) 572.

[12] S. E. Cummins and L. E. Cross: Appl. Phys. Lett. **10** (1967) 14.

[13] Y. N. Venevtsev, G. Zhadanov, and S. Solov'ev: Sov. Phys. Crystallogr. **4** (1960) 538.

[14] G. Smolenskii, V. Isupov, A. Agranovskaya, and N. Kranik: Sov. Phys. Solid. State. **2** (1961) 2651.

[15] S. K. Singh, R. Ueno, H. Funakubo, H. Uchida, S. Koda, and H. Ishiwara: Jpn. J. Appl. Phys. **44** (2005) 8525.

[16] J. F. Scott and C. A. Paz de Araujo: Science. **246** (1989) 1400.

[17] C. A. Paz de Araujo, J. D. Cuchiaro, L. D. McMillan, M. C. Scott, and J. F. Scott: Nature. **374** (1995) 627.

[18] M. Okuyama and Y. Ishibashi: *Ferroelectric Thin Films: Basis Properties and Device Physics for Memory Applications* (Springer, Berlin, 2005), Part 1.

[19] S. E. Cummins and L. E. Cross: J.Appl. Phys. **39** (1968) 2268.

[20] G. A. Smolenskii and I. Chupis: Sov. Phys. Ups. **25** (1982) 475.

[21] M. Takahashi, H. Sugiyama, T. Nakaiso, K. Kodama, M. Noda, and M. Okuyama: Jpn. J. Appl. Phys. **40** (2001) 2923.

[22] U. Ueda, H. Tabata, and T. Kawai, Appl. Phys. Lett. **75** (1999) 555.

[23] H. Ogata, K. Kanayama, M. Ohtani, K. Fujiwara, H. Abe, and H. Nakayama: Thin Solid Films. **48** (1978) 333.

[24] H. Xu, T. Kiyomoto, Y. Morikawa, M. Okuyama, and C. Lin: Jpn. J. Appl. Phys. **7** (1998) L809.

[25] W. Zhu, S. A. Akbar, R. Asiaie, and P. K. Dutta: J. Elec. Ceramics. **2** (1998) 21.

[26] T. Morita and Y. Cho: J. Korean. Phys. Soc. **46** (2005) 10.

[27] W. L. Suchanek and E. Riman: Advances in Science and Technology **45** (2006) 184.

[28] R. Gunavan, M. Y. L. Jung, E. G. Seebauer, and R. D. Braatz: J. Process. Control. **14** (2004) 423.

[29] G. Mannino, P. A. Stolk, N. E. B. Cowern, W. B. de Boer, A. G. Dirks, F. Roozeboom, J. G. M. van Berkum, and P. H. Woerlee: Appl. Phys. Lett. **78** (2001) 889.

[30] T. Morita, Y. Wagatsuma, Y. Cho, H. Morioka, F. Funakubo and N. Setter: Appl. Phys. Lett. **84** (2004) 6535.

[31] T. Morita and Y. Cho: Appl. Phys. Lett. **85** (2004) 2331.

[32] T. Kaoyama, Y. Sakioka, M. Noda, M. Okuyama and K. Saito: Jpn. J. Appl. Phys. **44** (2005) 6873.

[33] T. Naoyama, A. Inoue, K. Takei, M. Noda, and M. Okuyama: Jpn. J. Appl. Phys. **45** (2006) 7283.

[34] A. A. Belik, S. Iikubo, K. Kodama, N. Igawa, S. Shamoto, S. Niitaka, M. Azuma, Y. Shimakawa, M. Takano, F. Izumi, and E. Takayama-Muromachi: Chem. Mater. **18** (2006) 798.

CHAPTER 2

Low Temperature Preparation of $Bi_4Ti_3O_{12}$ Ferroelectric Powder and Thin Films by Hydrothermal Synthesis

2.1 INTRODUCTION

In recent years, nonvolatile ferroelectric random access memory (FeRAM) with medium integration has been developed for practical uses such as Integrated Circuit cards (IC-cards) and Radio Frequency tags (RF-tags). In the conventional planar-type fabrication process, a ferroelectric thin film is deposited in a previous process to the Al wiring and requires high deposition temperature for crystallization in the thin film. This becomes a serious issue in the stacked-type capacitor of FeRAMs, because the high process temperature for the ferroelectric film thermally damages device components fabricated beneath the film [1-3]. If the deposition temperature is lower than 400 °C described in chapter 1, the ferroelectric thin films can be deposited on the large scale integration (LSI) structure in an end-process without damage to either the Al wire or the low-k layer, and mutual diffusion between the layers can be avoided. Also, the contamination of ferroelectric film preparation does not affect the ultra-clean LSI process.

Not only the deposition method, it is also important to select the material having a low crystallization temperature. In the case of Pb(Zr, Ti)O_3 (PZT) thin film, typical deposition temperature is about 500-600 °C, but lead is consisted in this material. $SrBi_2Ta_2O_9$ (SBT) is a lead free ferroelectric material, but crystalline temperature is high (about 700-750 °C [4]). On the other hand, crystalline temperatures of $BaTiO_3$ (BTO) and $Bi_4Ti_3O_{12}$ (BIT) are 500 °C or less [5, 6], but Curie temperature of BTO (120 °C) is much lower than that of BIT (675 °C).

Ferroelectric $Bi_4Ti_3O_{12}$ (BIT) thin films deposited on Pt electrodes are expected to be used in FeRAM [7]. Pb(Zr,TiO)$_3$ (PZT) has been considered to be one of the promising candidates for this application, but the PZT thin film deposited on Pt shows a serious

degradation of ferroelectric properties, i.e. fatigue, after cumulative polarization switch. Since polarization must be reversed to read or write data in a memory cell, the fatigue is a critical obstacle for practical use. BIT contains unstable Bi ions, which are easily evaporated during the heating process. This volatility of Bi ions affects the ferroelectric and fatigue characteristics of thin films, and improvement of the electrical properties of BIT thin films by rare earth ion modification has been reported [8]. Especially, in lanthanum substituted BIT fatigue free behavior is observed [9]. From this viewpoint, BIT is a hopeful material [10-12]. Moreover, BIT has a Bi-layer structure with a pseudo-perovskite phase whose lattice constants are a = 0.5448, b = 0.5410, and c = 3.284 nm. It shows coercive fields (E_c) of 3.5 kV/cm and 50 kV/cm, and remanent polarization (P_r) values of 4 μC/cm^2 and 50 μC/cm^2, in the c-axis and a-b plane directions, respectively [13]. The low-coercive field along the c-axis makes BIT an attractive gate dielectric in a ferroelectric field effect transistor. However, there is a problem such as high processing temperature.

The low-temperature deposition of BIT thin films has been extensively investigated using several techniques such as metal-organic chemical vapor deposition (MOCVD) [14, 15], and atomic layer deposition (ALD) [16]. So far, there have also been reports on preparing (Pb,Ba)TiO_3 (PBT) thin films by hydrothermal treatment using the precipitation reaction in the alkaline solution at a low temperature of 200 °C [1, 3]. A similar method of hydrothermal synthesis has been investigated in this chapter as a low-temperature preparation method for BIT. It can be expected that the hydrothermal method will also be effective for below 400 °C-thin film preparation of BIT.

2.2 EXPERIMENTAL

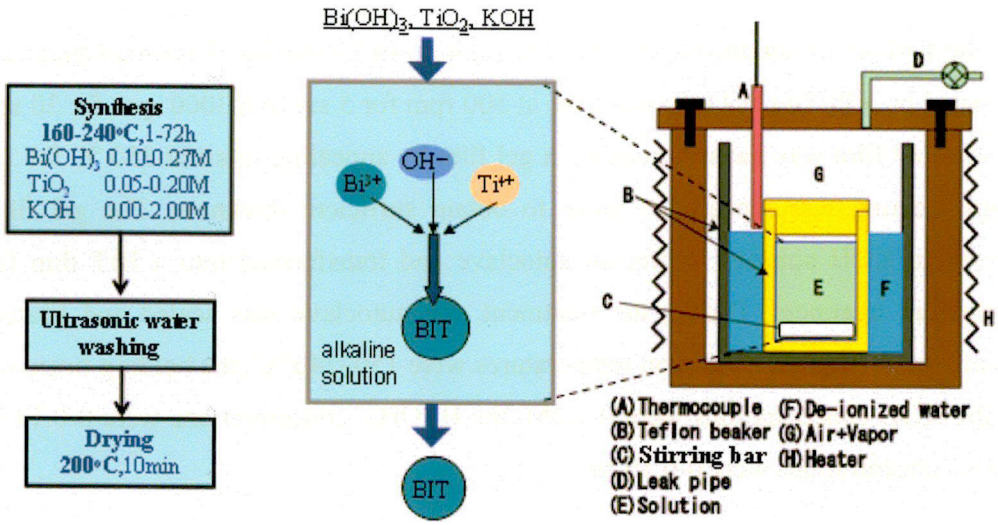

Figure 2.1 Flow chart for preparation of BIT powder by hydrothermal synthesis in solution.

First, BIT powder preparation by hydrothermal synthesis has been examined before the preparation of BIT thin films, as shown in Fig. 2.1. In a typical synthesis for BIT, $Bi(OH)_3$, TiO_2 and KOH were added to 15 ml deionized water. The mixture was then sealed in a teflon-lined stainless steel autoclave with magnetic stirring and kept at 160-240 °C for 0-45 h. After hydrothermal synthesis, the autoclave was cooled down to less than 100 °C and opened. The product was washed with deionized water several times, and dried at 120 °C [17]. The conditions of hydrothermal synthesis for BIT powders are listed in Table I. Crystalline state was studied using an X-Ray Diffractometer (XRD; Rigaku, RINT2000) with CuKα radiation. The morphologies of the BIT powders were observed by Scanning Electron Microscopy (SEM; JEOL, JSM-6340F). The composition of the products was estimated by X-Ray Fluorescence analysis (XRF; PHILIPS, PW2400).

Next, BIT thin films were prepared under two hydrothermal conditions and the crystallinity and ferroelectric properties were studied. The hydrothermal synthesis technique requires a long growth time (several hours to tens of hours) and high concentrated KOH (a few M). So, it is important to apply this synthesis technique to LSI process in which deposition speed is increased and concentration of KOH is decreased. Because the use of KOH induces the deterioration of the device, and the preparation time becomes significantly

longer to obtain appropriate film thickness in the precipitation reaction. Thus, a TiO_2 thin film or amorphous BIT film is used as a precursor or a promoter to obtain good crystalline BIT [1, 2].

In the first set of conditions, the BIT sol solution (0.33 mol/kg, Toshima Chemical) was spin-coated on a $Pt/TiO_x/SiO_2/Si$ substrate at 500 rpm for 5 sec and 3000 rpm for 30 sec, and the coated sol film was transformed into a gel film by annealing in air at 350 °C for 20 min. The spin-coating was repeated 5 times to obtain sufficient thickness. The gel film was immersed in KOH solution within an autoclave and transformed into a BIT thin film by hydrothermal treatment. During the treatment, the autoclave was sealed and heated at a constant temperature. The solution temperatures were 150–240 °C, the holding times were 3-24 h, the KOH concentrations were 0-0.2M, the $Bi(OH)_3$ concentrations were 0-0.14 M and the TiO_2 concentrations were 0-0.10 M.

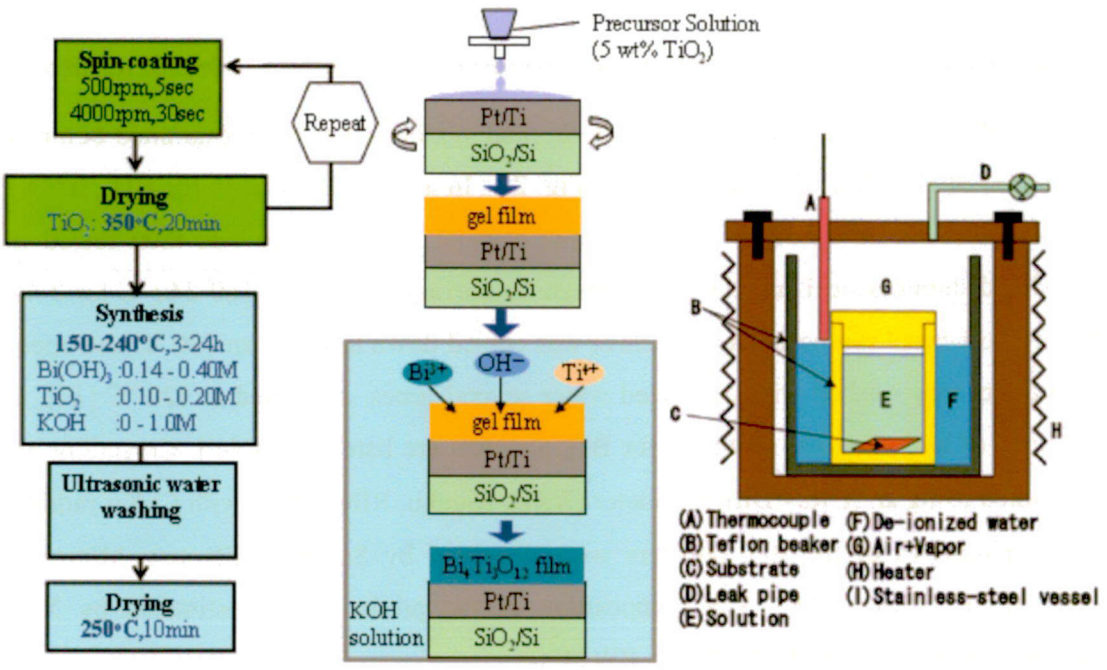

Figure 2.2 Flow chart for preparation of BIT thin films by hydrothermal synthesis using the TiO_2 gel film as a nucleation.

Next, as you can see in Fig. 2.2, the sol solution of 5 wt% TiO_2 was spin-coated on $Pt/TiO_x/SiO_2/Si$ substrates under the same rotation and pre-baking temperature conditions, as the ones in the first set. The hydrothermal synthesis of the BIT thin films was carried out in

0.1-0.25 M $Bi(OH)_3$, 0.01-0.02 M KOH and 0.1 M TiO_2 for 2-6 h at temperatures of 180, 190, 200, 210, 220 and 230 °C.

Pt top electrodes (ϕ190 μm) were deposited on the treated film by rf sputtering at room temperature for electrical measurement. The polarization-electric field (*P-E*) hysteresis loops were evaluated using a ferroelectric test system with virtual ground circuit (Toyo Corp., FCE-1) at 1.2 kHz.

Table 2.1 Hydrothermal condition for BIT powders.

Solution temperature (°C)	160 - 240
Holding time (h)	0 - 45
$Bi(OH)_3$ concentration (M)	0.10 - 0.27
TiO_2 concentration (M)	0.05 - 0.20
KOH concentration (M)	0 - 2.0
Solution volume (ml)	15

2.3 RESULT AND DISCUSSION OF BIT POWDER AND THIN FILMS PREPARED BY HYDROTHERMAL METHOD

2.3.1 X-ray Diffraction Analysis of BIT Powders and Thin Films

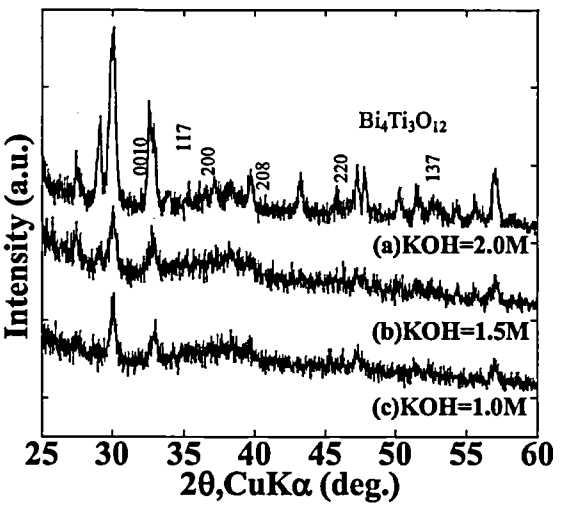

Figure 2.3 XRD patterns of BIT powders prepared by hydrothermal synthesis in solution with various KOH concentrations (a) 2.0M, (b) 1.5M and (c) 1.0M.

Figure 2.3 shows the XRD patterns of BIT powders prepared by hydrothermal synthesis under conditions of 240 °C, 24 h, $Bi(OH)_3$ 0.27 M, TiO_2 0.20 M and various KOH concentrations. It was found that the crystallization of BIT powders is greatly affected by KOH concentration because the XRD intensity increases with increasing the KOH concentration up to 2.0 M. The elemental ratio Bi/Ti of BIT powders prepared in KOH concentration 1.0, 1.5 and 2.0 M were 1.80, 1.77 and 1.56, respectively. The Bi/Ti ratio becomes close to the ratio of pure BIT (Bi/Ti = 4/3) with increasing the KOH concentration. Treatment temperatures are from 160 to 240 °C, and the optimal one is decreased with increasing the treatment time.

Figure 2.4 shows the XRD patterns of BIT powders prepared by hydrothermal synthesis for various holding times. Temperature and concentration are 240 °C, $Bi(OH)_3$ 0.27 M, TiO_2 0.20 M and KOH 1.5 M for 24 h and 45 h. Utilizing more time in the synthesis process allows for better BIT crystalline state because the XRD intensity of (a) is larger than that of (b).

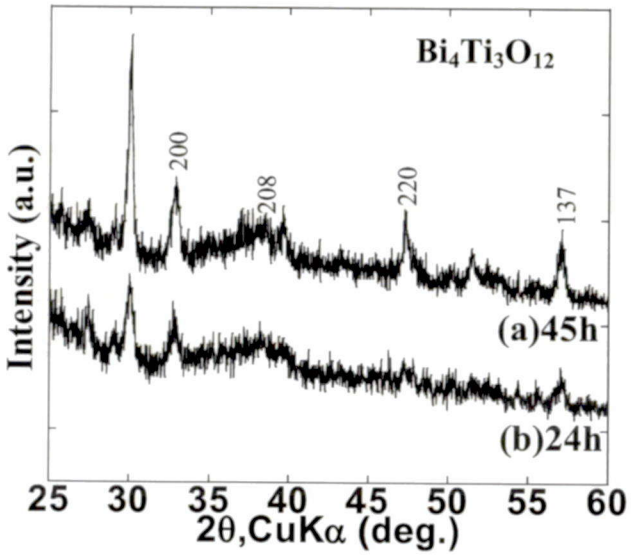

Figure 2.4 XRD patterns of BIT powders prepared by hydrothermal synthesis for (a) 45 h and (b) 24 h.

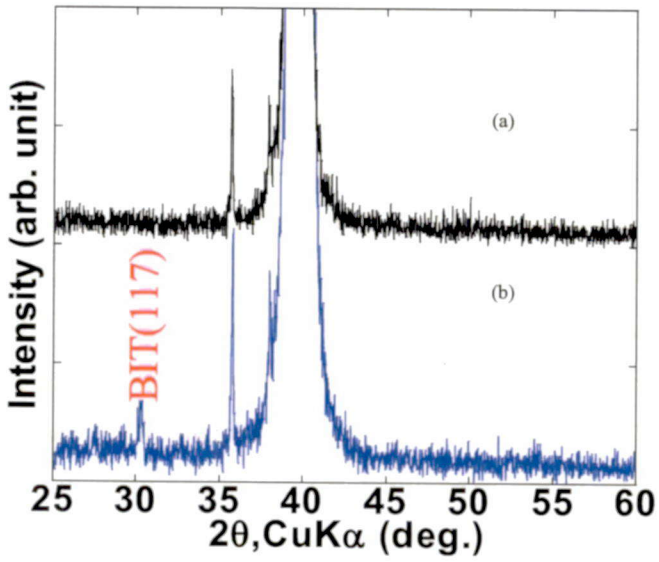

Figure 2.5 XRD patterns of (a) the BIT gel and (b) the BIT thin film prepared with post hydrothermal treatment in a mixture solution of $Bi(OH)_3$ 0.14 M, TiO_2 0.1 M and KOH 0.01 M at 150 °C for 3 h.

Figure 2.5 shows XRD patterns of the BIT gel film and the BIT thin film obtained from hydrothermal treatment in a mixture solution of $Bi(OH)_3$ 0.14 M, TiO_2 0.01 M and KOH 0.01 M at 150 °C for 3 h. In this study, the dependence of the crystallization on treatment time was examined. When the treatment time increases, the BIT (117) peak intensity increases. However, when the time is longer than 3 h, the intensity is decreased and the other BIT peaks appear. Therefore, 3 h is the best condition for the crystallization of BIT thin films.

The difficulty of preparing BIT thin films having high peak XRD intensity is related to the removal of BIT gel films from the $Pt/TiO_x/SiO_2/Si$ substrate by the alkaline solution. After the pre-bake process to form the precursor film, most of the organic materials such as solvent were removed by vaporization, but an annealing did not carried out. Thus, the obtained BIT gel films for the precursor including a small amount of organic residuals are amorphous (Fig. 2.5 (a)), which means they are not attached strongly to the substrate and are not so stable, chemically. Thus, it is thought that gel film is removed at eary stage. In addition, during the hydrothermal treatment, the pressure increases with increasing the processing temperature and reactivity of KOH becomes to be high. The removal of the BIT gel films may be prevented by long prebaking or high temperature pre-baking. However, such a process, especially the high temperature baking, reduces the merit of hydrothermal annealing.

In order to obtain the crystalized BIT thin films having high BIT peak in XRD, the hydrothermal synthesis was carried out by replacing the BIT sol solution with TiO_2 sol solution. Because, it is reported that $BaTiO_3$ thin films with a perovskite structure have been prepared by the hydrohermal treatment of TiO_2 gel films at temperatures below 210 °C [2]. Figure 2.6 shows the XRD patterns of TiO_2 gel solution and BIT thin films obtained by hydrothermal treatment under various conditions. After the spin-coating process, the TiO_2 gel film was crystallized as shown in Fig. 2.6(a), so the TiO_2 layer was attached tightly to the surface of the substrate. In this experiment, the processing temperature of the hydrothermal synthesis played a key role on the crystallization of the BIT thin films. When the temperature was lower than 210 °C, no BIT peak was found. On the other hand, when the temperature was higher than 220 °C, BIT thin films were removed from the substrate. Therefore, hydrothermal treatments were carried out for various holding time at the fixed temperature of 220 °C. After hydrothermal treatment for 3 h, the TiO_2 anatase (101) peak is found as shown in Fig. 2.6(b). BIT or pyroclore structures appeared in the films treated for 3.5 h and then BIT thin films

were crystallized as shown in Fig. 2.6(d), (e) and (g). If the holding time is longer than 5 h, no BIT peak could be observed in Fig. 2.6(f). The lattice parameters of the TiO_2 anatase are a = 0.378 nm and c = 0.949 nm. The interval of oxygen ion along (101) of the TiO_2 anatase is considered to be relatively closer to the a- and b-axis lattice parameters (0.5448 and 0.5410 nm) than that to c-axis parameter of BIT (3.284 nm). The lattice mismatch between BIT and TiO_2 anatase is estimated to be approximately 5.4 %. Moreover, it is reporte that a- and b-axes-oriented BIT thin films can be obtained on the TiO_2 anataze buffer layer deposited on $Pt/Ti/SiO_2/Si$ substrate using MOCVD technique and it is considered that TiO_2 anatase enhances the possibility of crystallization of BIT thin films oriented to a- and b-axes as an intermediate layer during the treatment process [15]. In my result, TiO_2 anatase is formed at the first stage of hydrothermal synthesis, and BIT is grown after that. So, it is thought that enhancement of formation of BIT occues in hydrothermal synthesis.

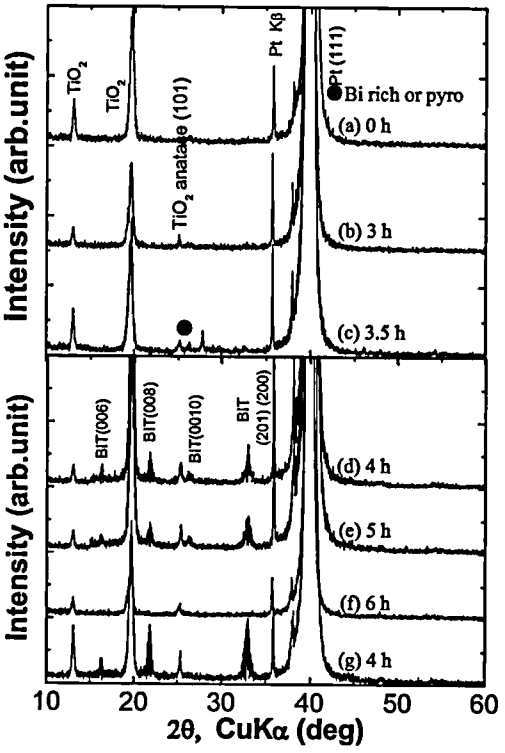

Figure 2.6 XRD patterns of the TiO_2 gel film and thin films prepared by hydrothermal treatment at 220 °C: (a) TiO_2 gel film and BIT thin films prepared by hydrothermal treatment in the mixture solution of $Bi(OH)_3$ 0.2 M, TiO_2 0.1 M and KOH 0.015 M for (b) 3 h, (c) 3.5 h, (d) 4 h, (e) 5 h and (f) 6 h; and (g) the thin film treated in the mixture solution of $Bi(OH)_3$ 0.2 M, TiO_2 0.1 M and KOH 0.012 M for 4 h to characterize the depencency of KOH concentration.

The effect of the alkali concentration and holding time on the crystallization in the treatment are also showed in Fig. 2.6 by XRD patterns of BIT thin films. There are two hydrothermal conditions corresponding to the high and the low concentrations of KOH in this figure. Alkali of KOH is used as a mineralizer. Two main mechanisms of a combination of these mechanisms have been suggested for the hydrothermal reaction of ferroelectric powders: dissolution-precipitation and in-situ transformation [18]. The rate of dissolution-precipitation is limited by OH^- concentration. Thus, under the low KOH condition, first step of hydrothermal reaction is limited. So, it can be assumed that the higher alkali concentration can facilitate the better chemical reaction. The BIT (0010) peak appears in Fig. 2.6(d), but disappears in the case of the low concentration of KOH shown in Fig. 2.6(g). On the other hand, the intensity of the BIT (200) (201) peak in the case of a low concentration of KOH is larger than that in the case of high concentration, so the BIT thin film is preferentially oriented in *a-b* plane direction in the high KOH concentration [19]. The concentration of the entrapped hydroxyl groups increases with increasing the pH of the mixture solution within the hydrothermal autoclave. As a result, ferroelectric properties may be degraded with the increase of the concentration of hydroxyl groups.

Hydrothermal processes can further be categorized into oxidation, precipitation, decomposition, and crystallization processes [18]. The oxidation requires a metal to transform to an oxide while in water. In this study, oxidation process does not occur because metal is not used. In the precipitation process, two metal salts dissolve in water and coprecipitate under hydrothermal conditions,

$$4Bi(OH)_3 + 3TiO_2 + 3KOH + H_2O \rightarrow Bi_4Ti_3O_{12} + H_2O + \text{ions}.$$

In the decomposing process a precursor (TiO_2) decomposes under hydrothermal conditions,

$$TiO_2 + H_2O + x\,KOH \rightarrow Ti(OH)_x + H_2O + \text{other spicies}.$$

In the crystallization process a hydrous precursor crystallizes to form a crystallite while in water,

$$4Bi(OH)_3 + 3TiO_2 + H_2O \rightarrow Bi_4Ti_3O_{12} + H_2O + \text{ions}.$$

Based on the treatment process, I have proposed two possible mechanisms for hydrothermal growth of BIT thin films. (1) In-situ transformation mechanism. The TiO_2 particle reacts initially with dissolved bismuth hydroxide to produce a continuous layer of BIT; the additional bismuth hydroxide must diffuse through this layer and react with TiO_2 until the TiO_2 reacts fully. (i.e. crystallization process is dominant.) (2) Dissolution-precipitation. The TiO_2 particle is dissolved to form hydroxyl titanium complexes ($Ti(OH)_n^-$) which then react with bismuth ions in the solution to precipitate BIT. (i.e. decomposing and precipitation processes are dominant.) In this study, BIT thin films were prepared using hydrothermal synthesis with the fixed concentration of TiO_2 0.1 M. According to this method, the BIT thin films are obtained with the concentration of $Bi(OH)_3$ 0.2 M and that of KOH from 0.012 to 0.015 M.

2.3.2 Morphologies of BIT Powders and Thin Films

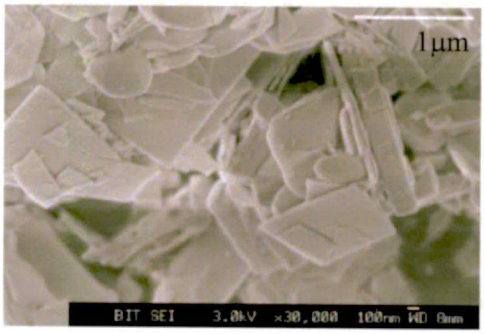

Figure 2.7 SEM photograph of the BIT powder prepared by hydrothermal treatment in the mixture solution of $Bi(OH)_3$ 0.14 M, TiO_2 0.10 M, KOH 2.0 M at 240 °C for 24 h.

The powder products are yellowish gray. According to the SEM photograph shown in Fig. 2.7, the BIT powder consists of microscopic lamellar platelets of 0.5-1.5 μm corresponding to the layer structure.

Figure 2.8 shows the cross-sectional and the surface morphology micrographs of the BIT thin film treated in the mixture solution of $Bi(OH)_3$ 0.2 M TiO_2 0.1 M and KOH 0.012 M. The grain shape is spherical and the grain size is 120 nm in a film thickness of 473 nm.

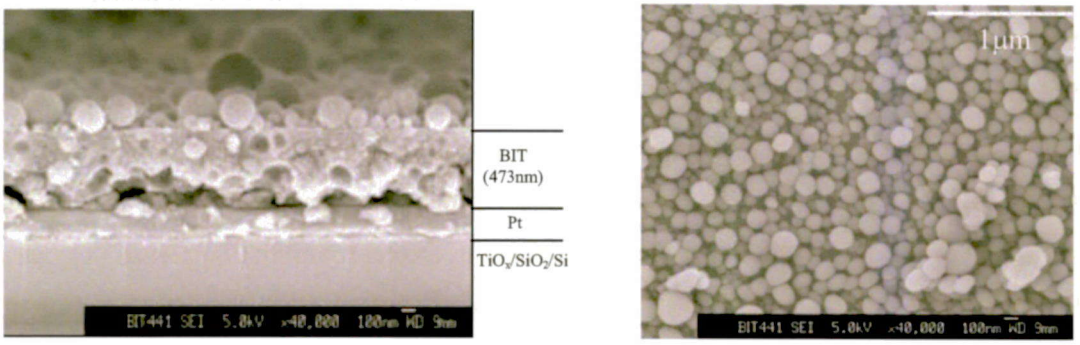

Figure 2.8 (a) SEM cross-sectional micrograph and (b) surface morphology of the BIT thin film prepared by hydrothermal treatment of TiO_2 gel film in a mixture solution of $Bi(OH)_3$ 0.2 M, TiO_2 0.1 M and KOH 0.012 M.

BIT powders have grains of lamellar platelet shape, while BIT thin films prepared by the hydrothermal synthesis have spherical grains. It can be assumed that this is caused by the difference in chemical reaction. Powder is direct synthesized from the ions in the solutions. On the other hand, a TiO_2 precursor is used in the case of the thin film, and hydroxyl ions and/or ions attached to the TiO_2 and react with each other under the same condition as in the case of hydrothermal synthesis.

2.3.3 *P-E* Hysteresis Loops of BIT Thin Film

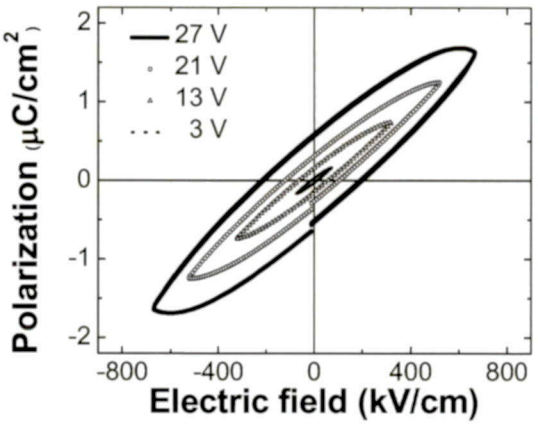

Figure 2.9 *P-E* hysteresis loops of the BIT thin film with 473 nm thickness under the condition of $Bi(OH)_3$ concentration 0.2 M, TiO_2 0.1 M and KOH 0.012 M.

Figure 2.9 shows the *P-E* hysteresis loops of the BIT thin film with 473 nm thickness as a parameter of applied electric field. The hysteresis loops were measured at room temperature of about 20 °C with a triangular wave (27 V, 1.2 kHz). The difference of polarizations at zero electric field, 1.16 μC/cm^2 and the difference of electric fields at zero polarization, 422 kV/cm have been obtained. The polarization value is small, but it appears to be ferroelectric.

2.3.4 *J-E* Characteristic of BIT Thin Film

Figure 2.10 shows the *J-E* curve of the BIT thin film. If the applied voltage is above 10 V, the current will increase unexpectedly. This explains why the hysteresis loops corresponding to 21 V and 27 V of applied voltage in Fig. 2.9 are not closed. The leakage current increases quickly when the applied voltage on the surface of two electrodes is high enough.

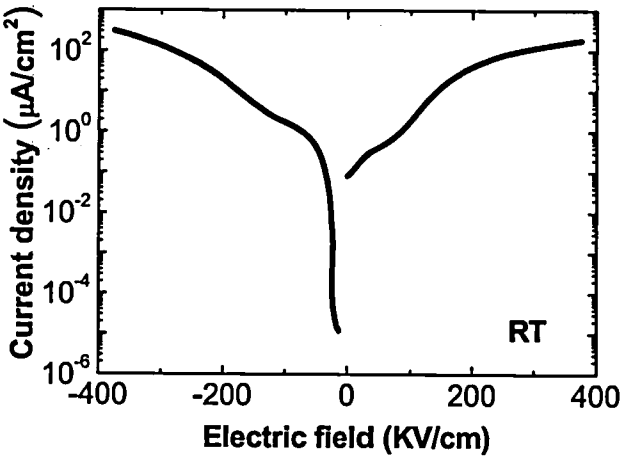

Figure 2.10 The *J-E* curve of the BIT thin film with 473 nm thickness under the condition of $Bi(OH)_3$ concentration 0.2 M, TiO_2 0.1 M and KOH 0.012 M.

2.4 CONCLUSION

BIT ferroelectric thin films have been prepared by sol-gel and successive hydrothermal treatment using BIT and TiO_2 gel precursor films for low temperature deposition. BIT poweder were prepared at 240 °C in $Bi(OH)_3$-TiO_2-KOH solution by hydrothermal synthesis. BIT thin films were obtained at the maxium prrocess temperature of 350 °C for 4 h in $Bi(OH)_3$ 0.2 M-TiO_2 0.1 M-KOH 0.015 M solution by the sol-gel process and hydrothermal

treatment. This temperature is relatively low comparison with the other method, and is acceptable for electronic device production. BIT thin film is oriented *a*- and *c*-axis by the effect of TiO_2 precursor film. Moreover, there is a complete difference of grain shape and grain size between powder and thin film. Power shape is lamellar, and its size is 0.5-1.5 μm. Grain shape of the thin film is spherical and its size is 120 nm. Thus, in the case of the film, substrate and precursor film affects the reaction to form BIT. On the other hand, BIT thin film cannot be prepared by using BIT gel as a precursor, because precursor film is easliy removed from the substrate during hydrothermal process.

The *P-E* saturation characteristic may be insufficient for the thin film treated hydrothermally owing to TiO_2. The BIT thin film prepared under optimized conditions had a hysteresis loop and the polarization difference at zero electric field is 1.16 $\mu C/cm^2$.

REFERENCES

[1] T. Naoyama, A. Inoue, K. Takai, M. Noda, and M. Okuyama: Jpn. J. Appl. Phys. **45** (2006) 7283.

[2] T. Naoyama, Y. Sakioka, M. Noda, M. Okuyama, and K. Saito: Jpn. J. Appl. Phys. **44** (2005) 6873.

[3] T. Naoyama, M. Noda, M. Okuyama, H. Fujisawa, and M. Shimizu: Trans. Mat. Res. Soc. Jpn. **31** (2006) 181.

[4] K. A. Vorotilov, A. S. Sigov, E. P. Turevskaya, V. B. Bergo, and S. V. Sokolov: Russian Microelectronics. **28** (1999) 161.

[5] Y. Lu, D. T. Hoelzer, W. A. Schulze, B. Tuttle, and B. G. Potter: Mater. Scien. Eng. B. **39** (1996) 41.

[6] P. Li and T. M. Lu: App. Phys. Lett. **59** (1991) 1064.

[7] W. B. Wu, Y. Oishi, M. Okuyama, and Y. Hamakawa: J. Korean Phys. Soc. **29** (1996) S660.

[8] S. I. Hirano, T. Hayashi, W. Sakamoto, K. Kikuta, and T. Yogo: *Ferroelectric Thin Films* (Springer), Topics in Applied Physics **98** (2005) 25.

[9] D. C. Lupascu: *Fatigue in ferroelectric ceramics and related issues* (Springer, Heidelberg, 2004), chapter 6.

[10] N. Maffei and S.B. Krupanidhi: Appl. Phys. Lett. **60** (1992) 781.

[11] R. Ramesh, A. Inam, B. Wilkens, W. K. Chan, T. Sands, J. M. Tarascon, D. K. Fork, T. H. Geballe, J. Evans, and J. Bullington: Appl. Phys. Lett. **59** (1991) 1782.

[12] H. Buhay, S. Sinharoy, W. H. Kasner, M.H. Francombe, D.R. Lampe, and E. Stepke: Appl. Phys. Lett. **58** (1991) 1470.

[13] S. E. Cummins and L. E. Cross: J.Appl. Phys. **39** (1968) 2268.

[14] T. Kijima, M. Ushikubo, and H. Matsunaga: Jpn. J. Appl. Phys. **38** (1999) 127.

[15] M. Nakamura, T. Higuchi, Y. Hachisu, and T. Tsukamoto: Jpn. J. Appl. Phys. **43** (2004) 1449.

[16] M. Vehkamaki, T. Hatanpaa, M. Kemell, M. Ritala, and M. Leskela: Chem. Matter. **18** (2006) 3883.

[17] H. Xu, K. J. Bowman, and E. B. Slamovich: J. Am. Ceram. Soc. **38** (2003) 1815.

[18] B. L. Gersten, (Edited by: K. Byrappa, T. Ohachi, W. Michaeli, H. Warlimont, and E. Weber): *Crystal Growth Technology* (Elsevior, ScienceDirect e-book), chapter 9.

[19] T. Watanabe and H. Funakubo: Jpn. J. Appl. Phys. **44** (2005) 1337.

CHAPTER 3

Preparation of $BiFeO_3$ Powder and Thin Films by Hydrothermal Synthesis

3.1 INTRODUCTION

During the past decade considerable attention has been devoted to investigations of perovskite type crystals, particularly concerning phase transitions associated with magnetic and electric properties. In this class, $BiFeO_3$ (BFO) based thin films have recently generated great attention due to their prominent polarization values of 50–150 $\mu C/cm^2$. This value is largest one in typical inorganic ferroelectric materials such as Rochelle salt, $BaTiO_3$, $LiNbO_3$, $KNbO_3$, $PbTiO_3$, $PbZrO_3$, $Pb(Zr_x,Ti_{1-x})O_3$, $SrBi_2Ta_2O_9$, $Ba_{0.73}Sr_{0.72}TiO_3$ and $Bi_4Ti_3O_{12}$ [1]. It is though that such large remanent polarization is well adapted for FeRAM application. Many approaches have been undertaken for the preparation of BFO thin films, such as chemical solution deposition (CSD), metal organic chemical vapor deposition (MOCVD), pulse laser deposition (PLD) [2-9]. In general, the temperature for the BFO thin film preparation is from 500 to 700 °C. In order to decrease the process temperature for suppression of thermal damage to FET metal wire or impurity rediffusion in the stacked-typed capacitor of FeRAMs described in Chapter 1, a similar method of hydrothermal synthesis has been investigated as a low-temperature preparation method for BFO powder and thin films. In this chapter, BFO thin films are prepared by hydrothermal process at the temperature below 400 °C and characterize the ferroelectric properties.

3.2 EXPERIMENTAL

In order to try to prepare BFO thin films, BFO powder preparation has been examined by hydrothermal synthesis before preparation of BFO thin films. It needs to determine the source materials and concentrations. There are some reports on preparation of hydrothermal synthesis. $Bi(NO_3)_3{\cdot}5H_2O$ and $Fe(NO_3)_3{\cdot}9H_2O$ are commonly used as sources of Bi and Fe, respectively [10-13]. KOH is also used as a mineralizer, commonly. However, the concentrations of these sources are different. It is thought that the molars of $Bi(NO_3)_3{\cdot}5H_2O$ and $Fe(NO_3)_3{\cdot}9H_2O$ must be same value to obtain stoichiometric BFO. This idea is different from that in the case of PLD/CSD/MOCVD, because the processing temperature of hydrothermal synthesis is relatively low comparison with the other methods, and evaporation of Bi is suppressed. Moreover, I want to apply the BFO thin film for electronic device. Thus, it is better to decrease a concentration of KOH, because K ions degrade the device. So, KOH concentrations used in this study are varied 0.5-5 M that are smaller than that of reported value of about 10 M. In a typical synthesis for BFO, $Bi(NO_3)_3{\cdot}5H_2O$ 0.1 M, $Fe(NO_3)_3{\cdot}9H_2O$ 0.1 M and KOH with the concentration from 0.5–5 M were added to 15 ml deionized water. The mixture was then sealed in a teflon-lined stainless steel autoclave with magnetic stirring and kept at 200 °C for 6-12 h. After hydrothermal synthesis, the autoclave was cooled down to less than 100 °C and opened. The product was washed with deionized water several times, and dried at 120 °C. The crystalline state was studied using an X-Ray Diffractometer (XRD; Rigaku, RINT2000) with CuKα radiation.

However, it is difficult for prepration of BFO thin film from the solutions of $Bi(NO_3)_3.5H_2O$, $Fe(NO_3)_3.9H_2O$, and KOH on the $Pt/Ti/SiO_2/Si$ substrates, directly. Therefore, the BFO thin films were prepared by using precursor BFO film. The precursor film must be deposited at low temperature, because one of the merits of hydrothermal synthesis is that crystalline film or powders can be grown at low temperature. Thus, the BFO thin films were prepared by hydrothermal synthesis as follows. First, $Bi_{1.1}FeO_3$ precursor solution (Toshima Manufacture Co. LTD) was spin-coated on a $Pt/Ti/SiO_2/Si$ substrate at 500 rpm for 5 sec and 3000 rpm for 30 sec, and the coated sol film was transformed to a gel film by annealing in air at 250 °C for 5 min. The samples were annealed by rapid thermal annealing at 430 °C in nitrogen for 15 min. This process was repeated 5 times to create a BFO precursor layer. In order to obtain BFO thin films, $Bi(NO_3)_3.5H_2O$ 0.1 M and $Fe(NO_3)_3.9H_2O$ 0.1 M reacted together in alkali solution of KOH. Second, the hydrothermal

synthesis of BFO thin films was carried out on $Bi(NO_3)_3.5H_2O$ 0.1 M, $Fe(NO_3)_3.9H_2O$ 0.1 M and KOH 1, 2, 3 and 5 M at 200 °C for 10h30m - 17h30m. The deposition temperature of the precursor is 430 °C, and is not so low, but high concentration of KOH 5M is used for comparison with the case of BIT.

3.3 CRYSTALLIZATION OF BFO POWDER PREPARED BY HYDROTHERMAL METHOD

The crystalline property of BFO powder obtained by hydrothermal synthesis for 12 h in solution of $Bi(NO_3)_3.5H_2O$ 0.1 M, $Fe(NO_3)_3.9H_2O$ 0.1 M with KOH concentration from 0.5–5 M was investigated using θ-2θ XRD patterns from 20° to 60° as shown in Fig. 3.1. At low concentration of KOH 0.5 M, intensities of BFO rhombohedral are quite small, while the intensity of $Bi_2Fe_4O_9$ peak increases. The intensities of the rhombohedral peaks increase and the $Bi_2Fe_4O_9$ peak decreases when the KOH concentration increases from 0.5 to 1 M. However, the crystallization of the BFO becomes weakly at KOH concentration above 3 M. Moreover, BFO could not be obtained with a KOH concentration about 5 M. From the above results, I concluded that BFO powder with having high XRD peak intensities can be prepared by hydrothermal synthesis at 200 °C for 12 h in a solution of $Bi(NO_3)_3.5H_2O$ 0.1 M, $Fe(NO_3)_3.9H_2O$ 0.1 M with optimized concentration of KOH 1 M. If the concentration is low, BFO peak is small. Impurity phase such as Bi_2O_3 was detected for the sample synthesized with the KOH concentration of 5 M. In the hydrothermal process, the presence of alkaline medium was found to be essential [10]. So, the concentration of KOH is low, hydrothermal reaction is suppressed. The dissolution-precipitation and in-situ transformation processes can be used to describe the hydrothermal synthesis. If the concentration of KOH is too high, precipitated species by the reaction with Bi^+ and Fe^+ under the KOH may causes etching or dissociation of BIT, or formation of BIT may be prevented. Thus, the other phase is grown under the non-optimized condition.

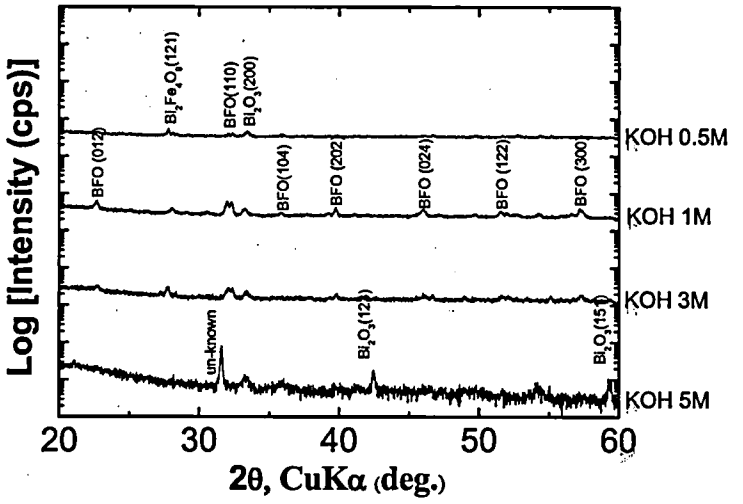

Figure 3.1 XRD patterns of BFO powders prepared by hydrothermal synthesis at 200 °C for 12h with various KOH concentrations.

3.4 CRYSTALLIZATION OF BFO THIN FILMS PREPARED BY HYDROTHERMAL METHOD

Figure 3.2 shows XRD patterns of the $Pt/TiO_x/SiO_2/Si$ substrate, BFO precursor thin film deposited on the substrate using RTA at 430 °C in nitrogen and BFO thin films obtained by the hydrothermal treatment under various conditions of KOH concentration and processing time. Although the BFO powder prepared with KOH 1 M has largest BFO peaks in XRD measurements, higher KOH concentration is necessary to deposit BFO thin films prepared by hydrothermal synthesis. Next, I have carried out a comparative study of the crystallization of BFO thin films prepared at KOH concentration from 1 to 5 M and the BFO precursor thin film annealed by RTA in nitrogen. When the KOH concentration increases from 1 to 3 M, the intensities of the BFO rhombohedral peak intensity in XRD measurements seems not to be increased at any processing time from 10 to 15 h. On the other hand, the removal of the BFO precursor film appears when processing time increases up to 12 h with KOH 1 M, as in the case of the removal of BIT thin film [9]. My data shows that a KOH concentration below 3 M is not enough to deposit a BFO thin film by hydrothermal synthesis.

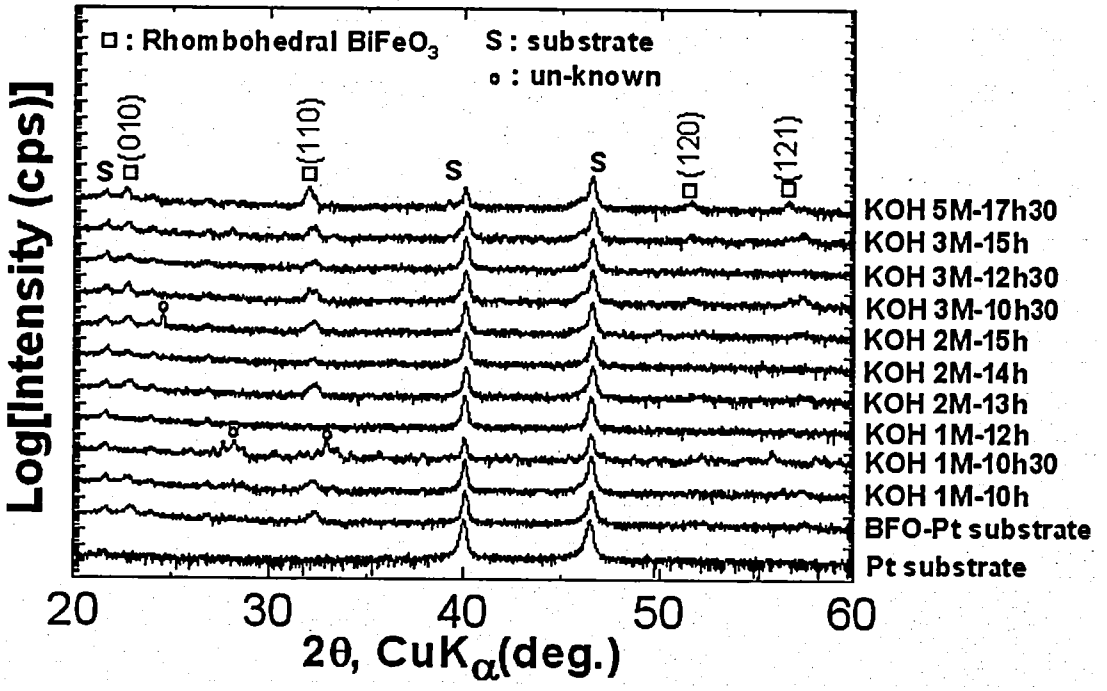

Figure 3.2 XRD patterns of the $Pt/TiO_x/SiO_2/Si$ substrate, BFO precursor thin film deposited on the substrate using RTA at 430 °C in nitrogen and BFO thin films obtained by hydrothermal treatment at 200 °C for 12 h under various conditions of KOH concentration and processing time.

By increasing the KOH concentration and processing time, BFO thin films with better crystallization compared to that of the BFO precursor layer can be obtained by hydrothermal synthesis at 200 °C for 17.5 h in solution of $Bi(NO_3)_3.5H_2O$ 0.1 M, $Fe(NO_3)_3.9H_2O$ 0.1 M with KOH 5 M. However, the ferroelectric P-E hysteresis loops of the thin film are not obtained. This may suggest that the leakage current is large. Also, The BFO thin film with improved crystallized BFO rhombohedral structure can not be obtained by increasing the KOH concentration and processing time, due to the damage to BFO precursor film and Pt layers in the substrate.

3.5 CONCLUSION

I have attempted to prepare BFO powder and thin films by hydrothermal synthesis. Crystallization of BFO powder can be obtained through the treatment at 200 °C for 12 h in solution of $Bi(NO_3)_3.5H_2O$ 0.1 M, $Fe(NO_3)_3.9H_2O$ 0.1 M with KOH 1 M. On the other hand, by creating a BFO precursor layer deposited by using RTA at 430 °C in nitrogen, BFO thin films can be obtained by hydrothermal syntehsis at 200 °C for 17.5 h in solution of $Bi(NO_3)_3.5H_2O$ 0.1 M, $Fe(NO_3)_3.9H_2O$ 0.1 M with very high KOH concentration of 5 M.

However, the film has not shown ferroelectric property yet, because of high leakage current. Meanwhile, when I increased the processing time and KOH concentration, the substrate was damaged. It has been reported that BFO crystalline powder is obtained by using high concentration of KOH [10-13], [15, 16]. However, ferroelectric properties were not described in the report, and such highly concentrated KOH is not applicable in the case of devices such as a semiconductor memory. It is reported that the optimum conditions to retain pure-phase BFO were determined to be a KOH concentration of 8 M for a reaction time of 6 h at 175-225 °C [16], and process window is narrow. Moreover, under the low KOH concentration, $Bi(NO_3)_3$ reacts with KOH and Bi_2O_3 is formed and remained. Thus, pure BFO cannot be obtained. I think it is very difficult to obtain ferroelectric BFO thin film by hydrothermal treatment, and the deposition method has been changed.

REFERENCES

[1] N. Izyumskaya, Y. I. Alivov, S. J. Cho, H. Morkoc, H. Lee, and Y. S. Kang: Crit. Rev. Solid. Stat. Mate. Sci. **32** (2007) 111.

[2] J. Wang, J. B. Neaton, H. Zheng, V. Nagarajan, S. B. Ogale, B. Liu, D. Viehland, V. Vaithyanathan, D. G. Schlom, U. V. Waghmare, N. A. Spaldin, K. M. Rabe, M. Wuttig, and R. Ramesh: Science **299** (2003) 1719.

[3] J. Li, J. Wang, M. Wuttig, R. Ramesh, N. Wang, B. Ruette, A. P. Pyatakov, A. K. Zvezdin, and D. Viehland: Appl. Phys. Lett. **84** (2004) 5261.

[4] K. Y. Yun, D. Ricinschi, T. Kanashima, M. Noda and M. Okuyama: Jpn. J. Appl. Phys. **43** (2004) L647.

[5] K. Y. Yun, D. Ricinschi, T. Kanashima and M. Okuyama: Appl. Phys. Lett. **89** (2006) 192902-1.

[6] G. Smolenskii, V. Yudin, E. Sher, and Y. E. Stolypin: Sov. Phys. JETP. **16** (1963) 622.

[7] Y. N. Venevtsev, G. Zhadanov, and S. Solov'ev: Sov. Phys. Crystallogr. **4** (1960) 538.

[8] G. Smolenskii, V. Isupov, A. Agranovskaya, and N. Kranik: Sov. Phys. Solid State. **2** (1961) 2651.

[9] S. K. Singh, H. Ishiwara, K. Sato, and K. Maruyama: J. Appl. Phys. **102** (2007) 094109.

[10] D. Rout, S. H. Han, K. S. Moon, H. G. Kim, C. I. Cheon, and S. J. L. Kang: Appl. Phys. Lett. **95** (2009) 122509.

[11] S. Basu, M. Pal, and D. Chakravorty: J. Mag. and Mag. Mater. **320** (2008) 3361.

[12] J. T. Han, Y. H. Huang, X. J. Wu, C. L. Wu, W. Wei, B. Peng, W. Huang, and J. B. Goodenough: Adv. Mater. **18** (2006) 2145.

[13] C. Chen, J. Cheng, S. Yu, L. Che, and Z. Meng: J. Crystal Growth **291** (2006) 135.

[14] N. T. Tho, A. Inoue, M. Noda and M. Okuyama: IEEE. Trans. Ultra. Ferro. Freq. Control. **54** (2007) 2603.

[15] Y. Mao, T. J. Park, and S. S. Wong: Chem. Comm. **46** (2005) 5721.

[16] S. H. Han, K. S. Kim, H. G. Kim, H. G. Lee, H. W. Kang, J. S. Kim, and C. I. Cheon. Ceramics International **36** (2010) 1365.

CHAPTER 4

Characterization of $Bi_{1.1}Fe_{1-x}Co_xO_3$ Thin Films Prepared by Chemical Solution Deposition Using Rapid Thermal Annealing in Nitrogen

4.1 INTRODUCTION

In recent years, multiferroic materials have attracted a lot of interest as they display numerous interesting properties, such as ferroelectric, piezoelectric and ferromagnetic phenomena. Among many multiferroelectric materials, bismuth ferrite ($BiFeO_3$, BFO) gathers much attention as it is G-type antiferromagnetic below Néel temperature of 643 K and ferroelectric below Curie temperature of 1103 K, and the magnetoelectric effect is expected to occur even at room temperature. Also, high remanent polarizations of 50–150 $\mu C/cm^2$ were reported in thin films [1-7]. However, BFO has one serious problem as a ferroelectric material that is a quite large leakage current density, especially at room temperature (RT). Therefore, dielectric breakdown occurs easily even in low electric field conditions and implies difficulty in poling the film. Moreover, leakage current makes BFO undesirable in the use for ferroelectric memories. The proposed high density FeRAM has a Metal-Ferroelectric-Insulator-Semiconductor (MFIS) structure, and the insulator is generally very thin. Therefore, leakage current in the ferroelectric layer causes the increase of power consumption and the decrease of memory retention time. A depolarization electrical field is applied to the ferroelectric layer when the memorized data is held in the FeRAM, and thus, polarization is decreased through leakage current, and memory retention time is shortened [8].

To overcome this problem, various approaches have been proposed, particularly the substitution techniques using Mn, Ti, Cr, Sc, Ti, Ni, V, Zn and Co at B-sites or/and La and Nd at A-sites, or the formation of a solid solution [9-20]. In the case of Mn-substituted BFO,

P_r is 85 μC/cm^2 in a 10 at. % Mn-substituted, but the leakage current density in the 10 at. % Mn-substituted BFO (BFMO) film was higher than that in a pure BFO film. In the case of Mn and Ti co-doped BFO (BFMT) the well-saturated *P-E* hysteresis curves were observed at RT. P_r was 75 μC/cm^2. BFMT film shows a greatly reduced leakage current compared with other films. In the case of Cr-doped $BiFeO_3$ thin films, the 3 mol% Cr-doped BFO thin film showed a low leakage current density, but P_r is 16 μC/cm^2 at room temperature. In the case of $(1-x)BiFeO_3$-$xBiScO_3$ the surface of the films became smooth for the increase in x of up to 0.15, and the leakage current density at room temperature decreased. Well-saturated polarization and electric field hysteresis loops were obtained and the P_r of the films was 70 μC/cm^2. In the case of La-doped BFO (BLFO), P_r is about 15.5 μC/cm^2, and the leakage current density up to the level of 10^{-3} A/cm^2. In the case of La^{3+}- and Nd^{3+}-substituted BFO films, the leakage current at room temperature was too high, and saturated *P-E* hysteresis was not obtained. In the case of Co-, Ni-, Zn-, Nb-, Ba-, Sr- and Ca-doped BFO, only the magnetic properties were reported. These results show that there are no single-metal doped BFO thin films having low leakage current and large remanent polarization. Since, some co-coped BFO thin films have small leakage current density, but co-doping is difficult to control the rate ration of elements comparison with single-metal doped BFO. So, I focused on Co. It is reported Co-doped BFO has relatively large remanent magnetic [16], and Co and Ni are compatible with electrical devices such as FeRAM.

Moreover, it is well known that $BiCoO_3$ is isostructural with tetragonal $PbTiO_3$ and has tetragonal anisotropy (c/a = 1.267) [20]. BFO thin films are reported to have rhombohedral or tetragonal structure and BFO with large tetragonality has large remanent polarization. Hence, Co-substitution might enhance the ferroelectric property around phase transition or give stable tetragonality. It is believed that Co successfully substitutes Fe [21, 22]. The atomic radius of Co is 0.116 nm and this value is very similar to that of Fe (0.117 nm). (Atomic radius of Bi is 0.15 nm) Fe in BFO is trivalent. The ionic radii of Co^{3+} are 0.075 nm (high spin; HS) and 0.072 (low spin; LS). These values are similar to 0.079 nm (HS) and 0.069 nm (LS) of Fe^{3+}. So, if Co in $BiFeCoO_3$ is trivalent, the tolerance factor is hardly changed and the perovskite structure can be obtained. Because of the large size of Co^{2+}, I assume that Co^{3+} may be able to occupy to position of Fe^{2+} and Fe^{3+} [23]. However, its size is slightly larger than that of Fe^{3+} ion, so there is a limited amount of Co occupied at position of Fe^{3+} ions even with the increase of Co concentration [20]. Also, the thermodynamic stability of Co^{3+} is

smaller than that of Fe^{3+}. Thus, if some of the cobalt ions become divalent by heavy doping, the crystal structure and electrical/magnetic properties are expected to change.

In this chapter, I will enlarge upon the preparation of BFCO thin films by RTA in nitrogen, meant to improve their structural and ferroelectric property. Rapid thermal annealing (RTA) following spin-coating and drying is repeated to promote the necessary chemical reaction. I suppose that rapid thermal annealing $BiFe_{1-x}Co_xO_3$ films layer by layer could suppress strains and damage inside thin films induced by temperature during annealing. It is expected that iterative annealing will be appropriate for thermal reaction at low temperatures in comparison with one-time annealing.

As mention in chapter 1, all perovskite structures depend on temperature. Therefore, the distortion of the ferroelectric structures may also be enhanced by increasing the processing temperature rate. In the case of rapid thermal annealing (RTA), temperature can be increased from RT to 520 °C in about 10 sec. Thus, RTA was selected to prepare ferroelectric BFCO thin films. I also suppose that thermal annealing $BiFe_{1-x}Co_xO_3$ films layer by layer could suppress strains and damage inside thin films induced by temperature during annealing. On the other hand, Naganuma *et al.* prepared BFCO thin films by chemical solution deposition (CSD) using one-time RTA at 500 °C in air, which is dominated by nitrogen and oxygen [24]. Therefore, in this chapter, I will enlarge upon the preparation of BFCO thin films by RTA in nitrogen, meant to improve their structural, insulation, and ferroelectric property. RTA following spin-coating and drying is repeated (iterative RTA) to promote the necessary chemical reaction.

4.2 EXPERIMENTAL

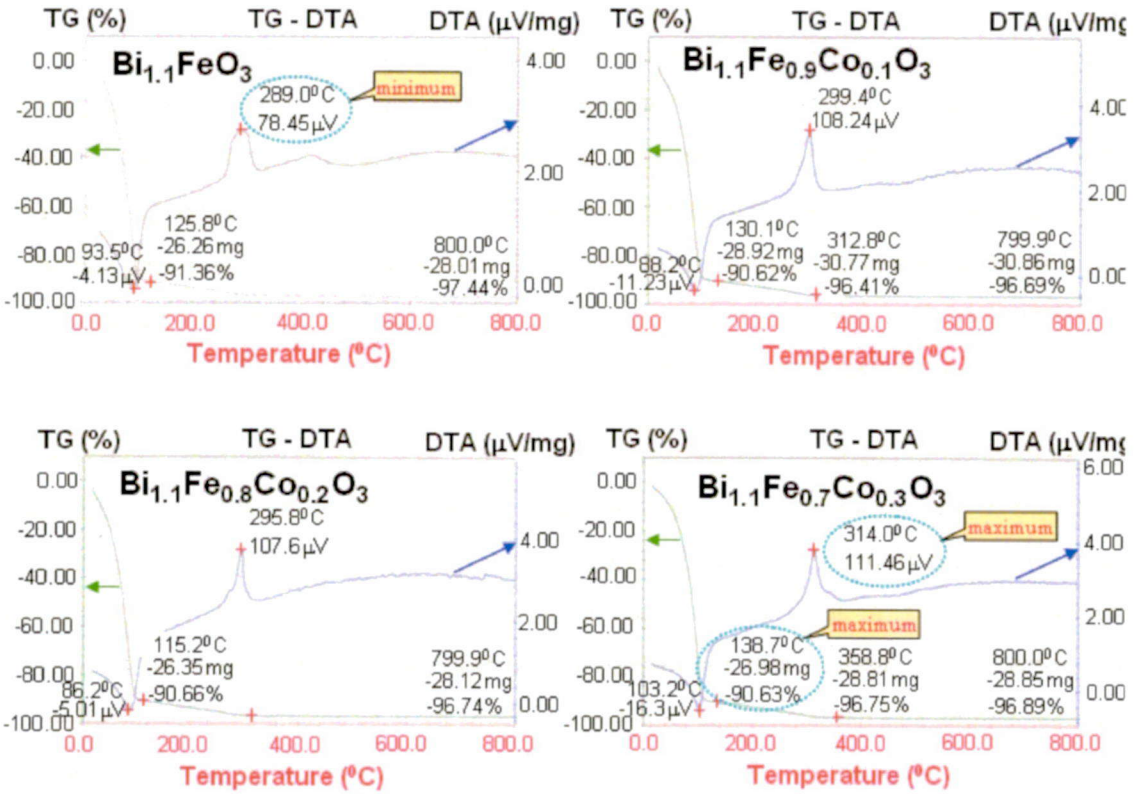

Figure 4.1 Data for thermal gravimetric (TG) and differential thermal analysis (DTA) of (a) $Bi_{1.1}FeO_3$, (b) $Bi_{1.1}Fe_{0.9}Co_{0.1}O_3$, (c) $Bi_{1.1}Fe_{0.8}Co_{0.2}O_3$ and (d) $Bi_{1.1}Fe_{0.7}Co_{0.3}O_3$ precursor solutions. (Toshima MFG Co., Ltd.)

BFCO thin films were prepared by CSD. In this method, a BFCO solution that is a mixture of metal organic source dissolved in solvent is used for thin film preparation. BFCO solutions with various Co concentrations from Toshima Manufacture Co., LTD were used. To form a crystalline film, the solvent is evaporated by a drying-process, and then the residual that is the precursor of the film is reacted and annealed at a suitable temperature. The data for differential thermal analysis (DTA) and thermo-gravimetric analysis (TG) from Toshima Manufacture Co. LTD were used to determine the thermal decomposition behavior of the $Bi_{1.1}Fe_{1-x}Co_xO_3$ 0.2 mol/kg (with x = 0, 0.05, 0.1, 0.2, and 0.3) and toluene 88 wt% in precursor solutions, and to select the appropriate temperatures for baking, as shown in Fig.4.1. I was able to conclude that the DTA curves of the $Bi_{1.1}Fe_{1-x}Co_xO_3$ precursor solutions show endothermic peaks at 93.5, 88.2, 86.2 and 103.4 °C corresponding to solvent evaporation, and exothermic peaks at 289.0, 299.4, 295.8, and 314.0 °C corresponding to precursor

decomposition and formation of BFCO compound when x is equal to 0, 10, 20 and 30%, respectively. Similarly, TG curves of these BFCO solutions also show that the total mass of the investigated liquid decreases rapidly, the solution loss 91.36, 90.62, 90.66 and 90.63 % corresponding to temperature at 125.8, 130.1, 115.2 and 138.7 °C when x is equal to 0, 0.1, 0.2 and 0.3, respectively. The solution loss is slow when temperature increases from 300 to 360 °C. The weight loss is insignificant above 360 °C. From these results, drying temperature of 250 °C and baking temperature above 400 °C were selected to ensure full solvent evaporation in short time and to minimize as much as possible the stress and defects caused by a further weight reduction during annealing and complete precursor decomposition and BFCO creation in a limited time.

BFCO thin films were deposited on $Pt/Ti/SiO_2/Si$ substrates by CSD. The substrates were spin-coated by the $Bi_{1.1}Fe_{1-x}Co_xO_3$ precursor solution (Toshima Manufacturing Co. LTD) at 3000 rpm for 30 s and dried at 250 °C for 5 min. The samples were annealed by using RTA in a temperature range from 450 to 560 °C for 20 min. The annealing temperature is comparatively low as thermal damage in the device structure should be suppressed. The films were cooled down quickly after each RTA process. This coating and drying processes were repeated 8 times to obtain a film having the thickness of 100 nm. This process is named iterative RTA preparation, and shown in Fig.4.2(a).

Moreover, in order to confirm the improvement of leakage current and polarization versus electric field (*P-E*) hysteresis loops of the BFCO thin films prepared by iterative RTA, conventional CSD preparation of BFCO thin films was also carried out by a one time of RTA, called mono-RTA, as shown in Fig.4.2(b). In the conventional CSD, annealing is done just once, and afterwards spin-coating and drying are repeated until sufficient thickness is obtained. The substrates were spin-coated by using the $Bi_{1.1}Fe_{0.9}Co_{0.1}O_3$ precursor solution under the same conditions of rotation speed and time and drying temperature as those of iterative RTA. This process was repeated 8 times and then the 100nm-BFCO thin films were obtained by mono-RTA for 20 min in nitrogen.

The crystal structure was determined by X-ray diffraction (XRD) [Rigaku, RINT2000] at RT. The morphology was also measured by a field emission scanning electron microscope (FESEM) [JSM-6340F]. Chemical bondings in BFCO thin films were identified by X-ray photoelectron spectroscopy (XPS) [Kratos Analytical Axis-HSI2]. Pt dot top electrodes were deposited on the BFCO thin films by RF sputtering [Anelval-250S-FH]. The diameter of the

top electrode is 200 μm. Leakage current density versus electric field (*J-E*) characteristic was measured with a semiconductor parameter analyzer (Agilent, 4155C). The resistance of Pt electrodes (~10 μΩ cm) is considerably smaller than that of BFCO (>100 kΩ cm) and film thickness of BFCO is small compared with the width, so the fringing field can be neglected. Polarizations versus electric field *P-E* hysteresis loops were evaluated by using a ferroelectric test system with virtual ground circuitry (Toyo Corporation, FCE-1). The field-induced piezoelectric hysteresis loops of the BFCO thin films were measured with Piezoresponse Force Microscopy (PFM). The chemical composition of the thin film, prepared from the $Bi_{1.1}Fe_{0.9}Co_{0.1}O_3$ precursor solution in nitrogen at 520 °C by iterative RTA, was analyzed by inductively coupled plasma atomic emission spectroscopy (ICP-AES).

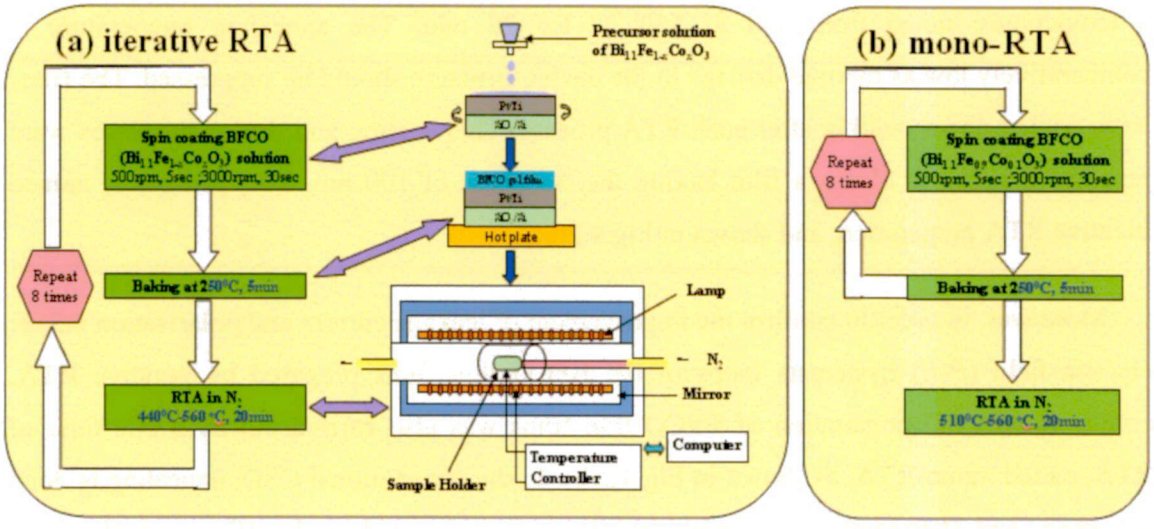

Figure 4.2 Flow charts for preparation of BFCO thin films by CSD method using (a) iterative RTA and (b) mono-RTA in nitrogen.

4.3 RESULTS AND DISCUSSION

4.3.1 X-ray Diffraction Analysis of BFCO thin films annealed in nitrogen by iterative RTA

Reciprocal space mapping of the $Bi_{1.1}Fe_{0.9}Co_{0.1}O_3$ thin film annealed at 520 °C in nitrogen by iterative RTA for 20 times is shown in Fig. 4.3. The results show that the (110) $BiFeO_3$ rhombohedral phase is oriented strongly. Pt substrate is observed and oriented in the (111) direction. BFCO thin film does not have epitaxial growth and polycrystalline BFCO is obtained. Also, small Bi_2O_3 peaks are observed. The origin of existence of Bi_2O_3 is thought as follows. Bi is easily vaporized and evaporated during annealing. Therefore, excess Bi solution is generally used to obtain BFO, BFCO, BIT, etc. having a large remanent polarization, high XRD peak intensity, small leakage current, and so on. It is believed that a part of excess Bi may be presented and crystallized in the film under this deposition condition.

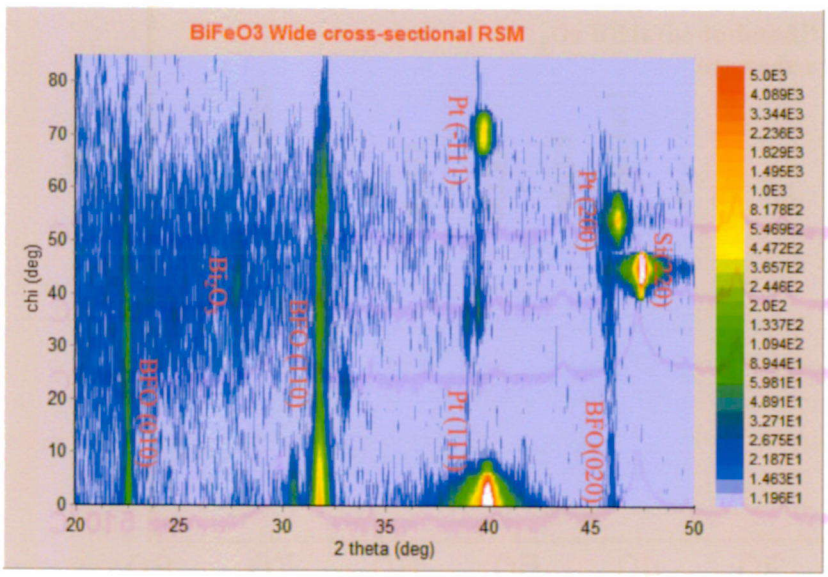

Figure 4.3 Reciprocal space mapping of the $Bi_{1.1}Fe_{0.9}Co_{0.1}O_3$ thin film annealed at 520 °C in nitrogen by iterative RTA for 20 times.

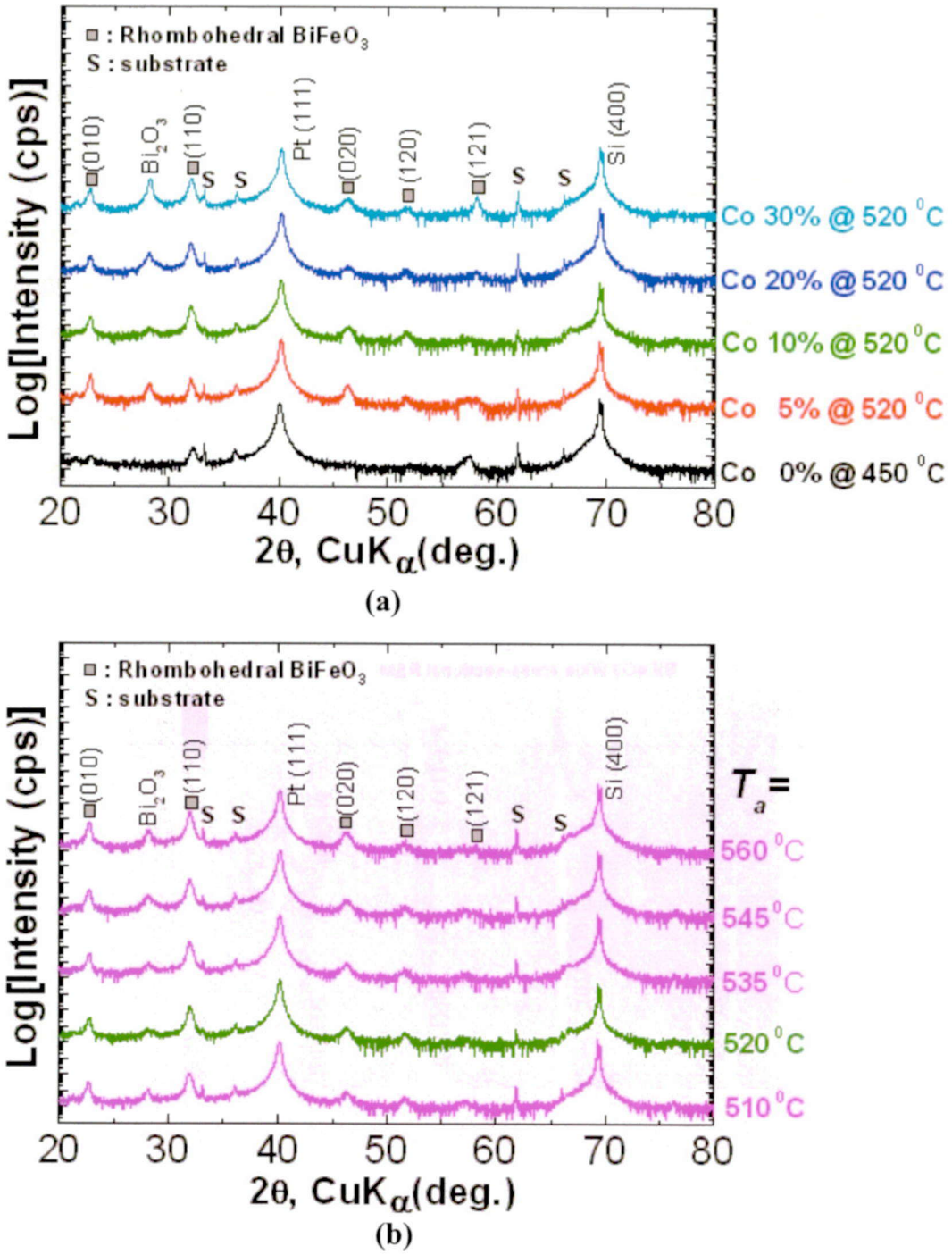

Figure 4.4 XRD θ-2θ patterns of (a) $Bi_{1.1}FeO_3$ thin films annealed at 450 °C and $Bi_{1.1}Fe_{1-x}Co_xO_3$ (x = 0.05, 0.1, 0.2 and 0.3) thin films at 520 °C, and (b) $Bi_{1.1}Fe_{0.9}Co_{0.1}O_3$ thin films annealed at various temperatures (T_a) by iterative RTA.

The crystalline property of the BFO thin film annealed at 450 °C and the BFCO thin films (x = 0.05, 0.1, 0.2 and 0.3) annealed at 520 °C was investigated by the θ-2θ XRD patterns from 20° to 80° as shown in Fig.4.4(a). On the other hand, the crystallization of $Bi_{1.1}Fe_{0.9}Co_{0.1}O_3$ thin films prepared at various annealing temperatures is shown in Fig.4.4(b). Polycrystalline perovskite phases with rhombohedral structure of $BiFeO_3$ are observed clearly. Moreover, the Bi_2O_3 phase appears too. I was able to observe that the $Bi_{1.1}Fe_{0.9}Co_{0.1}O_3$ film annealed in N_2 at 520 °C has the highest intensity of the rhombohedral (110) $BiFeO_3$ peak and a relatively low intensity of the Bi_2O_3 phase in all thin films. Moreover, the Bi_2O_3 phase also appears, and XRD intensity of Bi_2O_3 is smallest in the film annealed at 520 °C in Fig.4.4(b). The intensities of all the peaks seem to increase gradually with the increase of the annealing temperature. However, the intensity change is not so large. So, it is thought that 520 °C is the optimum temperature from the viewpoint of XRD peak height of Bi_2O_3.

According to the XRD pattern of the $BiFeO_3$ powder (calculated from 2000 JCPDS-International Centre for Diffraction Data, No.74-2493), the intensity ratio of (010), (110), (020), (120) and (121) is 658:999:497:126:153 ≈ 0.66:1:0.5:0.13:0.15. Meanwhile, the intensity ratio of the corresponding peaks in XRD pattern of the BFCO thin films is much different. For example, the ratio of the $Bi_{1.1}Fe_{0.9}Co_{0.1}O_3$ thin film annealed in nitrogen at 520 °C is 31.8:157.2:6:3.67:0.66 ≈ 0.18:1:0.034:0.021:0.004. It is found that the percentage of (010), (020), (120) and (121) intensities over the (110) intensity in the BFCO thin film are very smaller than that of these intensities in BFO powder. This is another proof of the strong orientation in (110) direction in the BFCO thin films. The ferroelectric behavior of BFO thin films is strongly dependent on the film orientation. In the case of rhombohedral $BiFeO_3$, it is reported that the easy axis of spontaneous polarization lies close to (111) [25], and the (110) orientation gives rise to a relatively higher polarization than the (100) orientation [25]. Therefore, the ferroelectric behavior

Lattice constants of all BFCO thin films annealed in nitrogen is about 3.9 Å. However, their value can slightly differ, as they depend on ambient (as mentioned in next chapter) and cobalt concentration, as shown in Fig.4.5.

In BFCO thin films annealed in nitrogen, the lattice constant increases to maximum at a Co concentration of 10%. The values of lattice constants of BFCO become larger with the

increase of cobalt concentration due to the larger size of Co^{+3}, as compared to Fe^{+3}. In order to find out the reason, the radii of Fe^{+2}, Fe^{+3}, Co^{+2}, and Co^{+3} have been considered. The results show that the radii of Fe^{+2} and Fe^{+3} ions are 0.078 and 0.069 nm, respectively. Meanwhile, the radii of Co^{+2} and Co^{+3} ions are 0.084 and 0.072 nm, respectively. Because of the large size of Co^{+2}, I assumed that Co^{+3} may just be able to occupy to the position of Fe^{+2} and Fe^{+3} [23]. However, its size is slightly larger than that of the Fe^{+3} ion, so there is a limited amount of Co occupied at position of Fe^{+3} ions even when the Co concentration increases. Thus, there is a very small amount of Co^{+3} occupied at Fe^{+3} positions due to the larger radius of Co^{+3} ions. Therefore, a very small $BiCoO_3$ exists in BFCO thin films. Moreover, the deviation in the $BiCoO_3$ structure can easily occur due to the appearance of cobalt oxides with unidentified valences of cobalt embedded into the grains of $BiCoO_3$, as mentioned in the XPS analysis of the BFCO thin films.

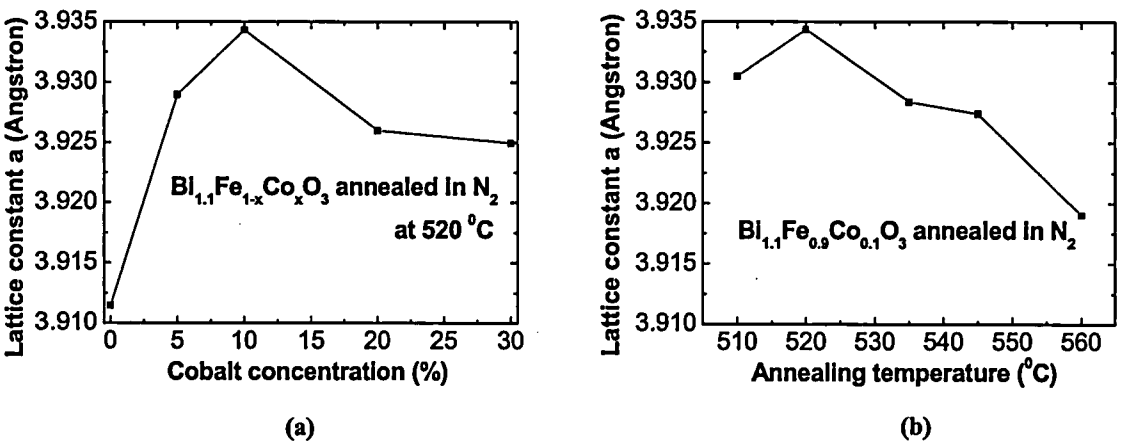

Figure 4.5 Dependence of lattice constants of $Bi_{1.1}Fe_{1-x}Co_xO_3$ thin films on (a) cobalt concentration annealed at 520 °C and (b) at various annealing temperatures with $x = 0.1$ in nitrogen.

In order to determine the evidence of $BiCoO_3$ in BFCO thin films, the chemical composition of the thin film, prepared from the $Bi_{1.1}Fe_{0.9}Co_{0.1}O_3$ precursor solution in nitrogen at 520 °C by iterative RTA, was analyzed by inductively coupled plasma atomic emission spectroscopy (ICP-AES). The analysis shows that the weight percentage of Bi, Fe, and Co is 81.37, 18.27, and 0.37%, respectively. However, the percentage of Bi, Fe, and Co in the chemical formula $Bi_{1.1}Fe_{0.9}Co_{0.1}$ is 80.37, 17.57, and 2.06%, respectively. The decrease of bismuth concentration is confirmed by the volatilization at high annealing temperature. As above mention, the precursor solution made from Toshima manufacturer includes $Bi_{1.1}Fe_{0.9}Co_{0.1}O_3$, toluene and unknown substances. It is assumed that during temperature

increasing, a considerable cobalt amount may react chemically with the unknown substances or/and nitrogen to create new substances, which are easy to volatile at temperatures below 520 °C. Therefore, the marked decrease of cobalt concentration in the thin film is induced by volatilization of the new substances at low temperatures and deviation of the $BiCoO_3$ structure. This is the reason why $BiCoO_3$ structure has not been determined clearly in XRD patterns.

4.3.2 Morphologies of BFCO thin films annealed in nitrogen by iterative RTA

Figure 4.6 shows the morphology of $Bi_{1.1}Fe_{0.9}Co_{0.1}O_3$ thin films of about 100 nm of thickness prepared at various temperatures. The cross-section and surface of these BFCO thin films become smoother as the annealing temperature decreases. On the other hand, the crystallization of these films including monoclinic Bi_2O_3 and rhombohedral $BiFeO_3$ phases increases, and grains associate with each other strongly and are larger with the increase in the annealing temperature above 520 °C. However, the surface and thickness morphology of the thin film annealed at 520 °C is smoother than that of other films. This is expected that the insulation of the 520 °C-film is better than that of others thin films.

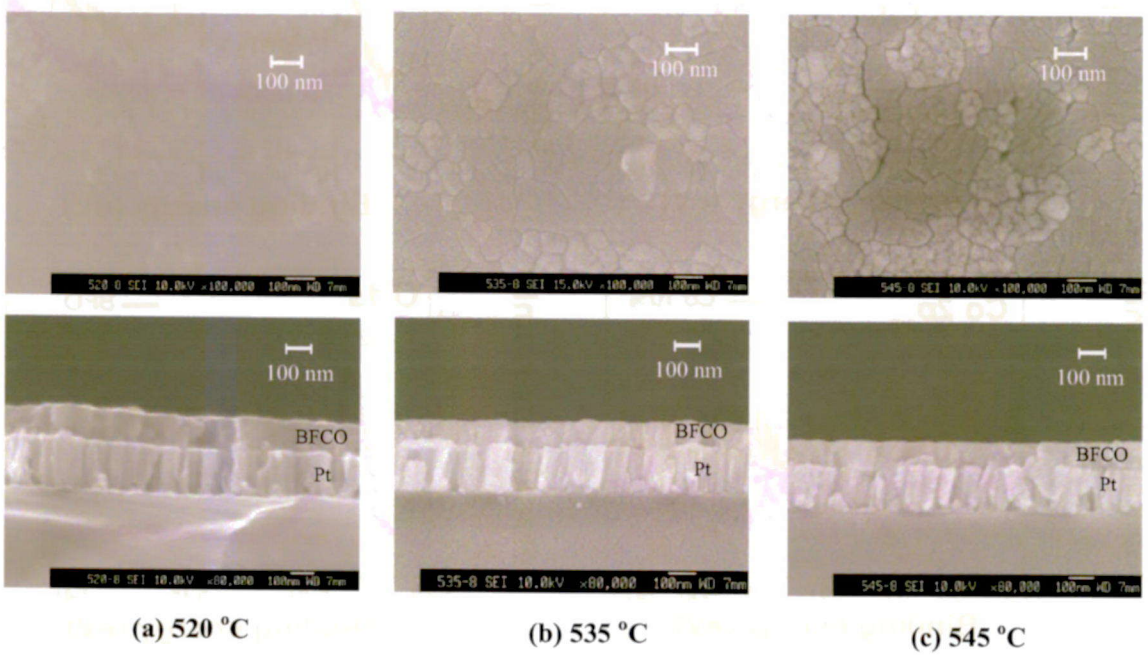

(a) 520 °C **(b) 535 °C** **(c) 545 °C**

Figure 4.6 Surface and cross-sectional morphologies observed by SEM of the $Bi_{1.1}Fe_{0.9}Co_{0.1}O_3$ thin films prepared by iterative RTA at (a) 520, (b) 535 and (c) 545 °C.

4.3.3 XPS spectra of BFCO thin films annealed in nitrogen by iterative RTA

Figure 4.7 shows the XPS spectra of Bi *4f*, Fe *2p*, Co *2p* and O *1s* in BFO annealed at 450 °C in N_2, and $Bi_{1.1}Fe_{0.9}Co_{0.1}O_3$ and $Bi_{1.1}Fe_{0.8}Co_{0.2}O_3$ thin films annealed at 520 °C in N_2. Co^{2+} and Co^{3+} ions in chemical bonding of Co *2p* are not clear in the spectrum because of their weak intensities, which are below the XPS detection limit. However, concentration change of cobalt in $Bi_{1.1}Fe_{1-x}Co_xO_3$ thin films induces a decrease in the ratio of Bi 4f and Fe *2p* intensities when *x* increases in all XPS spectra. Bi $4f_{7/2}$ at 158.5 eV and Fe $2p_{3/2}$ at 710.7 eV shift to lower energy. Because BFO and BFCO thin films are insulators, they were charged up by photoelectrons when the X-ray comes and emit. However, the signal around Fe $2p_{3/2}$ peak has a considerable amount of background noises that prevents to obtain an accurate estimation. On the other hand, bismuth peaks are observed at 157.8 eV in both the thin films annealed in nitrogen and oxygen, and they demonstrate the trivalent bismuth [26].

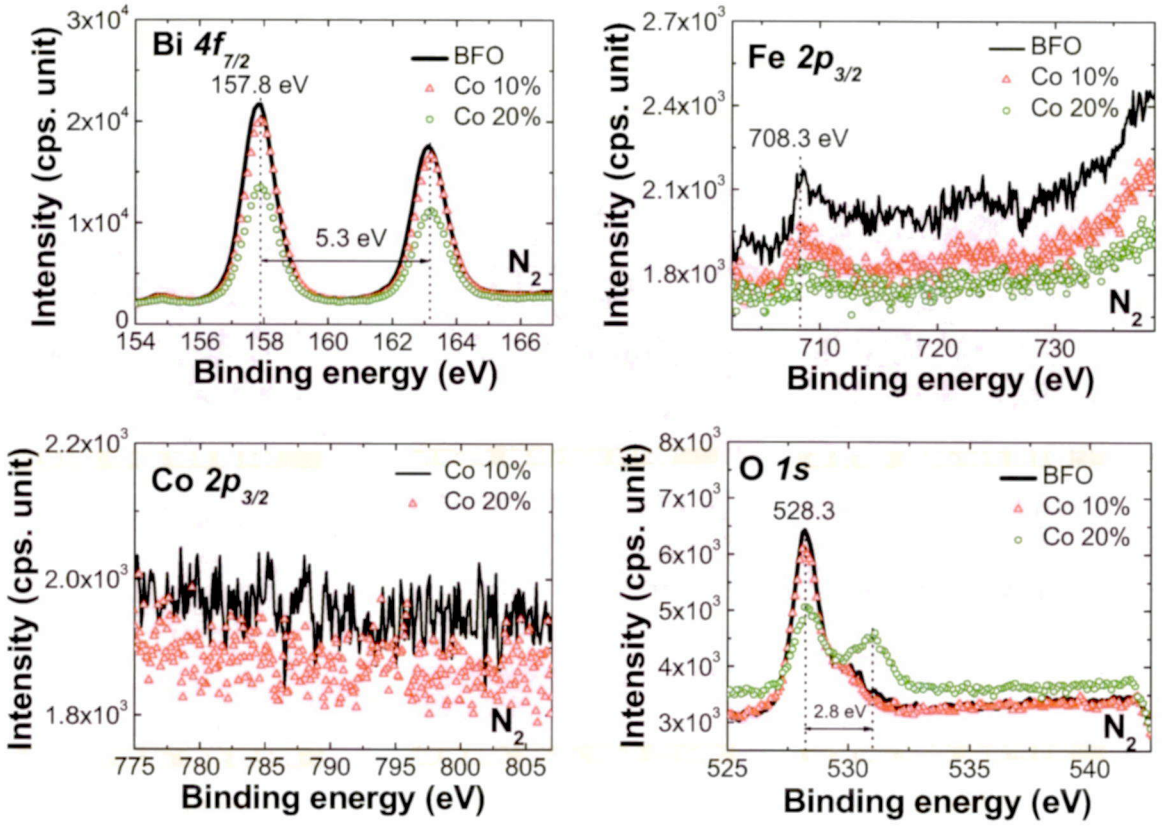

Figure 4.7 XPS spectra of Bi 4f, Fe 2p, Co2p and O 1s in BFO annealed at 450 °C, $Bi_{1.1}Fe_{0.9}Co_{0.1}O_3$ (Co 10%) and $Bi_{1.1}Fe_{0.8}Co_{0.2}O_3$ (Co 20%) thin films annealed at 520 °C in N_2.

Although it is difficult to estimate the iron valence from the Fe $2p_{3/2}$ spectra by the shift of binding energy and the background noises, its valence can be implied by O *1s* XPS spectra of all thin films. There is a small additional satellite peak at 530 eV in O *1s* XPS spectra of BFO thin films annealed in N_2, which is corresponds to O–Fe bonding with the iron trivalent in rhombohedral BFO structure [26]. When Co concentration in $Bi_{1.1}Fe_{1-x}Co_xO_3$ thin films annealed in N_2 increases up to 20 %, the satellite peak increases, expands and shifts in the direction of the higher binding energy direction. The shift of the peak might imply that a small amount of iron may change valence, but its valence is unidentified. It means that almost all iron ions in the BFCO thin films with low cobalt concentration are in the BFO structure, but a small amount of iron in BFCO thin films with high cobalt concentration does not belong to the BFO structure. Meanwhile, the amount of iron in the $Bi_{1.1}Fe_{1-x}Co_xO_3$ with low Co concentration is smaller than that in $Bi_{1.1}Fe_{1-x}Co_xO_3$ with high Co concentration. This supports the idea that the intensity of (110) BFO rhombohedral phase in the $Bi_{1.1}Fe_{0.9}Co_{0.1}O_3$ thin film is a little higher than that of the $Bi_{1.1}Fe_{0.8}Co_{0.2}O_3$ thin film as shown in Fig. 4.4 (a). And Co might react with oxygen to create O–Co bonding, although this peak at 531 eV can not be assigned.

The appearance of the O-Co bonding may be related to results such as those reported by Belik et al. [20]. Hence, grains of cobalt oxides might be embedded into the grains of $BiCoO_3$, so that the stoichiometry of $BiCoO_3$ may deviate from the ideal formula. On the other hand, oxygen vacancies may be created by the valence fluctuation of Fe ions in BFCO thin films annealed in nitrogen [8, 27]. This may be the reason why O-Fe bonding with unidentified valence of iron appears in the BFCO thin films.

4.3.4 *J-E* characteristic property of BFCO thin films annealed in nitrogen by iterative and mono-RTA

Current density versus applied electric field values of BFCO thin films annealed at 520 °C and BFO thin films annealed at 450 °C in N_2 measured at RT are shown in Fig.4.8. For applications such as ferroelectric memories, leakage current at RT is crucial. Moreover, maximum applied field is also important to reverse a polarization at RT. The BFCO thin film with 10 % cobalt concentration, annealed in nitrogen at 520 °C, does not breakdown electrically even under 2 MV/cm of electric field. However, its leakage current density from

about 10^{-2} to 2×10^{-2} A/cm^2 is considerably large under high external electric field from 1 to 2 MV/cm.

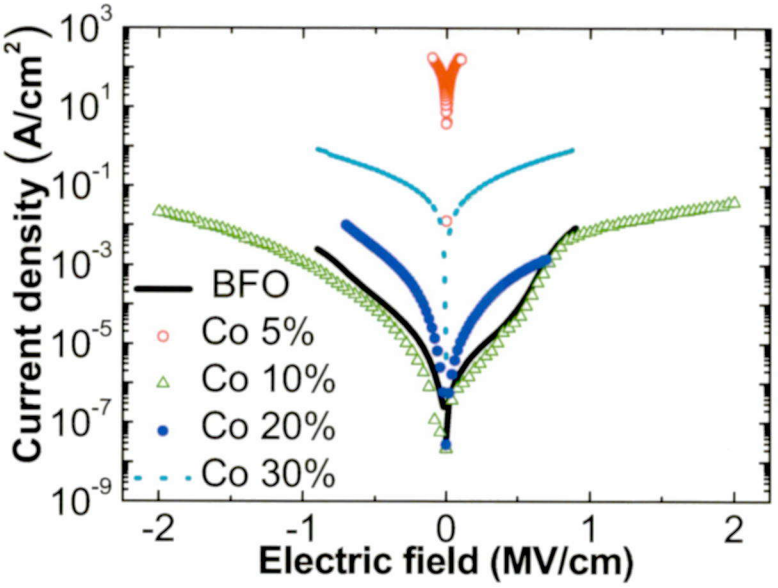

Figure 4.8 *J-E* characteristics of BFCO thin films annealed at 520 °C and the BFO thin film annealed at 450 °C in N_2 by iterative RTA measured at RT.

In Fig.4.8, it can be observed that BFCO thin films with a cobalt concentration of 5 %, annealed at 520 °C in nitrogen have large leakage current density. Based on crystallization of all films in Fig.4.4, I assumed that there is a relation between the intensities of monoclinic Bi_2O_3 peaks and the leakage current of $Bi_{1.1}Fe_{1-x}Co_xO_3$ with high cobalt concentration (over 10%). The $Bi_{1.1}Fe_{0.9}Co_{0.1}O_3$ thin film annealed at 520 °C in nitrogen has low intensities of the Bi_2O_3 peak and also shows a large breakdown field. Since it is reported some solid solutions based on trivalent metallic oxide, that is Bi_2O_3 were found to be high oxide ion conductor [28], this may imply that some of the crystalline Bi_2O_3 clusters might create conductive paths between metallic electrodes, which may suppress the insulation property of other films [29]. This means that the optimization of the condition to decrease intensity of monoclinic Bi_2O_3 phase is necessary for the preparation of the good insulation BFCO thin films, although a Bi-excess precursor solution needs to be used for volatilization suppression of bismuth at high annealing temperature. Addition to this, it is reported that recent work was focused on solid solutions of $BiFeO_3$ with other ABO_3 perovskite materials, such as $BaTiO_3$, which can prevent second phase formation and increase sample resistivity, and $BiFeO_3$ density is

lowered by existing Bi_2O_3 [28]. So, it is thought that second phase of Bi_2O_3 affects the leakage current in BFCO.

I assume that the asymmetry of *J-E* characteristic is caused by the difference in roughness between the top and bottom electrodes. Because BFCO thin films were prepared on a Pt bottom electrode, the BFCO interface between the thin film and the electrode is smoother. On the other hand, the top Pt electrode was prepared after BFCO preparation, so the growth of the BFCO thin films is oriented but quite free to develop. Thus, the surface of films that contact to the top electrode may be rougher. So, the interface properties such as contact resistance, barrier height between bottom electrode and BFCO is different from those between bottom electrode and BFCO in spite of the same Pt electrodes. This may be the reason why the *J-E* characteristic of BFCO thin films shows asymmetry.

Improvement in leakage current, especially at RT, has been the prime problem in the preparation of ferroelectric BFO and doped BFO thin films. Yasui *et al.* reported that the leakage current of highly-oriented BFCO thin films on $SrRuO_3/SrTiO_3$ prepared by MOCVD at 700 °C was less than 10^{-1} A/cm^2 at 100 KV/cm at RT. Ferroelectric *P-E* hysteresis loops have not been obtained at RT, although the well-saturated loops were shown at 80 K and their remanent polarization, $2P_r$ was about 100 μC/cm^2 at 310 KV/cm [30]. Naganuma *et al.* prepared BFCO thin films by the CSD method using mono-RTA at 500 °C in air and improved the leakage current and *P-E* hysteresis loops at RT. The current was suppressed, showed about 10^{-3} A/cm^2 at applied electric field of 300 KV/cm, and the difference of polarizations at a zero field was about 70 μC/cm^2 at 1.25 MV/cm. However, the leakage current of BFCO thin films was not observed under a high electric field larger than 300 KV/cm, although high electric field was used to apply up to around 1.25 MV/cm in the *P-E* hysteresis measurement [24].

In order to compare electric and ferroelectric properties of $Bi_{1.1}Fe_{0.9}Co_{0.1}O_3$ thin films, I also prepared the films by the conventional CSD method using mono-RTA for 20 min, and characterized their leakage current and *P-E* hysteresis loop properties. Figs. 4.9(a) and (b) show the *J-E* characteristics of the $Bi_{1.1}Fe_{0.9}Co_{0.1}O_3$ thin film measured at RT and 80 K, prepared by mono-RTA. The leakage current density of the films decreases with the decrease of the measuring temperature from RT to 80 K. The result shows that it can be said that the leakage current of all BFCO thin films annealed from 510 °C to 560 °C is improved.

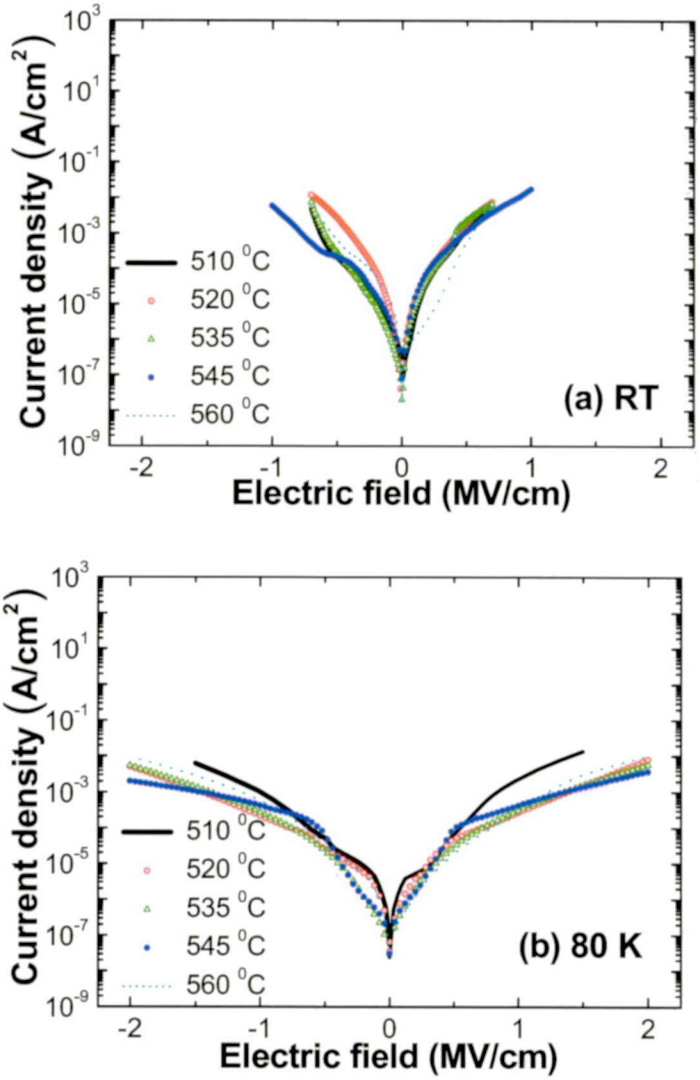

Figure 4.9 *J-E* characteristics of $Bi_{1.1}Fe_{0.9}Co_{0.1}O_3$ thin films annealed by mono-RTA at 510, 520, 535, 545 and 560 °C, measured at (a) RT and (b) 80 K.

I have also focused on which annealing temperature is optimal for obtaining good insulation in $Bi_{1.1}Fe_{0.9}Co_{0.1}O_3$ thin films annealed in nitrogen. The *J-E* characteristics of the $Bi_{1.1}Fe_{0.9}Co_{0.1}O_3$ thin film annealed by iterative RTA are shown in Fig.4.10. $Bi_{1.1}Fe_{0.9}Co_{0.1}O_3$ films annealed at 510 °C and at 560 °C show a very large leakage current. Meanwhile, a high electric field of 2 MV/cm in all of the thin films annealed from 520 °C to 545 °C can be applied at 80 K without dielectric breakdown, and the current density below 10^{-2} A/cm^2 is similar to that of $Bi_{1.1}Fe_{0.9}Co_{0.1}O_3$ thin films RTA annealed by mono-RTA from 510 °C to 560 °C. At RT, these thin films annealed at 535 °C and 545 °C also have almost the same *J-E* characteristics as those of $Bi_{1.1}Fe_{0.9}Co_{0.1}O_3$ thin films annealed by mono-RTA at various

temperatures other than 545 °C. An external electric field of only 0.7 MV/cm can be applied and the leakage current density was about 2×10^{-2} A/cm^2. However, it was interesting to notice that the BFCO thin film annealed at 520 °C shows a good *J-E* characteristic at RT. It shows about 2×10^{-2} A/cm^2 of leakage current density at even at an applied electric field of 2 MV/cm, which is much better than that of the $Bi_{1.1}Fe_{0.9}Co_{0.1}O_3$ thin film prepared by mono-RTA at 545 °C. The lowest current density of the thin film annealed at 520 °C by iterative RTA may be related to the fact that the Bi_2O_3 peak is the smallest as shown in Fig.4.4(b).

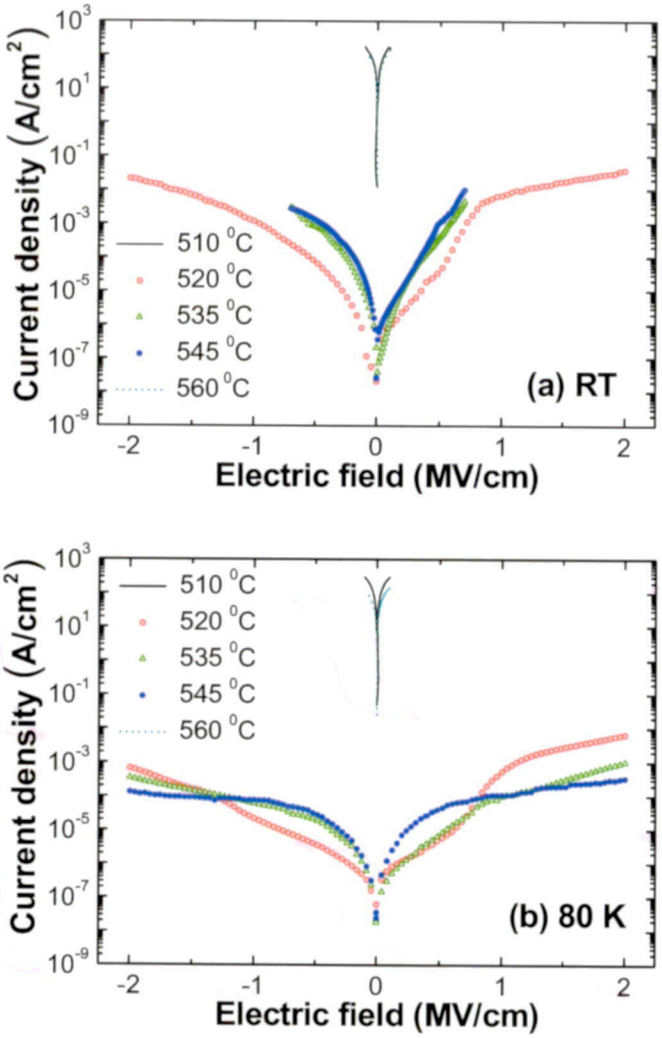

Figure 4.10 *J-E* characteristics of $Bi_{1.1}Fe_{0.9}Co_{0.1}O_3$ thin films annealed by iterative RTA at 510, 520, 535, 545 and 560 °C, measured at (a) RT and (b) 80 K.

4.3.5 *P-E* hysteresis loops of $Bi_{1.1}Fe_{0.9}Co_{0.1}O_3$ thin films annealed in nitrogen by iterative and mono-RTA

The *P-E* hysteresis loops of the $Bi_{1.1}Fe_{0.9}Co_{0.1}O_3$ thin films annealed by iterative RTA at various temperatures were measured at RT and 80 K and are shown in Fig.4.11. The leakage current affects the shape of *P-E* hysteresis loops, and the value of the applied voltage and polarization as well. The thin films annealed at 510 °C and 560 °C show no ferroelectric *P-E* hysteresis loop due to high leakage current at low applied electric field. Ferroelectric *P-E* hysteresis loops are obtained at RT and 80 K in $Bi_{1.1}Fe_{0.9}Co_{0.1}O_3$ thin films annealed from 520 °C to 545 °C. The loops look more saturated in the films measured at 80 K than at RT. The difference in polarization at zero field increases with the increase of the annealing temperature. The polarizations of the $Bi_{1.1}Fe_{0.9}Co_{0.1}O_3$ thin film prepared by iterative RTA at 520 °C are 150 $\mu C/cm^2$ at applied electric field of 3MV/cm and RT and 120 $\mu C/cm^2$ at applied electric field of 4 MV/cm and 80 K. A large polarization can be obtained as the high field can be applied to the films, and the polarization increases with increase of applied electric field in the polycrystalline $BiFeO_3$ [4].

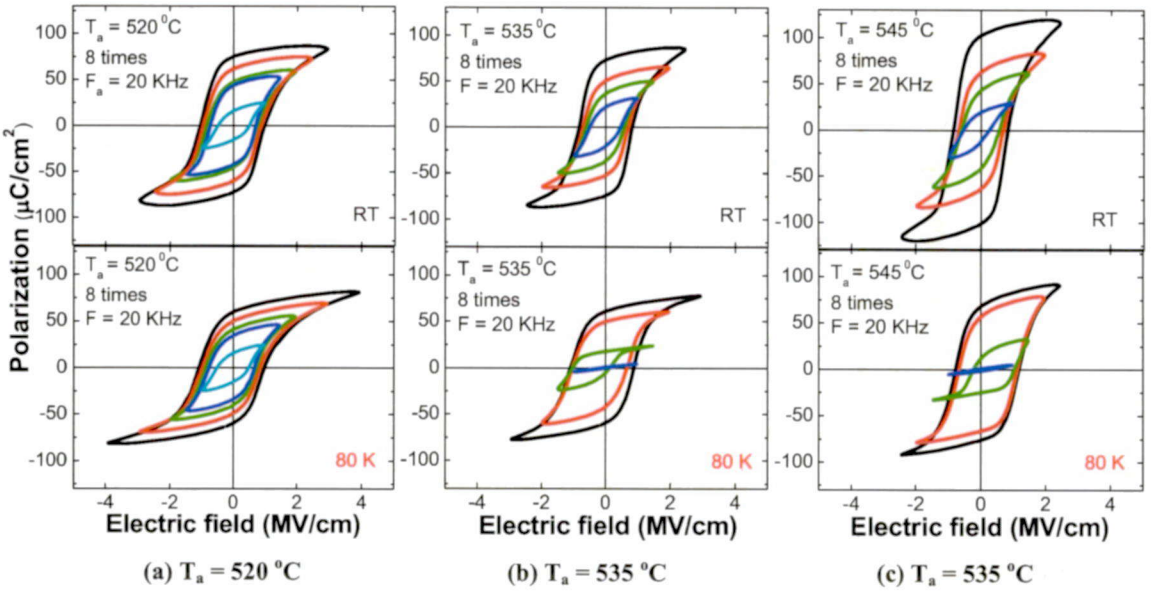

Figure 4.11 *P-E* hysteresis loops of $Bi_{1.1}Fe_{0.9}Co_{0.1}O_3$ thin films annealed by iterative RTA at (a) 520, (b) 535 and (c) 545 °C, measured at RT and 80 K using 20 KHz triangular wave.

On the other hand, *P-E* hysteresis loops can be obtained from in any $Bi_{1.1}Fe_{0.9}Co_{0.1}O_3$ thin films annealed by mono-RTA at temperatures from 510 to 560 °C and are shown in Fig.4.12, but the polarizations are smaller than those of iterative RTA. The polarization of the 545 °C-thin film shows the largest values, which are 108 $\mu C/cm^2$ at applied electric field of 2.5 MV/cm and RT and 114 $\mu C/cm^2$ at applied electric field of 4 MV/cm and RT. Based on the value of the leakage current and *P-E* hysteresis loops, it can be said that $Bi_{1.1}Fe_{0.9}Co_{0.1}O_3$ thin films prepared by RTA in nitrogen have better electric and ferroelectric properties compared to the preparation method of RTA in air [24], and the $Bi_{1.1}Fe_{0.9}Co_{0.1}O_3$ thin film annealed at 520 °C by iterative RTA has the best properties in our experiment.

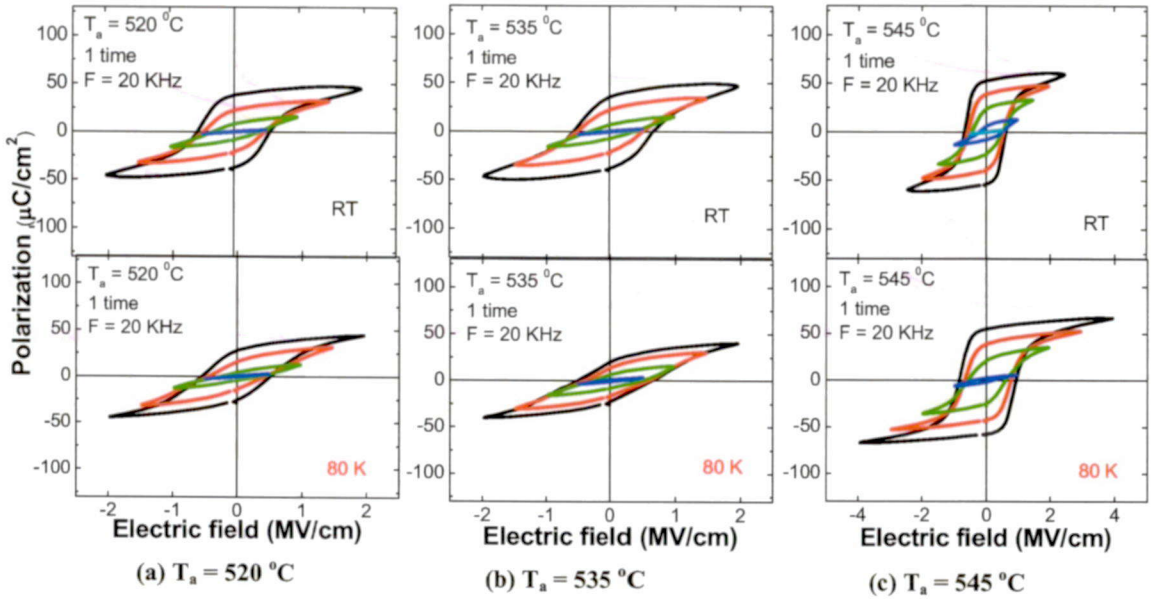

Figure 4.12 *P-E* hysteresis loops of $Bi_{1.1}Fe_{0.9}Co_{0.1}O_3$ thin films annealed by mono-RTA at (a) 520, (b) 535 and (c) 545 °C measured at RT and 80 K using 20 KHz triangular wave.

In order to suppress the effect of the current in the *P-E* hysteresis loops generated by applying an external electric field, BFO thin films were usually measured at high scanning frequency because leakage current can be suppressed due to displacement current. Scanning frequency dependence of *P-E* hysteresis loops of $Bi_{1.1}Fe_{0.9}Co_{0.1}O_3$ thin films prepared by iterative RTA, measured at 80 K and RT, are shown in Fig. 4.13. By applying the electric field at 2 MV/cm, good hysteresis loops is obtained from 100 Hz to 20 KHz at 80 K, and from 10 KHz to 20 KHz at RT. It means that the effect of leakage current on ferroelectric

hysteresis loops of $Bi_{1.1}Fe_{0.9}Co_{0.1}O_3$ thin films is quite small at low temperature, and 10 KHz is the minimum scanning frequency for measurement of the saturated *P-E* hysteresis loop at RT. On the other hand, conventional BFO thin films show good *P-E* hysteresis loops above 20 KHz [31]. Therefore, the preparation of the $Bi_{1.1}Fe_{0.9}Co_{0.1}O_3$ thin film in nitrogen at 520 °C using iterative RTA makes the suppression of scanning frequency for obtaining the well hysteresis loops.

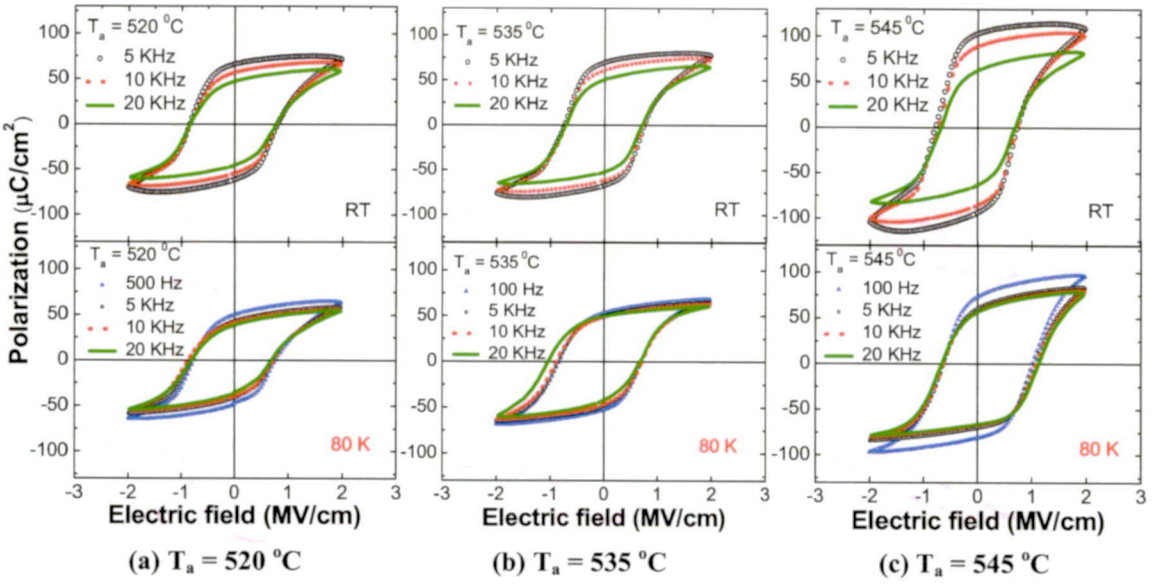

Figure 4.13 Frequency dependence of *P-E* hysteresis loops in $Bi_{1.1}Fe_{0.9}Co_{0.1}O_3$ thin films annealed by iterative RTA at (a) 520, (b) 535 and (c) 545 °C measured at RT and 80 K.

4.3.6 Electric and ferroelectric of $Bi_{1.1}Fe_{1-x}Co_xO_3$ thin films with x = 0~0.3 annealed in nitrogen by iterative RTA

Table 4.1 shows electric and ferroelectric properties of $Bi_{1.1}Fe_{1-x}Co_xO_3$ thin films with various Co concentrations annealed by iterative RTA in nitrogen, measured at RT. By selecting the appropriate annealing temperature, any $Bi_{1.1}Fe_{1-x}Co_xO_3$ thin film with x = 0~0.3 annealed in nitrogen by iterative RTA show ferroelectric property as shown in Table 4.1. The optimal annealing temperature for preparation of ferroelectric BFCO thin films depends on Co concentration. The result shows that the temperature becomes larger with the increase of Co concentration in the BFCO precursor solutions.

Figure 4.14 shows *P-E* hysteresis loops of $Bi_{1.1}FeO_3$, $Bi_{1.1}Fe_{0.95}Co_{0.05}O_3$, $Bi_{1.1}Fe_{0.8}Co_{0.2}O_3$ and $Bi_{1.1}Fe_{0.7}Co_{0.3}O_3$ thin films annealed at optimal temperatures measured at RT and 80 K. Except for the BFCO-Co 10% thin film, *P-E* hysteresis loops of the BFCO-Co 20% shows ferroelectric property at RT, although the loops are still unsaturated. This is induced by large leakage current density at high doped Co concentration and small applied electric field without dielectric breakdown at low doped Co concentration in the BFCO thin films.

Table 4.1 Summary of electric and ferroelectric properties of $Bi_{1.1}Fe_{1-x}Co_xO_3$ thin films prepared by CSD using iterative RTA in nitrogen, measured at RT. Red characters of values correspond to optimal condition of annealing temperature.

$Bi_{1.1}Fe_{1-x}Co_xO_3$	$T_a = 450\ ^oC$		$T_a = 490^oC$		$T_a = 520^oC$		$T_a = 545^oC$	
	J-E	*P-E*	*J-E*	*P-E*	*J-E*	*P –E*	*J-E*	*P-E*
$x = 0$ %	2×10^{-2} A/cm^2 at 500 KV/cm	44 μC/cm^2	Not ferroelectric		Not ferroelectric		Not ferroelectric	
$x = 5$ %	Not ferroelectric		2×10^{2} A/cm^2 at 500 KV/cm	Un-saturated	Not ferroelectric		Not ferroelectric	
$x = 10$ %	Not ferroelectric		Not ferroelectric		1.6×10^{-2} A/cm^2 at 2.0 MV/cm	Un-saturated	10^{-2} A/cm^2 at 700 KV/cm	Un-saturated
$x = 20$ %	Not ferroelectric		Not ferroelectric		10^{-2} A/cm^2 at 700 KV/cm	34 μC/cm^2	2.5×10^{-3} A/cm^2 at 700 KV/cm	25 μC/cm^2
$x = 30$ %	Not ferroelectric		Not ferroelectric		0.85 A/cm^2 at 900 KV/cm	Un-saturated	Not ferroelectric	

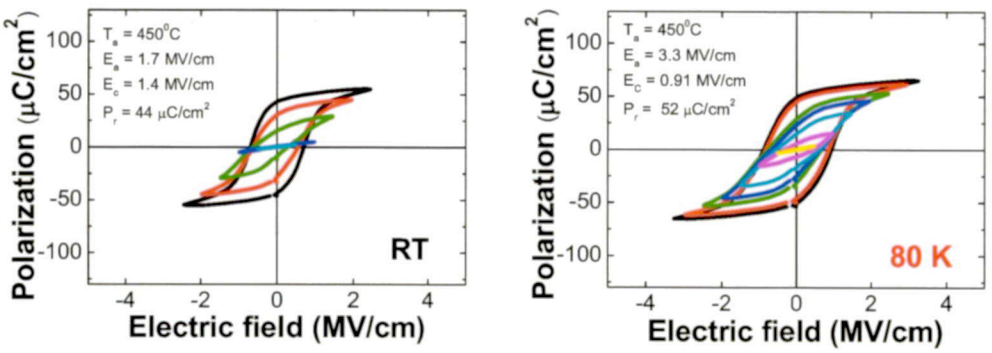

(a) $Bi_{1.1}FeO_3$

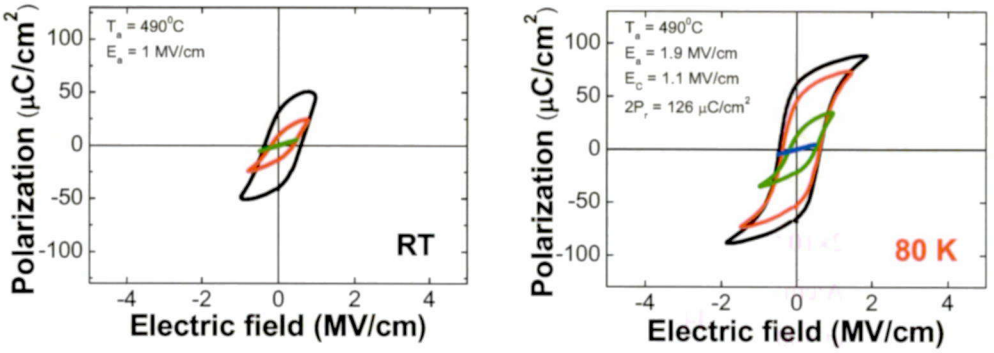

(b) $Bi_{1.1}Fe_{0.95}Co_{0.05}O_3$

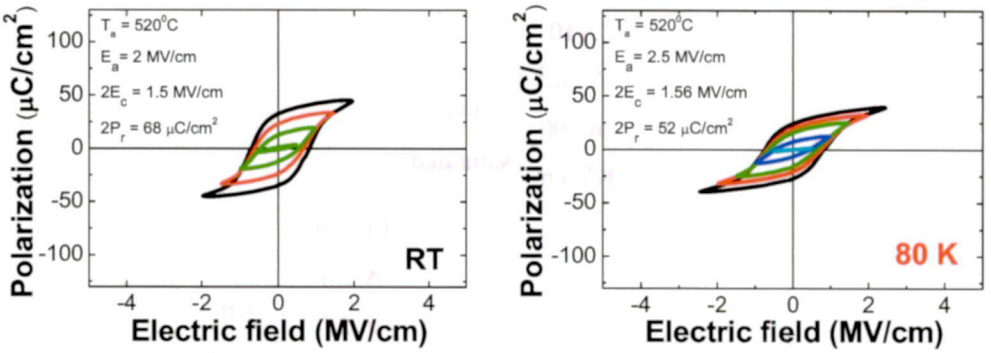

(c) $Bi_{1.1}Fe_{0.8}Co_{0.2}O_3$

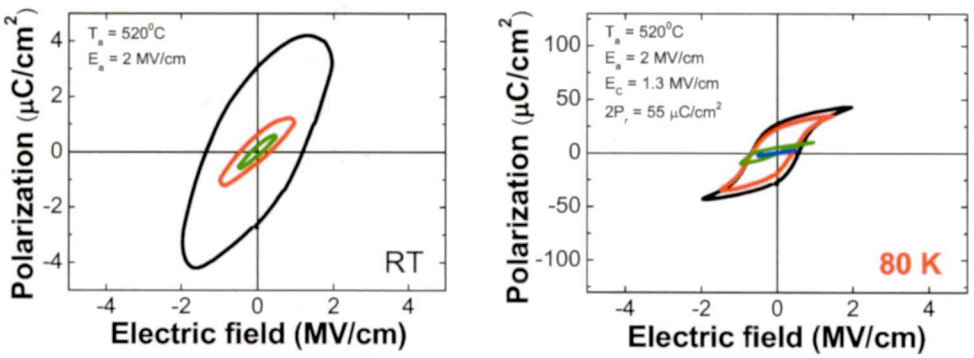

(d) $Bi_{1.1}Fe_{0.7}Co_{0.3}O_3$

Figure 4.14 *P-E* hysteresis loops of $Bi_{1.1}FeO_3$, $Bi_{1.1}Fe_{0.95}Co_{0.05}O_3$, $Bi_{1.1}Fe_{0.8}Co_{0.2}O_3$ and $Bi_{1.1}Fe_{0.7}Co_{0.3}O_3$ thin films annealed at optimal temperatures measured at RT and 80 K.

4.3.7 Ferroelectric domain switch of the $Bi_{1.1}Fe_{0.9}Co_{0.1}O_3$ thin film annealed at 520 °C in nitrogen by iterative RTA

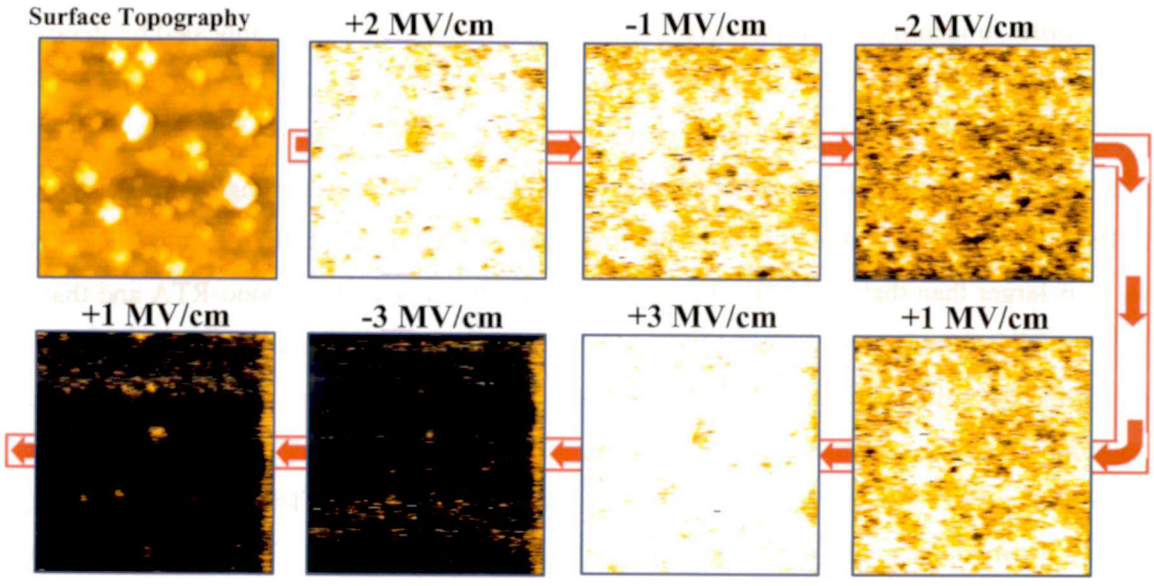

Figure 4.15 Ferroelectric domain switch of the $Bi_{1.1}Fe_{0.9}Co_{0.1}O_3$ thin film annealed 520 °C in nitrogen by iterative RTA measured at RT.

The switch of ferroelectric domains of the $Bi_{1.1}Fe_{0.9}Co_{0.1}O_3$ thin film at RT is characterized as shown in Fig. 4.15. The external DC electric field applied to the surface of the thin film is set as +2, -1, -2, +1, +3, -3 and +1 MV/cm subsequently. Domains seem to be switched at low electric field from -1 to 1 MV/cm. When the field changes from +3 to -3 MV/cm, the switch of domains in orientation of the field seems to be complete. However, un-switch of domains appears when the field increases from -3 to +1 MV/cm. This means there is a dielectric breakdown at -3 MV/cm of applied electric field. Therefore, +2 and -2 MV/cm are selected to identify the switching of domains. The results show that the domains of the $Bi_{1.1}Fe_{0.9}Co_{0.1}O_3$ thin film are oriented incompletely. This confirms the un-saturation of *P-E* hysteresis loops of the film at RT.

4.3.8 Piezoelectric property of $Bi_{1.1}Fe_{0.9}Co_{0.1}O_3$ thin films annealed in nitrogen at 520 °C by iterative RTA and at 545 °C by mono-RTA

In order to identify which piezoelectric property of BFCO thin films annealed by iterative and mono-RTA is better, piezoelectric hysteresis loops of $Bi_{1.1}Fe_{0.9}Co_{0.1}O_3$ thin films annealed in nitrogen at 520 °C by iterative RTA and 545 °C by mono-RTA are shown in Fig.4.16. The piezoelectric coefficient value (d_{33}) of 77 pm/V, representing the piezoreponse of the $Bi_{1.1}Fe_{0.9}Co_{0.1}O_3$ thin film annealed by iterative RTA in the fully clamped state. This value is larger than that in the $Bi_{1.1}Fe_{0.9}Co_{0.1}O_3$ thin film annealed by mono-RTA and that in 300 nm-BFO thin films heteroepitaxially constrained to the STO single crystal substrates in which the d_{33} value decreases with the decrease of the film thickness [1]. Nakashima *et at.* reported that the polycrystalline 350 nm-BFO thin film on $Pt/TiO_2/SiO_2/Si$ substrate deposited by PLD shows litle different d_{33} at various directions [33]. The result indicated that the d_{33} components of (001)- and (110)-orient domains were 27.8 and 26.4 pm/V, respectively. Therefore, it is concluded that the $Bi_{1.1}Fe_{0.9}Co_{0.1}O_3$ thin film annealed by iterative RTA can improve the piezoelectric property of BFCO thin films.

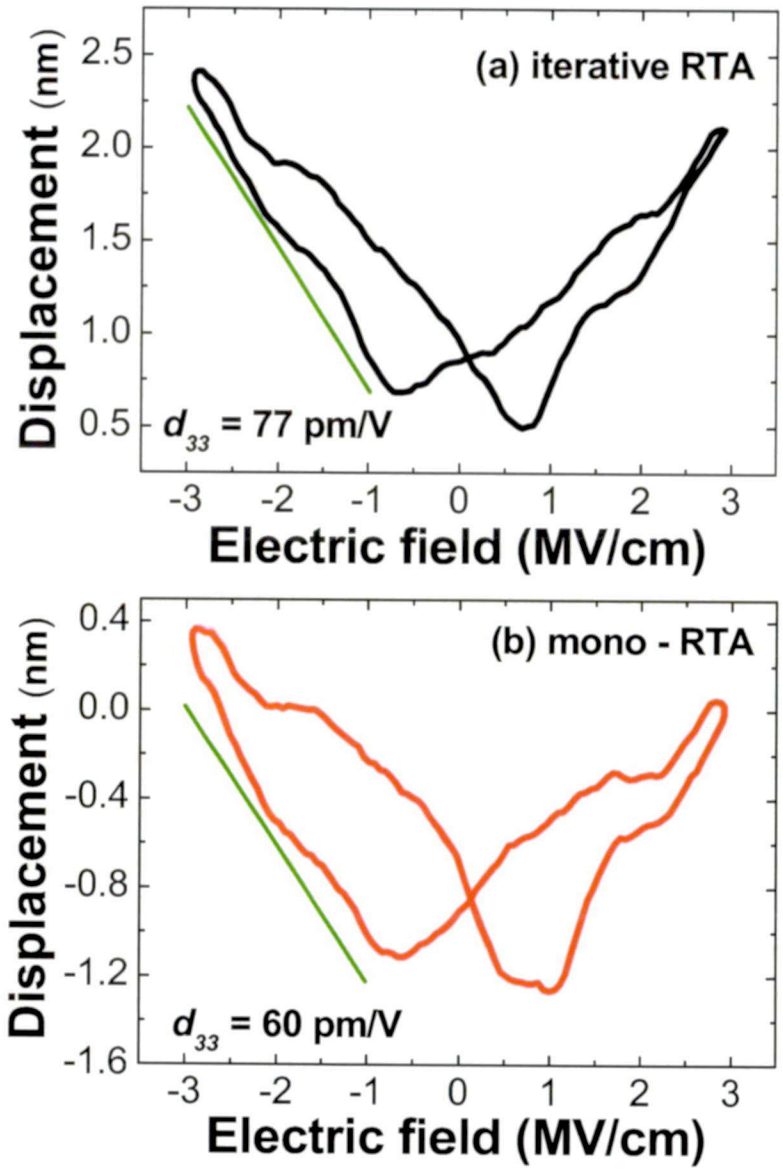

Figure 4.16 Piezoelectric hysteresis loops of $Bi_{1.1}Fe_{0.9}Co_{0.1}O_3$ thin films annealed in nitrogen at (a) 520 °C by iterative RTA and (b) 545 °C by mono-RTA measured at RT.

4.4 CONCLUSION

To reduce the leakage current in ferroelectric BFO for the electronic device application, Co-substituted BFO has been prepared iterative-RTA. $Bi_{1.1}Fe_{1-x}Co_xO_3$ thin films (x = 0~0.3) of 100 nm of thickness by the CSD method using iterative RTA at 450–560 °C in nitrogen have been characterized the electric and ferroelectric properties. The polycrystalline perovskite phases with rhombohedral structure of $BiFeO_3$ were observed clearly. Using the $Bi_{1.1}Fe_{0.9}Co_{0.1}O_3$ precursor solution, it was possible to obtain ferroelectric thin films annealed in nitrogen by iterative and mono-RTA that show good insulation. The cross-section and surface of the BFCO thin films became smooth when thin films were annealed at temperatures lower than 520 °C. While the BFCO thin film annealed by mono-RTA at 545 °C in nitrogen shows the best insulation at RT with 2×10^{-2} A/cm^2 at 1 MV/cm of applied electric field, the electric and ferroelectric properties of the BFCO film annealed by iterative RTA at 520 °C in nitrogen are improved comparatively at 80 K and RT. However, the *P-E* hysteresis loops of the $Bi_{1.1}Fe_{0.9}Co_{0.1}O_3$ thin film annealed at 520 °C by iterative RTA as well as the thin film annealed at 545 °C by mono-RTA seem to be un-saturated at RT. Such behavior of *P-E* loop causes the large leakage current density above 10^{-2} A/cm^2 at applied electric field from 1 to 2 MV/cm. This tendency is confirmed by the completed domain switch of these thin films

On the other hand, the piezoelectricity of the $Bi_{1.1}Fe_{0.9}Co_{0.1}O_3$ thin film annealed at 520 °C by iterative RTA has been improved in comparison with that of the thin film annealed by mono-RTA.

REFERENCES

[1] J. Wang, J. B. Neaton, H. Zheng, V. Nagarajan, S. B. Ogale, B. Liu, D. Viehland, V. Vaithyanathan, D. G. Schlom, U. V. Waghmare, N. A. Spaldin, K. M. Rabe, M. Wuttig, and R. Ramesh: Science **299** (2003) 1719.

[2] J. Li, J. Wang, M. Wuttig, R. Ramesh, N. Wang, B. Ruette, A. P. Pyatakov, A. K. Zvezdin, and D. Viehland: Appl. Phys. Lett. **84** (2004) 5261.

[3] K. Y. Yun, D. Ricinschi, T. Kanashima, M. Noda and M. Okuyama: Jpn. J. Appl. Phys. **43** (2004) L647.

[4] K. Y. Yun, D. Ricinschi, T. Kanashima and M. Okuyama, Appl. Phys. Lett. **89** (2006) 192902-1.

[5] G. Smolenskii, V. Yudin, E. Sher, and Y. E. Stolypin: Sov. Phys. JETP. **16** (1963) 622.

[6] Y. N. Venevtsev, G. Zhadanov, and S. Solov'ev: Sov. Phys. Crystallogr. **4** (1960) 538.

[7] G. Smolenskii, V. Isupov, A. Agranovskaya, and N. Kranik: Sov. Phys. Solid State. **2** (1961) 2651.

[8] M. Takahashi, H. Sugiyama, T. Nakaiso, K. Kodama, M. Noda, and M. Okuyama: Jpn. J. Appl. Phys. **40** (2001) 2923

[9] S. K. Singh, H. Ishiwara, K. Sato, and K. Maruyama: J. Appl. Phys. **102** (2007) 094109.

[10] T. Kawae, Y. Terauchi, H. Tsuda, M. Kumeda, and A. Morimoto: Appl. Phys. Lett. **94** (2009) 112904.

[11] S. Yasui, H. Uchida, H. Nakaki, H. Funakubo, and S. Koda: Jpn. J. Appl. **45** (2006) 7321.

[12] V. R. Singh, A. Garg, and D. C. Agrawal: Soli. Stat. Comm, **149** (2009) 734.

[13] M. Azuma, S. Niitaka, N. Hayashi, K. Oka, M. Takano, H. Funakubo, and Y. Shimakawa: Jpn. J. Appl. Phys. **47** (2008) 7579.

[14] H. Uchida, R. Ueno, H. Funakubo, and S. Koda: J. Appl. Phys. **100** (2006) 014106.

[15] S. K. Singh and H. Ishiwara: Jpn. J. Appl. Phys. **45** (2006) 3194.

[16] P. Kharel, S. Talebi, B. Ramachandran, A. Dixit, V. M. Naik, M. B. Sahana, C. Sudakar, R. Naik, M. S. R. Rao, and G. Lawes: J. Phys. Cond. Mater. **21** (2009) 036001.

[17] N. Izyumskaya, Y. Alivov, and H. Morkoç: Crit. Rev. Sol. Stat. Mat. Sci. **34** (2009) 89.

[18] B. Bhushan, A. Basumallick, S. K. Bandopadhyay, N. Y. Vasanthacharya, and D. Das: J. Phys. D. **42** (2009) 065004.

[19] B. Yu, M. Li, J. Liu, D. Guo, L. Pei, and X. Zhao: J. Phys. **41** (2008) 065003.

[20] A. A. Belik, S. Iikubo, K. Kodama, N. Igawa, S. Shamoto, S. Niitaka, M. Azuma, Y. Shimakawa, M. Takano, F. Izumi, and E. Takayama-Muromachi: Chem. Mater. **18** (2006) 798.

[21] A. Haj: Crys. Res. Tech. **45** (2010) 89.

[22] Y. Wang, G. Xu, L. Yang, Z. Ren, X. Wei, W. Weng, P. Du, G. Shen, and G. Han: Mater. Lett. **62** (2008) 3806.

[23] N. TruongTho, T. Kanashima, M. Sohgawa, D. Ricinschi, M. Noda, and M. Okuyama: "Ferroelectric Property of $Bi_{1.1}Fe_{1-x}Co_xO_3$ Thin Films Prepared by Chemical Solution Deposition Using Iterative Rapid Thermal Annealing in N_2 and O_2", Jpn. J. Appl. Phys. (to be published)

[24] H. Naganuma, J. Miura, M. Nakajima, H. Shima, S. Okamura, S. Yasui, H. Funakubo, B. Nishida, T. Iijima, M. Azuma, Y. Ando, K. Kamishima, K. Kakizaki, and N. Hiratsuka: Jpn. J. Appl. Phys. **47** (2008) 7574.

[25] J. Wu and J. Wang: J. Appl. Phys. 107 (2010) 034103.

[26] C. D. Wagner, W. M. Riggs, L. E. Davis, and J. F. Moulder, G. E. Muilenberg: *Handbook of X-ray Photoelectron Spectroscopy* (Perkin, Minnesota, 1979).

[27] U. Ueda, H. Tabata, and T. Kawai, Appl. Phys. Lett. **75** (1999) 555.

[28] T. Takahashi, T. Esaka, and H. Iwahara: J. Sol. Stat. Chem. **16** (1976) 317.

[29] Y. P. Wang, L. Zhou, M. F. Zhang, X. Y. Chen, J. M. Liu, and Z. G. Liu: Appl. Phys. Lett. **84** (2004) 1731.

[30] S. Yasui, H. Naganuma, S. Okamura, K. Nishida, T. Yamamoto, T. Iijima, M. Azuma, H. Morioka, K. Saito, M. Ishikawa, T, Yamada, and H. Funakubo: Jpn. J. Appl. Phys. **47** (2008) 7582.

[31] Y. Nakamura, S. Nakashima, and M. Okuyama: J. Appl. Phys. **105** (2009) 0616161.

[32] J. K. Yang, W. S. Kim, and H. H. Park: Appl. Surf. Sci. **169-170** (2001) 544.

[33] N. Nakashima, O. Sakata, Y. Nakamura, T. Kanashima, H. Funakubo, and M. Okuyama: Appl. Phys. Lett. 93 (2008) 0429071.

[34] S. K. Singh and H. Ishiwara: Jpn. J. Appl. Phys. **44** (2005) L734.

CHAPTER 5

Characterization of $Bi_{1.1}Fe_{1-x}Co_xO_3$ Thin Films Prepared by Chemical Solution Deposition Using Iterative Rapid Thermal Annealing in Oxygen

5.1 INTRODUCTION

In chapter 4, iterative rapid thermal annealing (iterative RTA) in nitrogen has been discussed, and the leakage current of $Bi_{1.1}Fe_{0.9}Co_{0.1}O_3$ (BFCO) thin films has been suppressed to 2×10^{-2} A/cm^2 under an applied electric field of 2 MV/cm at RT [1, 2]. Ferroelectric hysteresis loops has been obtained at RT in this film, but the leakage current of BFCO prepared in nitrogen ambient is large for electric device applications such as FeRAM. In the case of non-volatile 1T1C-type FeRAMs, a significant leakage component causes a hysteresis deformation [3]. Moreover, in the case of 1T type FeRAMs, leakage current much affects the retention time, since the leakage current due to the depolarization field is one of the main reasons for the short retention time. To suppress the leakage current, I draw attention to oxygen vacancies. Oxygen vacancies are easily generated in many ferroelectric materials such as PZT, BIT, and SBT, and oxygen vacancies are a common source of electrical degradation, fatigue, and ageing [4]. Moreover, it is though that the oxygen vacancies play a prominent role in leakage current of the films [5, 6]. BFCO thin films annealed in nitrogen could create oxygen vacancies as Belik et al. reported [7]. This is induced by the valence fluctuations of Fe ions (+2 and +3) in the thin films [8, 9]. According to defect equilibrium:

$$O_o \leftrightarrow \frac{1}{2} O_2 + V_o + 2e^-,$$

$$Fe^{3+} + e \leftrightarrow Fe^{2+}.$$

So, it is thought that many oxygen vacancies exit in BFCO prepared in nitrogen. In this chapter, in order to suppress the leakage current by the reduction of oxygen vacancies, I have prepared ferroelectric $Bi_{1.1}Fe_{1-x}Co_xO_3$ thin films with cobalt concentrations from 0 to 0.3 by CSD, using iterative RTA in oxygen at low annealing temperatures from 500 to 520 °C. I think that iterative annealing is more appropriate for thermal reaction at low temperature in comparison with mono-RTA. Deposition procedure is almost same to that described in previous chapter except for the ambient.

5.2 RESULTS AND DISCUSSION

5.2.1 Crystallization of BFCO thin films annealed in oxygen by iterative RTA

In my experiment, processing temperatures for preparation of BFO thin films depend on the ambient in which the thin films are annealed by iterative RTA. The results indicate that the $Bi_{1.1}FeO_3$ annealed at 500 °C and $Bi_{1.1}Fe_{0.8}Co_{0.1}O_3$ thin film annealed at 520 °C in oxygen by iterative RTA show good insulation and ferroeletricity as mention later. Thus, to determine the orientation of the films, reciprocal space mappings of the $Bi_{1.1}FeO_3$ annealed at 500 °C and $Bi_{1.1}Fe_{0.8}Co_{0.1}O_3$ thin film annealed at 520 °C in oxygen by iterative RTA are shown in Fig.5.1. Randomly oriented BFCO film is obtained, and BFCO is not polycrystalline and does not display epitaxial growth.

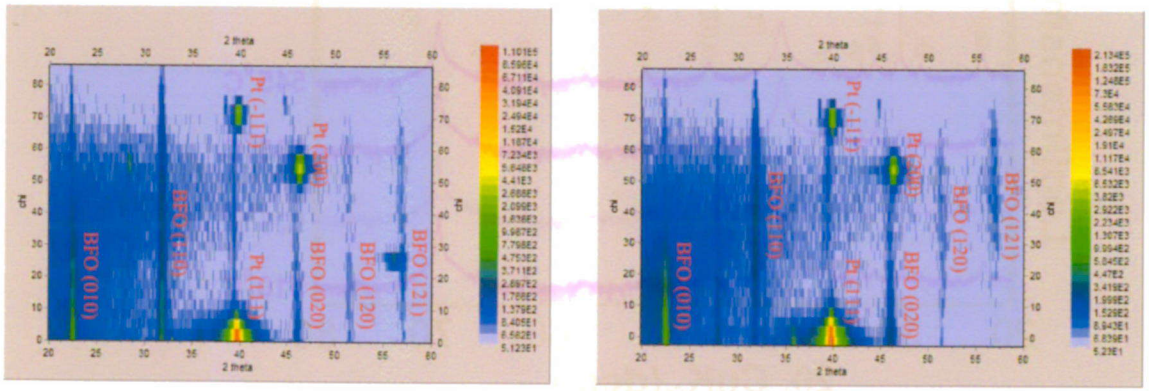

(a) $Bi_{1.1}FeO_3$ **(b) $Bi_{1.1}Fe_{0.8}Co_{0.2}O_3$**

Figure 5.1 Reciprocal space mappings of (a) the $Bi_{1.1}FeO_3$ thin film annealed at 500 °C and (b) the $Bi_{1.1}Fe_{0.8}Co_{0.2}O_3$ thin film annealed at 520 °C in oxygen by iterative RTA.

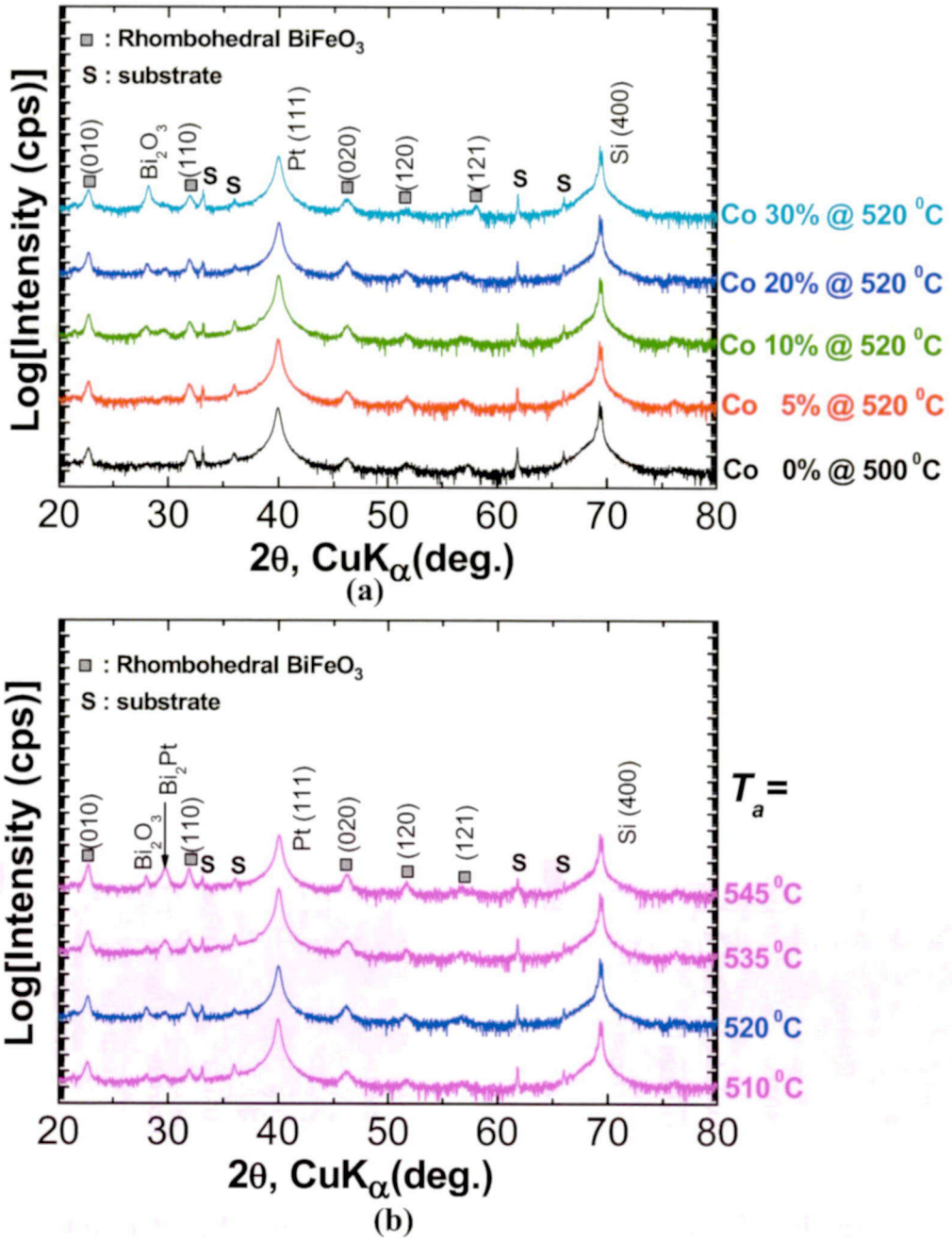

Figure 5.2 XRD θ-2θ patterns of (a) $Bi_{1.1}FeO_3$ thin films annealed at 500 °C and $Bi_{1.1}Fe_{1-x}Co_xO_3$ (x = 0.05, 0.1, 0.2 and 0.3) thin films at 520 °C in oxygen by iterative RTA, and (b) $Bi_{1.1}Fe_{0.8}Co_{0.2}O_3$ thin films annealed in oxygen at various temperatures by iterative RTA.

The crystalline property of the ferroelectric BFO thin films annealed at 500 °C in O_2 and $Bi_{1.1}Fe_{1-x}Co_xO_3$ thin films annealed at fixed temperature of 520 °C is also investigated on the ferroelectric BFO thin films annealed at 500 °C in O_2, as shown in Fig.5.2(a). Polycrystalline perovskite phases with *R3m* or *R3c* rhombohedral structure of $BiFeO_3$ are observed clearly in all of these thin films. The assignment of either *R3c* or *R3m* of BFO rhombohedral structure is not clarified by the results from our measurement, because all the peaks of the 2 kinds of rhombohedral structures are very close to each other in XRD patterns. Therefore, I was able to characterize perovskite crystallization from one of the structures. On the other hand, monoclinic Bi_2O_3 phase is also found and is considerably larger in Co-doped BFO thin films than BFO thin films. This Bi_2O_3 phase becomes the largest in the $Bi_{1.1}Fe_{0.7}Co_{0.3}O_3$ thin film. When Bi_2O_3 crystallization is enhanced, some of the Bi_2O_3 clusters might significant generate conductive spots between metallic electrodes and these spots would prevent the poling of BFCO thin films in ferroelectric measurements [10]. This may induce the degradation of ferroelectric property. In general, crystallization intensities of Co-doped BFO thin films annealed in nitrogen are higher than those of Co-doped BFO films annealed in oxygen at the same cobalt concentration and annealing temperatures. Thus, I suggest that bismuth in BFCO annealed in oxygen may be easy to volatilize at high pressure in oxygen ambient and BFCO thin films annealed in nitrogen might suppress Bi volatilization [11]. However, the intensity of Bi_2O_3 in the BFCO thin films annealed in oxygen is also smaller. It is expected that the value of leakage current density of these films at high electric field can be suppressed, so that the saturation of their *P-E* hysteresis loops can be improved at RT.

To characterize the effect of the annealing temperature, θ-2θ XRD patterns of $Bi_{1.1}Fe_{0.8}Co_{0.2}O_3$ thin films annealed at 510, 520, 535 and 540 °C in oxygen are shown in Fig.5.2(b). The intensity of Bi_2Pt assigned at 29.82° of 2θ also appears in the BFCO thin films annealed at temperature above 535 °C in oxygen. The appearance of the secondary peak of the Bi_2Pt suggesting the interface condition of the Pt bottom electrode/ the $Bi_{1.1}Fe_{0.8}Co_{0.2}O_3$ films was changed by high annealing temperature [12]. This suggests that Bi suffers from severe diffusing towards the surface due to volatility of Bi_2O_3, and at the same time, diffusing into the Pt layer at the Pt/BFCO interface. The inter-diffusion layer, occurring during annealing, has a reverse effect on the ferroelectric properties [12]. Therefore, it is expected to avoid or reduce this inter-diffusion phenomenon. During annealing (under O_2 atmosphere), metallic Bi diffuses out of the film and oxidizes into volatile Bi_2O_3 at the surface [13]. This reduces the chemical potential of Bi metal, creating the driving force for

more Bi to migrate from the film towards the surface [14]. This is in general agreement with the ferroelectric hysteresis data which have shown no perceptible improvement in polarization values.

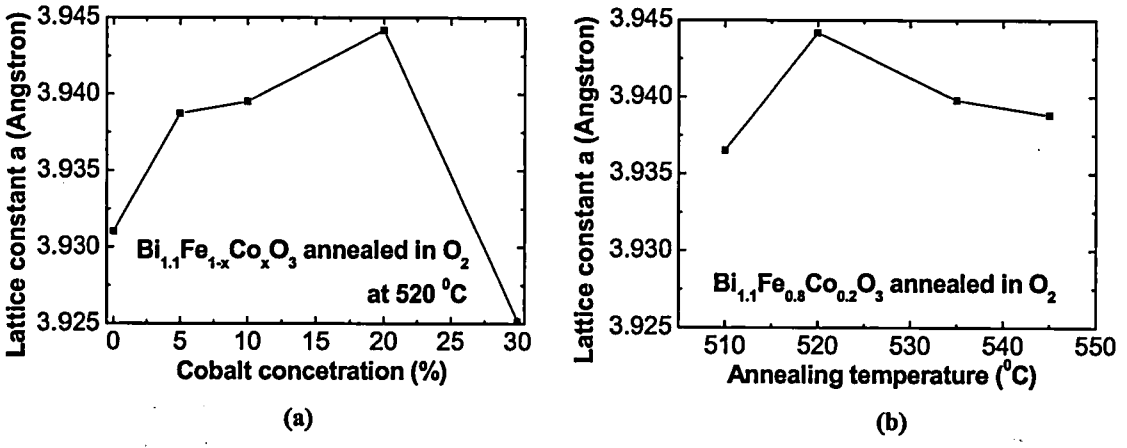

Figure 5.3 Dependence of lattice constants of $Bi_{1.1}Fe_{1-x}Co_xO_3$ thin films on (a) cobalt concentration annealed at 520 °C and (b) at various annealing temperatures with $x = 0.2$ in oxygen.

As mentioned in chapter 4, the lattice constant reaches its maximum at Co concentration of 20% in BFCO thin films annealed in oxygen. Oxygen vacancies may be suppressed by annealing BFCO thin films in oxygen. The main origin of oxygen vacancies is the valence change of iron ions from +3 to +2 [7]. Therefore, it could be concluded that most of the iron ions in BFCO thin films annealed in oxygen are trivalent. Meanwhile, the radius of trivalent iron ions is smaller than that of divalent iron ions. The result shows that more trivalent cobalt ions could be occupied at B-site in BFCO thin films annealed in oxygen in comparison with BFCO thin films annealed in nitrogen. However, the embedding of cobalt oxides makes $BiCoO_3$ structure easy to deviate. Therefore, there is a limited amount of Co occupied at position of Fe^{+3} ions even with the increase of Co concentration, and so no change appears in their crystal symmetry.

5.2.2 Morphologies of BFCO thin films annealed in oxygen by iterative RTA

Figure 5.4 shows the morphology of BFO thin films annealed at 500 °C and the $Bi_{1.1}Fe_{0.8}Co_{0.2}O_3$ films annealed at 520 °C in oxygen. There are small grains and large clusters grain agglomerations. The average of grain sizes in the BFO and the $Bi_{1.1}Fe_{0.8}Co_{0.2}O_3$ thin films is about 130 and 250 nm, respectively. Moreover, the thickness morphology of the BFCO film seems to be smoother than that of the BFO thin film. Grain size of the BFCO

annealed in oxygen is larger than that annealed in nitrogen. It is thought that crystalline temperature is changed by ambient, and crystal growth is enhanced by oxygen.

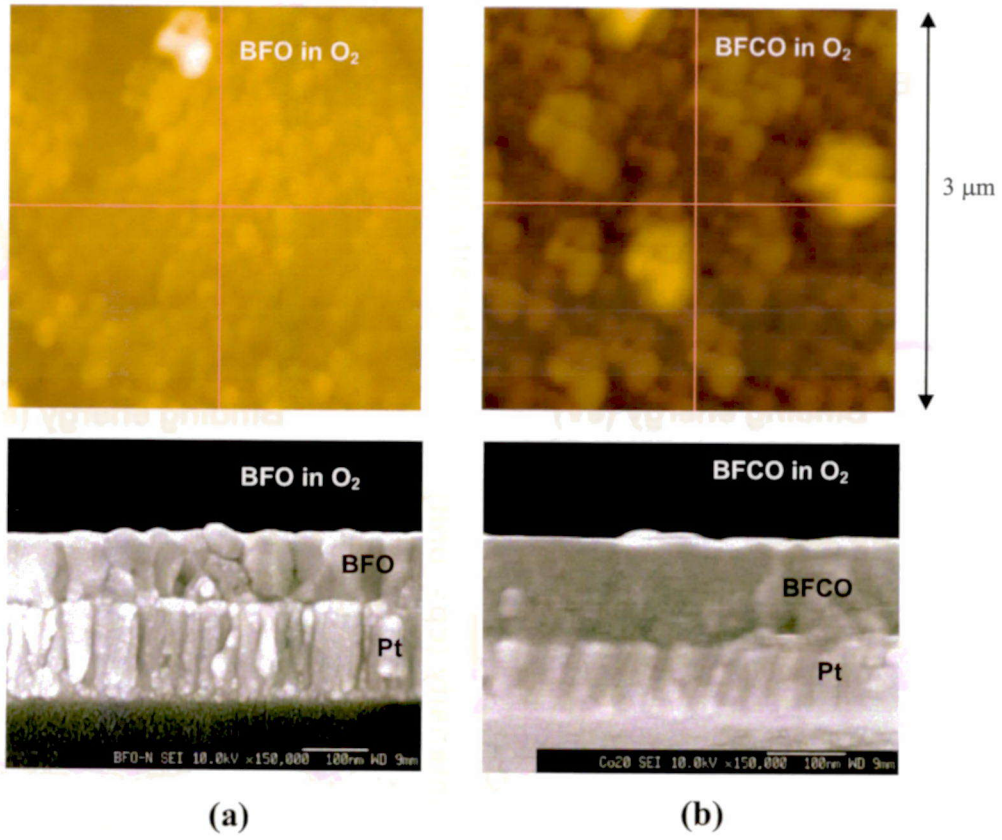

Figure 5.4 Surface morphology of (a) BFO thin film annealed at 500 °C and (b) $Bi_{1.1}Fe_{0.8}Co_{0.2}O_3$ thin film annealed at 520 °C in oxygen by iterative RTA.

5.2.3 XPS spectra of BFCO thin films annealed in oxygen by iterative RTA

Figures 5.5 show XPS spectra of BFO, $B_{1.1}Fe_{0.9}Co_{0.1}O_3$ and $Bi_{1.1}Fe_{0.8}Co_{0.2}O_3$ thin films annealed in oxygen. Co^{2+} and Co^{3+} ions in chemical bonding of Co *2p* show no different because of their weak intensities below the XPS detection limit. However, the change in the concentration of cobalt in $Bi_{1.1}Fe_{1-x}Co_xO_3$ thin films induces decrease of Fe *2p* intensities when x increases in all XPS spectra. Bi $4f_{7/2}$ at 158.5 eV and Fe $2p_{3/2}$ at 710.7 eV shift to lower energy, because the electrical charge of insulation BFO and BFCO thin films was induced by photoelectrons during XPS measurement. However, the signal around the Fe $2p_{3/2}$ peak includes a considerable amount of background noises that make the estimation

inaccurate. On the other hand, bismuth peaks are observed at 157.8 eV in three thin films and they demonstrate the trivalent bismuth [15].

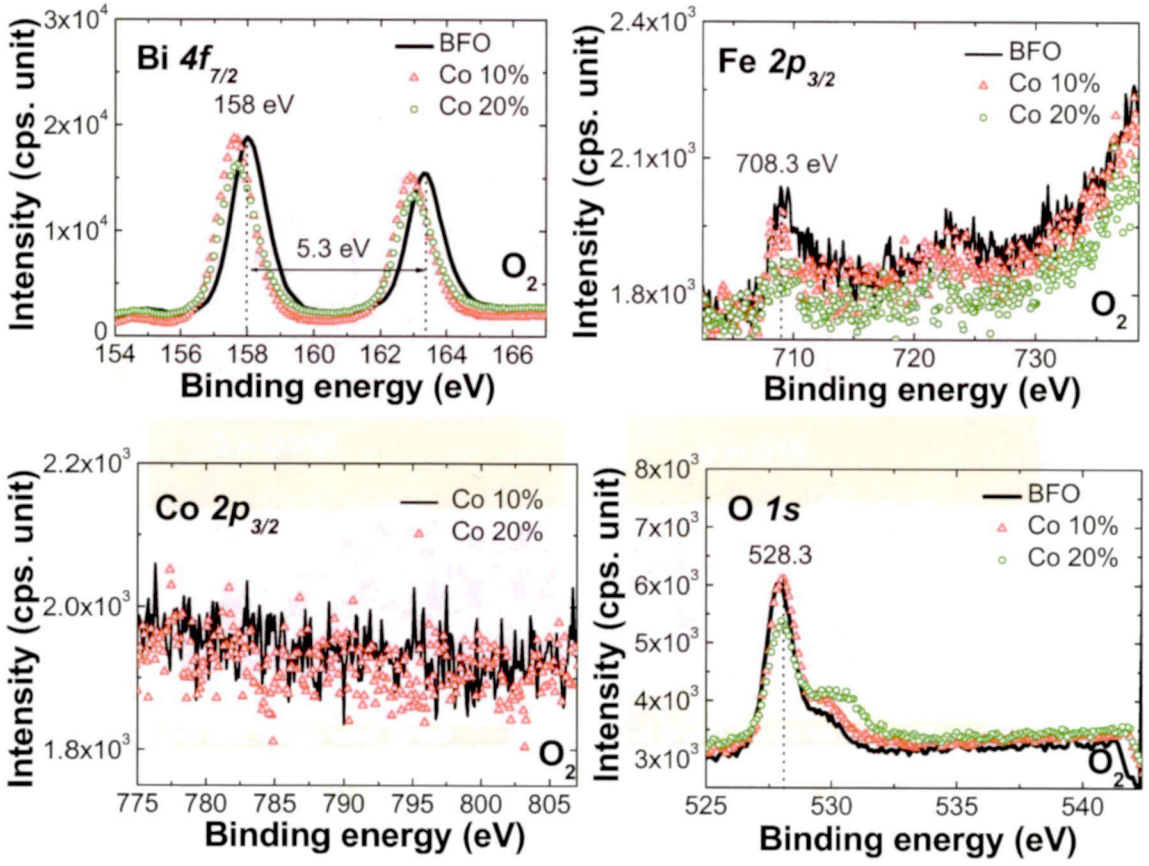

Figure 5.5 XPS spectra of Bi *4f*, Fe *2p*, Co *2p* and O *1s* in BFO annealed at 500 °C, $Bi_{1.1}Fe_{0.9}Co_{0.1}O_3$ (Co 10%) and $Bi_{1.1}Fe_{0.8}Co_{0.2}O_3$ (Co 20%) thin films annealed at 520 °C in O_2.

Although it is difficult to estimate the iron valence from the Fe $2p_{3/2}$ spectra by the shift of binding energy and the background noises, its valence could be implied by O *1s* XPS spectra of all thin films. There is a small additional satellite peak at 530 eV in O *1s* XPS spectra of BFO thin films, which corresponds to O–Fe bonding with iron trivalent [15]. When the cobalt concentration is increased to 20 % in the $Bi_{1.1}Fe_{1-x}Co_xO_3$ thin films annealed in O_2, the satellite peak becomes broad but does not increase. This means position of the satellite peak is not changed when Co concentration increases from 0 to 20% in BFCO thin films. Thus, almost all iron ions are still trivalent.

5.2.4 *J-E* characteristics of BFCO thin films

In order to compare electric and ferroelectric properties of BFCO thin films annealed in oxygen, I also prepared the films by conventional CSD using mono-RTA for 20 min, and characterized their leakage current and *P-E* hysteresis loop properties. The results indicate that these as-synthesized films show no ferroelectric *P-E* hysteresis loops due to high leakage current and weak crystallization of rhombohedral BFO. For example, the leakage current density of the film annealed at 520 °C by mono-RTA is 8×10^{-3} A/cm^2 at maximum applied electric field of 250 kV/cm without dielectric breakdown and RT, and 2.6×10^{-2} A/cm^2 at maximum applied electric field of 500 kV/cm without dielectric breakdown and 80 K. I have characterized the BFCO thin films prepared by iterative-RTA. Current density versus applied electric field of BFCO thin films annealed at 520 °C and BFO thin films annealed at 500 °C in oxygen, measured at RT are shown in Fig.5.6. The BFCO thin film with 20% cobalt concentration does not show electrical breakdown at 1.5 MV/cm of electric field, and the leakage current density of the thin film corresponding to the electric field is just about 8×10^{-3} A/cm^2. Moreover, its leakage current density is smallest at applied electric field above 700 KV/cm of all BFCO and BFO thin films. Thus, this is expected that the low leakage current of the $Bi_{1.1}Fe_{0.8}Co_{0.2}O_3$ thin film reinforces its saturation at RT.

As mentioned in chapter 4, the appearance of Bi_2O_3 clusters in BFCO thin films may create conductive paths between metallic electrodes, which may suppress the insulation property [1, 2, 8]. It means that optimization of the condition to decrease intensity of monoclinic Bi_2O_3 phase is necessary to enhance insulation of BFCO thin films, although a Bi-excess precursor solution needs to be used for volatilization suppression of bismuth at high annealing temperatures. However, the Co 5%-BFCO thin film, with no Bi_2O_3 peaks (in Fig.5.2), annealed at 520 °C in oxygen, shows large leakage current density and is easy to be electrical broken down at 800 KV/cm and RT (in Fig.5.6). Meanwhile, the $Bi_{1.1}Fe_{0.8}Co_{0.2}O_3$ thin film annealed at 520 °C in oxygen shows the low intensity of the Bi_2O_3 peak and the broken down field of 1.5 MV/cm at RT, as shown in Fig.5.6. Therefore, it is suggested that the suppression of leakage current in the $Bi_{1.1}Fe_{0.8}Co_{0.2}O_3$ film may be induced by the appearance of a sufficient $BiCoO_3$ amount. In order to explain the result, I suppose that almost all cobalt belongs to cobalt oxides in BFCO thin films with cobalt concentration below 20%. Inversely, the $BiCoO_3$ structure is easy to deviate by increase of embedded cobalt oxides in BFCO thin film with cobalt concentration above 20% [7]. Therefore, the

larger leakage current of the $Bi_{1.1}Fe_{1-x}Co_xO_3$ (x = 0.05, 0.1, and 0.3) thin films may be induced mainly by the domination of cobalt oxides. In *P-E* ferroelectric loops, the saturation will usually appear at a high electric field. Therefore, the $Bi_{1.1}Fe_{0.8}Co_{0.2}O_3$ thin film with low leakage current of 8.3×10^{-3} A/cm at the large electric field of 1.5 MV/cm at RT is considered as the optimal insulation thin films, which is expected to show saturation hysteresis loops.

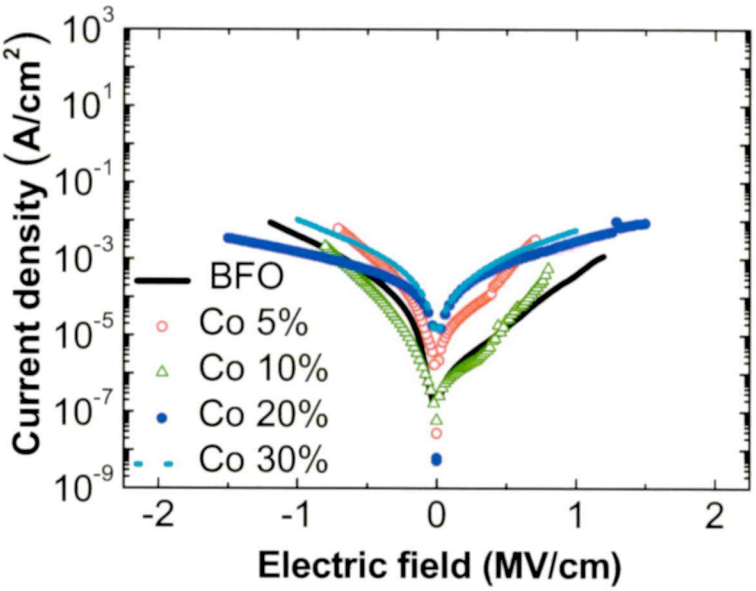

Figure 5.6 *J-E* characteristics of BFCO thin films annealed at 520 °C and the BFO thin film annealed at 500 °C in oxygen measured at RT.

In order to determine annealing temperature for the preparation of good insulation $Bi_{1.1}Fe_{0.8}Co_{0.2}O_3$ thin films by iterative RTA in oxygen, *J-E* characteristics of $Bi_{1.1}Fe_{0.8}Co_{0.2}O_3$ thin films annealed at 510, 520, 535, and 545 °C in oxygen were measured at 80 K and RT, and are shown in Fig.5.7. The result shows that there is little difference in the *J-E* characteristic at 80 K among thin films annealed from 520 °C to 545 °C, although the film annealed at 510 °C produces large leakage current. On the other hand, the $Bi_{1.1}Fe_{0.8}Co_{0.2}O_3$ thin film, annealed at 520 °C, shows low leakage current of 8.3×10^{-3} A/cm at the largest electric field of 1.5 MV/cm at RT. One of purposes in my experiment is the selection of the ferroelectric thin films which shows saturation polarization at the temperature as high as possible. Thus, I conclude that 520 °C is the optimal annealing temperature to obtain improved insulation thin films.

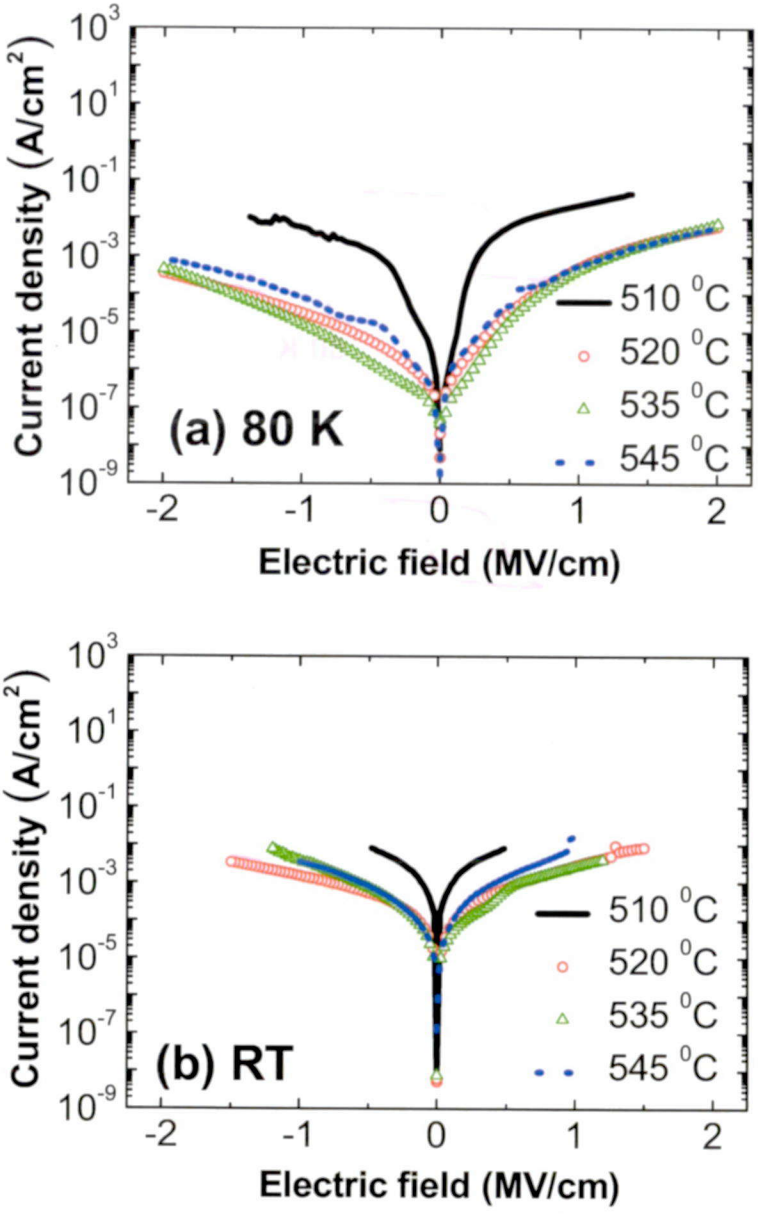

Figure 5.7 *J-E* characteristics of $Bi_{1.1}Fe_{0.8}Co_{0.2}O_3$ thin films annealed at 510, 520, 535 and 545 °C in oxygen, measured at (a) 80 K and (b) RT.

5.2.5 Electric and ferroelectric of $Bi_{1.1}Fe_{1-x}Co_xO_3$ thin films with $x = 0 \sim 0.3$ annealed in oxygen by iterative RTA

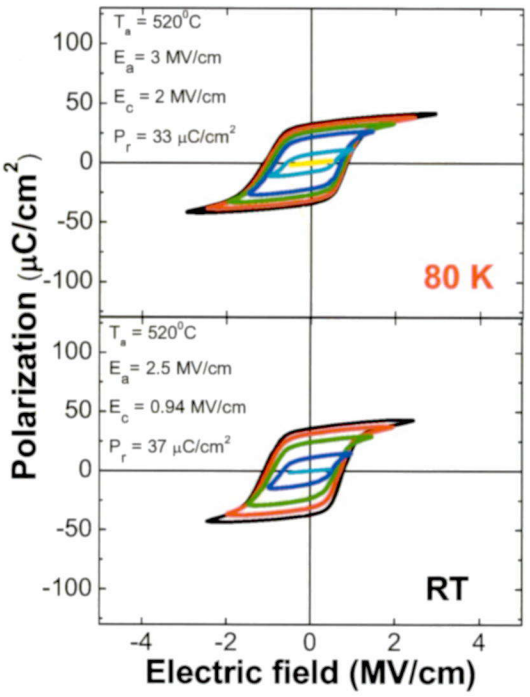

Figure 5.8 *P-E* hysteresis loops of the $Bi_{1.1}Fe_{0.8}Co_{0.2}O_3$ thin films annealed at 520 °C in oxygen, measured at 80 K and RT using 20 KHz triangular wave.

To characterize the ferroelectric property of BFCO thin films, *P-E* hysteresis loops of $Bi_{1.1}Fe_{0.8}Co_{0.2}O_3$ and $Bi_{1.1}Fe_{0.9}Co_{0.1}O_3$ thin films annealed at 520 °C in oxygen were measured at 80 K and RT and are shown in Figs.5.8 and 5.9. In order to compare ferroelectric of BFCO thin films to that of BFO thin films, the loops of BFO thin films annealed at 500 °C in oxygen measured at 80 K and RT, and the results are also shown in Fig.5.10. The results indicate that the leakage current affects the shape of the *P-E* hysteresis loops and the value of polarization. The $Bi_{1.1}Fe_{0.8}Co_{0.2}O_3$ thin films annealed at 520 °C in oxygen show low leakage current of 1.5 MV/cm at high electric field, its *P-E* hysteresis loops is saturated but remanent polarization (P_r) is small. Conversely, the *P-E* hysteresis loops of the $Bi_{1.1}Fe_{0.9}Co_{0.1}O_3$ film annealed at 520 °C in oxygen and the BFO thin film annealed at 500 °C in oxygen are less saturated due to higher leakage current at high electric field. However, the remanent polarization of $Bi_{1.1}Fe_{0.9}Co_{0.1}O_3$, BFO and $Bi_{1.1}Fe_{0.8}Co_{0.2}O_3$ thin films at RT is 68, 45 and 37 $\mu C/cm^2$, respectively. It may be induced by the maximum applied electric field without

electric breakdown. In this case, the applied electric field of $Bi_{1.1}Fe_{0.9}Co_{0.1}O_3$, BFO and $Bi_{1.1}Fe_{0.8}Co_{0.2}O_3$ thin films is 0.8, 1.2 and 1.5 MV/cm, respectively. At 80 K, remanent polarization of BFO thin film annealed at 500 °C in oxygen is the largest value, which is about 101 $\mu C/cm^2$. But, 68 $\mu C/cm^2$, the remanent polarization of the $Bi_{1.1}Fe_{0.9}Co_{0.1}O_3$ film annealed at 520 °C in oxygen is larger than in the case of BFO thin films annealed in N_2 and O_2 at RT. However, the $Bi_{1.1}Fe_{0.8}Co_{0.2}O_3$ thin films annealed at 520 °C in oxygen by iterative-RTA is considered as the candidate of ferroelectric thin films with saturation polarization at RT may be applied in preparation of FeRAM.

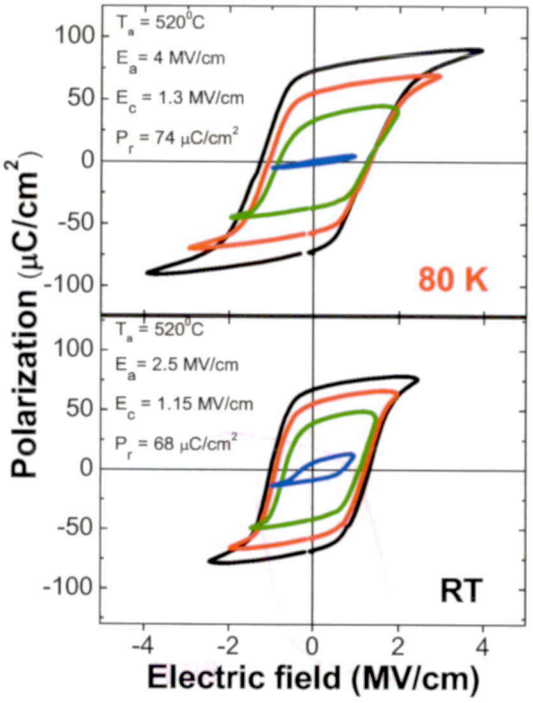

Figure 5.9 *P-E* hysteresis loops of the $Bi_{1.1}Fe_{0.9}Co_{0.1}O_3$ thin film annealed at 520 °C in oxygen, measured at 80 K and RT using 20 KHz triangular wave.

Table 5.1 shows the values of remanent polarization and leakage current density of all BFCO thin films annealed in oxygen at several different temperatures, measured at RT. By selecting appropriated annealing temperature, any $Bi_{1.1}Fe_{1-x}Co_xO_3$ thin film with x = 0~0.3 prepared in oxygen shows ferroelectric property. Especially, typical *P-E* ferroelectric loops of any $Bi_{1.1}Fe_{1-x}Co_xO_3$ thin film annealed in oxygen are observed if the necessary conditions of annealing temperature are fulfilled. The optimal annealing temperature for preparation of ferroelectric BFCO thin films depends on the Co concentration. The temperature becomes

larger with the increase of the Co concentration in the BFCO precursor solution. On the other hand, the temperatures for preparation of thin films with the same low cobalt concentration in oxygen are always larger than those in nitrogen. It may be induced that crystallization of the thin film annealed in nitrogen at the same temperature is better than that in oxygen. However, the saturation and the value of remanent polarization of the BFCO thin film annealed in oxygen are also better than those of films annealed in nitrogen with the same cobalt concentration of over 10% and the same annealing temperature.

The $Bi_{1.1}Fe_{0.8}Co_{0.2}O_3$ thin film has possible application in FeRAM because of its low leakage current and saturation polarization without imprint at RT. However, this has not been yet verified as measurements of charge retention ($\mu C/cm^2$) dependent on relaxation time (s) and polarization fatigue have not been carried out. The thin film could be used as capacitor material in the structure of Metal-Ferroelectric-Insulator-Semiconductor (MFIS) of FeRAM if the value of $(\pm P_{SW})-(\pm P_{NS})$ stays unchanged during a long relaxation time (where P_{SW} and P_{NS} are switching and non-switching polarizations of the thin film) and its remanent polarization is not reduced after a continuous cycling of negative and positive bias [3].

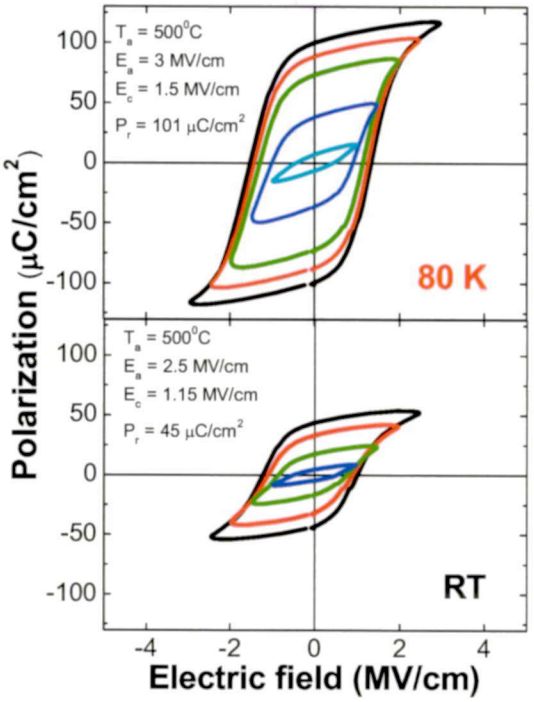

Figure 5.10 *P-E* hysteresis loops of $Bi_{1.1}FeO_3$ thin films annealed at 500 °C in oxygen, measured at 80 K and RT using 20 KHz triangular wave.

Table 5.1 Summary of electric and ferroelectric properties of $Bi_{1.1}Fe_{1-x}Co_xO_3$ thin films prepared by CSD using iterative RTA in oxygen measured at RT.

$Bi_{1.1}Fe_{1-x}Co_xO_3$	**Iterative RTA preparation in O_2**							
	T_a = 500 °C		**T_a = 510 °C**		**T_a = 520 °C**		**T_a = 545 °C**	
	J-E	***P-E***	***J-E***	***P-E***	***J-E***	***P -E***	***J-E***	***P-E***
***x* = 0 %**	10^{-2} A/cm^2 at 1.2 MV/cm	45 μC/cm^2	2.5×10^{2} A/cm^2 at 800 KV/cm	Un-saturated	Not ferroelectric		Not ferroelectric	
***x* = 5 %**	4.2×10^{-2} A/cm^2 at 500 KV/cm	Un-saturated	2×10^{-1} A/cm^2 at 1.0 MV/cm	44 μC/cm^2	Not ferroelectric		Not ferroelectric	
***x* = 10 %**	Not ferroelectric		Not ferroelectric		2×10^{-3} A/cm^2 at 800 KV/cm	68 μC/cm^2	1.4×10^{-2} A/cm^2 at 800 KV/cm	42 μC/cm^2
***x* = 20 %**	Not ferroelectric		Not ferroelectric		8.7×10^{-3} A/cm^2 at 1.5 MV/cm	37 μC/cm^2	1.3×10^{-2} A/cm^2 at 1.0 MV/cm	61 μC/cm^2
***x* = 30 %**	Not ferroelectric		Not ferroelectric		10^{-2} A/cm^2 at 1.0 MV/cm	34 μC/cm^2	Not ferroelectric	

5.2.6 Ferroelectric domain switch of the $Bi_{1.1}Fe_{0.8}Co_{0.2}O_3$ thin film annealed at 520 °C and $Bi_{1.1}FeO_3$ thin film annealed at 500 °C thin films in oxygen by iterative RTA

The domain switch of the $Bi_{1.1}FeO_3$ annealed at 500 °C and $Bi_{1.1}Fe_{0.8}Co_{0.2}O_3$ thin films annealed at 520 °C in oxygen measured at RT is characterized as shown in Fig.5.11. Although both films are applied at low electric field of 1 MV/cm in comparison with the $Bi_{1.1}Fe_{0.9}Co_{0.1}O_3$ thin film annealed at 520 °C in nitrogen as discussed in chapter 4, the switch of domains in orientation of the field seems to be complete. The electric saturation of the ferroelectric BFO and BFCO thin films annealed in oxygen is better than that of ferroelectric BFCO thin films annealed in nitrogen by iterative RTA at RT. Thus, annealing in oxygen ambient enhances ferroelectric domain switch of $Bi_{1.1}Fe_{1-x}Co_xO_3$ thin films so that their saturation is improved at RT.

5.2.7 Piezoelectric property of the $Bi_{1.1}Fe_{0.8}Co_{0.2}O_3$ thin film annealed at 520 °C and $Bi_{1.1}FeO_3$ thin film annealed at 500 °C thin films in oxygen by iterative RTA

The piezoelectric property of $Bi_{1.1}FeO_3$ annealed at 500 °C and $Bi_{1.1}Fe_{0.8}Co_{0.2}O_3$ thin films annealed at 520 °C in oxygen by iterative RTA is shown in Fig.5.12. The piezoelectric coefficient value (d_{33}) calculated from the data is very weak. The maximum d_{33} is 28.51 and 7.3 pm/V in the BFO and the BFCO thin films, respectively. It is smaller than that of the $Bi_{1.1}Fe_{0.9}Co_{0.1}O_3$ thin film annealed at 520 °C in nitroegn by iterative RTA. This fact shows that $Bi_{1.1}Fe_{1-x}Co_xO_3$ thin films annealed in oxygen suppress piezoelectric property.

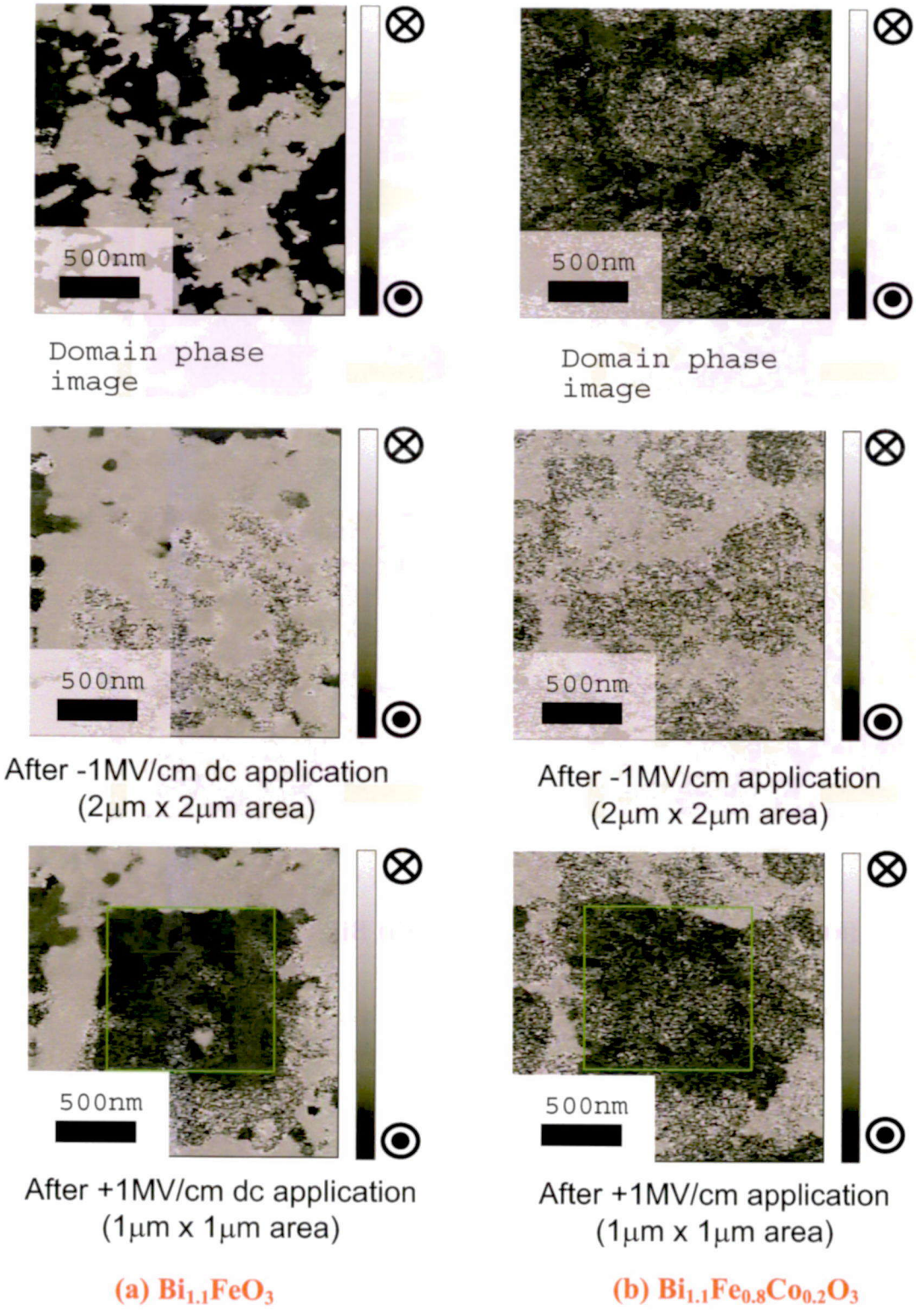

Figure 5.11 Ferroelectric domain switch of the $Bi_{1.1}FeO_3$ thin film annealed at 500 °C and the $Bi_{1.1}Fe_{0.9}Co_{0.1}O_3$ thin film annealed at 520 °C in oxygen by iterative RTA measured at RT.

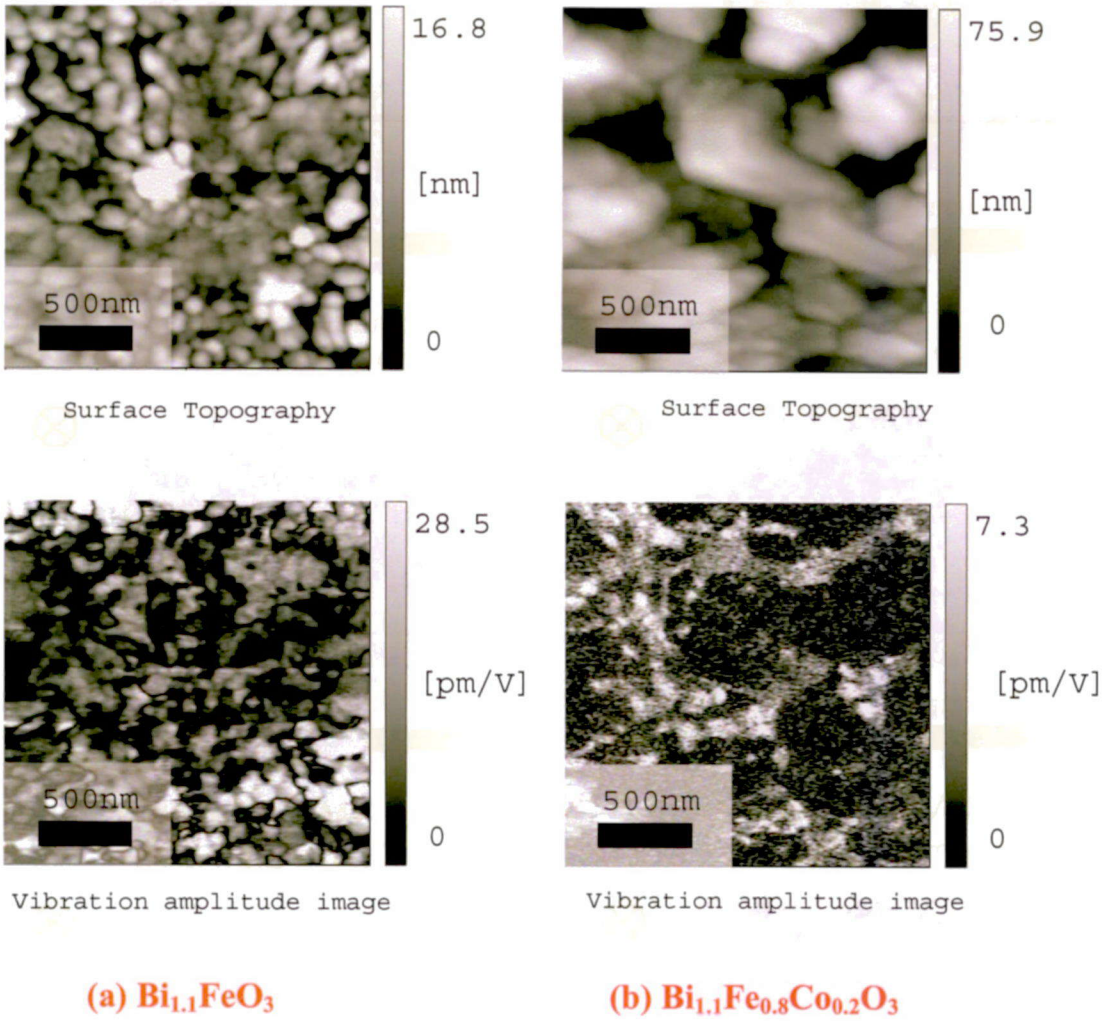

Figure 5.12 Piezoelectric hysteresis loops of the $Bi_{1.1}FeO_3$ thin film annealed at 500 °C and the $Bi_{1.1}Fe_{0.8}Co_{0.2}O_3$ thin film annealed at 520 °C in oxygen by iterative RTA measured at RT.

5.3 CONCLUSION

I have prepared $Bi_{1.1}Fe_{1-x}Co_xO_3$ thin films (x = 0~0.3) of 100 nm thickness by CSD using the iterative RTA in oxygen, although the ferroelectric $Bi_{1.1}Fe_{0.8}Co_{0.2}O_3$ thin film can not be obtained by mono-RTA in oxygen. The polycrystalline perovskite phases with rhombohedral structure of $BiFeO_3$ were observed clearly. The $Bi_{1.1}Fe_{0.8}Co_{0.2}O_3$ thin film annealed in oxygen at 520 °C does not break down electrically at 1.5 MV/cm at RT and its saturation polarization was improved due to smaller leakage current at quite high applied electric field. BFCO thin films with high cobalt concentrations of 10 and 20 % show lower leakage current and larger polarization compared to those of BFO thin films annealed in nitrogen and oxygen.

The suppression of leakage current and the enhancement of saturation of $Bi_{1.1}Fe_{1-x}Co_xO_3$ thin films annealed in oxygen by iterative RTA are further clarified by means of the completed switch of domains of the $Bi_{1.1}FeO_3$ annealed at 500 °C and $Bi_{1.1}Fe_{0.8}Co_{0.2}O_3$ thin films annealed at 520 °C in oxygen measured at RT.

The piezoelectric property of both thin films is weak, especially in the $Bi_{1.1}Fe_{0.8}Co_{0.2}O_3$ thin film. This is one of the evidences for weaker ferroelectric property in comparison with that of $Bi_{1.1}Fe_{1-x}Co_xO_3$ thin films annealed in nitrogen due to the BFO rhombohedral crystallization.

REFERENCES

[1] N. T. Tho, T. Kanashima, and M. Okuyama: Fall MRS Proc. (2009) in press.

[2] N. T. Tho, T. Kanashima, and M. Okuyama: Jpn. J. Appl. Phys (2010), in press.

[3] Y. Shimada: Testing and Reliability: *Ferroelectric Random Access Memories* (Springer, 2004) 177.

[4] S. B. Desu, I. K. Yoo: Integrat. Ferroelectr. **3** (1993) 365.

[5] M. S. Tsai and T.Y. Tseng: J. of the Electrochem. Soc. **145** (1998) 2853.

[6] Y. P. Wang and T. Y. Tseng: J. Appl. Phys. **81** (1997) 6762.

[7] A. A. Belik, S. Iikubo, K. Kodama, N. Igawa, S. Shamoto, S. Niitaka, M. Azuma, Y. Shimakawa, M. Takano, F. Izumi, and E. Takayama-Muromachi: Chem. Matter. **18** (2006) 798.

[8] Y. P. Wang, L. Zhou, M. F. Zhang, X. Y. Chen, J. M. Liu, and Z. G. Liu: Appl. Phys. Lett. **84** (2004) 1731.

[9] S. K. Singh and H. Ishiwara: Jpn. J. Appl. Phys. **44** (2005) L734.

[10] H. Bea, M.Bibes, A.Barthelemy, K. Bouzehouane, E. Jacquet, A. Khodan, J.P Contour, S. Fusil, F.Wyczisk, A. Forget, D. Lebeugle, D. Colson and M. Viret: Appl. Phys. Lett. **87** (2005) 072508.

[11] Y. Noguchi, H. Matsuo, Y. Kitanaka, and M. Miyayama: presented at Ceramics Congress, 12th Int. Montecatini Terme, Tuscany, Italy, 2010.

[12] T. Atsuki, N. Soyama, T. Yonezawa, and K. Ogi: Jpn. J. Appl. Phys. **34** (1995) 5096.

[13] Y. Li, S. Zhang, W. Fei, T. Sritharan, and C. Xu: Thin Solid Films **515** (2007) 8371.

[14] B.E. Watts, F. Leccabue, S. Guerri, M. Severi, M. Fanciulli, S. Ferrari, G. Tallarida, and C. Morandi: Thin Solid Films **406** (2002) 23.

[15] C. D. Wagner, W. M. Riggs, L. E. Davis, and J. F. Moulder, G. E. Muilenberg: *Handbook of X-ray Photoelectron Spectroscopy* (Perkin, Minnesota, 1979).

CHAPTER 6

Conclusions

As mentioned in this thesis, the purpose of this research is as follow; (1) suppression of processing temperature during preparation of ferroelectric thin films and (2) improvement of insulation, ferroelectric $Bi_4Ti_3O_{12}$ (BIT) and $BiFeO_3$ (BFO) thin films. These thin films have been prepared by a chemical solution deposition (CSD) method using hydrothermal synthesis and/or iterative RTA to enhance insulation and ferroelectric advantage of ferroelectric thin films in Ferroelectric Random Access Memory (FeRAM), which is in today's prototype of non-volatile memory cells.

In chapter 1, background of this thesis, properties of BIT and BFO and preparation methods of ferroelectric thin films were described.

The principal results obtained in this work are concluded in chapters 2-5.

In Chapter 2, low temperature preparation of BIT ferroelectric powder and thin films by hydrothermal synthesis has been carried out and characterized.

- BIT powders were obtained by hydrothermal synthesis under the condition of high KOH concentration of 1-2 M. XRD peak intensities increase with increasing synthesis time.
- BIT thin films were deposited by using the mixture solution of $Bi(OH)_3$ 0.2 M, TiO_2 0.1 M and KOH 0.012 M on TiO_2 film precursor film on $Pt/TiO_x/SiO_2/Si$ wafers by hydrothermal treatment at 220 °C. There are two possible mechanisms for crystallization of BIT thin films: (1) *in situ* transformation of the BIT thin films, and (2) dissolution-precipitation.
- These thin films are leaky but show ferroelectric property with the polarization difference at zero-electric field of 1.16 $\mu C/cm^2$.

In Chapter 3, preparation of BFO powder and thin films by a hydrothermal synthesis method has been carried out and characterized.

- From XRD analysis, BFO crystallization was observed in the powder prepared by hydrothermal treatment at 200 °C for 12 h with KOH 1M.
- The preparation of BFO thin film was obstructed not prepared successfully by the necessary of high KOH concentration to crystallize BFO. This problem makes the substrates and BFO gel films prepared by RTA at 430 °C in nitrogen damageable.

In Chapter 4, characterizations of $Bi_{1.1}Fe_{1-x}Co_xO_3$ (BFCO) thin films prepared CSD using rapid thermal annealing (RTA) in nitrogen were studied.

- Ferroelectric $Bi_{1.1}Fe_{1-x}Co_xO_3$ thin films (x = 0~0.3) were prepared on $Pt/Ti/SiO_2/Si$ substrates by CSD method using iterative RTA in nitrogen. Nitrogen was used as an ambient because annealing BFCO thin film can suppress the volatilization of bismuth at high temperature. Film thickness is 100 nm to decrease the polarization reversal voltage.
- The BFO thin film annealed at 450 °C and the BFCO thin films annealed at higher temperature in nitrogen by iterative RTA can show improved ferroelectric and piezoelectric properties at RT. One of them, the $Bi_{1.1}Fe_{0.9}Co_{0.1}O_3$ thin film annealed at 520 °C in nitrogen by iterative RTA show the best insulation.
- *P-E* hysteresis loops of the $Bi_{1.1}Fe_{0.9}Co_{0.1}O_3$ thin film is not saturated at RT because the leakage current density of 2×10^{-2} A/cm^2 at electric fields from 1 to 2 MV/cm is still large. Thus, domains of the film have not been switched completely at high electric field of ± 2MV/cm.
- The $Bi_{1.1}Fe_{0.9}Co_{0.1}O_3$ thin film annealed at 520 °C shows the piezoelectric coefficient (d_{33}) of 77 pm/V, which is larger than most of the value of BFO thin films reported.

In Chapter 5, characterizations of $Bi_{1.1}Fe_{1-x}Co_xO_3$ (BFCO) thin films prepared CSD using RTA in oxygen were studied.

- From the XPS results, the origin of leakage current, oxygen vacancies have been able to suppress in BFCO thin films annealed in oxygen by iterative RTA. One of these thin films, the $Bi_{1.1}Fe_{0.8}Co_{0.2}O_3$ thin film annealed at 520 °C in oxygen by iterative

RTA shows low leakage current density below 8.3×10^{-3} A/cm^2 at applied electric field of 1~1.5 MV/cm.

- Saturated *P-E* hysteresis loops of the $Bi_{1.1}Fe_{0.8}Co_{0.2}O_3$ thin film has been obtained.
- Domain switch measurement indicates that domains of the film can be switched completely at electric field of ± 1MV/cm.

Vita

Nguyen Truong Tho

Nguyen Truong Tho was born in Hue city, Vietnam, on August 26th 1976. He completed his undergraduate studies in physics in College of Science, Hue University in 1999. He received his M. S. degree from Hue University in 2005. From 1999 to 2006, he worked at College of Science and engaged in research and development of ferroelectric materials in bulk. He entered Graduate School of Engineering Science, Osaka University, Japan in 2006. He is a member of Japan Society of Applied Physics. Most of his works are related with ferroelectric properties of ferroelectric and multiferroic thin films.

Publications

Papers

1. Nguyen Truong Tho, Akihiro Inoue, Minoru Noda, and Masanori Okuyama, "Low Temperature Preparation of Bismuth-Related Ferroelectrics Powder and Thin Films by Hydrothermal Synthesis", IEEE. Trans. Ultra. Ferro. Freq. Contr. **54** (2007) pp.2603-2607.
2. Nguyen Truong Tho, Takeshi Kanashima, and Masanori Okuyama, "Leakage Current Reduction and Ferroelectric Property of $BiFe_{1-x}Co_xO_3$ Thin Films Prepared by Chemical Solution Deposition Using Iterative Rapid Thermal Annealing approximately 520 ^{0}C", Jpn. J. Appl. Phys., (in press).
3. Nguyen Truong Tho, Takeshi Kanashima, and Masanori Okuyama, "Ferroelectric Property of $Bi_{1.1}Fe_{1-x}Co_xO_3$ Thin Films Prepared by Chemical Solution Deposition Using Iterative Rapid Thermal Annealing in N_2 and O_2", Jpn. J. Appl. Phys., (in press).

Proceeding

1. Akihiro Inoue, Nguyen Truong Tho, Minoru Noda, and Masanori Okuyama, "Low Temperature Preparation of Bismuth-Related Ferroelectrics by Hydrothermal Synthesis", International Symposium on Applications of Ferroelectrics, May 2007, Nara, Japan.
2. Nguyen Truong Tho, Takeshi Kanashima, Masanori Okuyama, Leakage Current Reduction and Ferroelectric Property of $BiFe_{1-x}Co_xO_3$ Thin Films Prepared by Chemical Solution Deposition Using Rapid Thermal Annealing", Mater. Res. Soc. Symp. Proc., **1199E**, 1199-F06-19.

International Conferences

1. Nguyen Truong Tho, Takeshi Kanashima, and Masanori Okuyama, "Low Temperature Preparation of $Bi_4Ti_3O_{12}$ Thin Films by Hydrothermal Treament", 2nd International Workshop on Materials Science and Nano-Engineering", Awaji, Japan, December 2007, PB-33.
2. Nguyen Truong Tho, Takeshi Kanashima and Masanori Okuyama, "Low Temperature Preparation of $Bi_4Ti_3O_{12}$ Thin Films by Hydrothermal Treatment", 1st international workshop on nanotechnology and application IWNA, Vung Tau, Vietnam, November 2007, NMP-42-O.
3. Nguyen Truong Tho, Takeshi Kanashima and Masanori Okuyama, "Leakage Current Reduction and Ferroelectric Property of $BiFe_{1-x}Co_xO_3$ Thin Films Prepared by Chemical Solution Deposition Using Rapid Thermal Annealing", MRS Fall Meeting, Boston, USA, December 2009, F6.19.

Domestic Conferences

1. Nguyen Truong Tho, 井上成央, 野田 実, 奥山雅則, 「水熱合成法による$Bi_4Ti_3O_{12}$薄膜の低温作製」, 平成19(2007)年 第68回応用物理学会学術講演会, 北海道工業大学, 2007, 5a-ZL-1.
2. Nguyen Truong Tho, 金島 岳, 奥山 雅則, "RTAによる$BiFe_{1-x}Co_xO_3$薄膜の作製と評価", 平成21(2009)年 第70回応用物理学会学術講演会, 富山大, 2009, 10p-L-15.
3. 野田 実, 斎藤啓介, Nguyen Truong Tho, 山下 馨, 奥山雅則, 「X線回折による$Bi_{1.1}Fe_{0.9}Co_{0.1}O_3$ 薄膜の結晶特性評価」,2010年春季 第57回応用物理学関係連合講演会, 東海大学湘南キャンパス, 2010, 17p-TR-11.
4. Nguyen Truong Tho, T. Kanashima, M. Okuyama, M. Noda, and K. Saito, "Improvement of Ferroelectric Properties of $BiFe_{1-x}Co_xO_3$ Thin Films Prepared by Chemical Solution Deposition Using Iterative Rapid Thermal Annealing", The 27th Meeting on Ferroelectric Materials and Their Applications (FMA27), Kyoto, Japan, 2010, 27-T-12.